CHANNEL MORPHOLOGY, HYPORHEIC EXCHANGE, AND TEMPERATURE GRADIENTS WITHIN CHINOOK SALMON SPAWNING HABITAT

By

TIMOTHY PATRICK HANRAHAN

A dissertation submitted in partial fulfillment of
the requirements for the degree of

DOCTOR OF PHILOSOPHY

WASHINGTON STATE UNIVERSITY
Environmental and Natural Resource Sciences

May 2006

To the Faculty of Washington State University:

The members of the Committee appointed to examine the dissertation of TIMOTHY PATRICK HANRAHAN find it satisfactory and recommend that it be accepted.

Chair

ACKNOWLEDGMENT

I would like to extend my sincerest thanks to my advisor, Joan Wu, and the remainder of my graduate committee, Mike Barber and David Geist, for their insightful guidance throughout my graduate program. Their willingness to tolerate an unorthodox degree program and a non-traditional graduate student is much appreciated.

I owe a debt of gratitude to my employer, Battelle and the Pacific Northwest National Laboratory (PNNL), for their financial support and employment flexibility during my leaves of absence from PNNL. I would also like to thank PNNL staff Duane Neitzel for encouraging my early interest in fluvial geomorphology, Dennis Dauble for mentoring and encouraging me to pursue a Ph.D., and Charlie Brandt for giving me the management support necessary to complete a graduate program.

Lastly, I would like to thank my family, without whose love and support I would have never started graduate school. Heartfelt thanks go to my mom and dad, Rita and Don Hanrahan, for their endless support and continual encouragement of me to pursue my interests, despite me ending up 2000 miles from home. My warmest thoughts and appreciation go to my spouse, Stacey, and daughters, Quinlan and Norah, for their support, encouragement, and sacrifices during the past four years. If not for their strength, I would have given up on the "Pullman house" long ago and would have never completed my Ph.D.

CHANNEL MORPHOLOGY, HYPORHEIC EXCHANGE, AND TEMPERATURE GRADIENTS WITHIN CHINOOK SALMON SPAWNING HABITAT

Abstract

by Timothy Patrick Hanrahan, Ph.D.
Washington State University
May 2006

Chair: Joan Q. Wu

Snake River fall Chinook salmon (*Oncorhynchus tshawytscha*) populations in the Pacific northwestern United States (U.S.) have declined during the past 30 years, leading to their protection under the U.S. Endangered Species Act. Recovery activities and water management planning necessitate an understanding of the physical habitat characteristics affecting Snake River fall Chinook salmon spawning and incubation environments. The purpose of this research was to evaluate the relationships among channel morphology, river discharge, hydrologic exchange, and egg pocket water temperature in Snake River fall Chinook salmon spawning areas. The studies were completed at 15 fall Chinook salmon spawning sites distributed throughout 160 km of the Snake River in Hells Canyon, Idaho, U.S. The results indicate that 84% of fall Chinook salmon spawning areas are correlated with riffles (Chi-square=152.1, df=3, $p<0.001$), with 63% of those areas located on the upstream side of riffle crests. Differences in head pressure between the river and riverbed were small, often within ±2 cm. Measured temperature gradients in the riverbed indicated significant interactions between the surface and subsurface water. Neither hydraulic nor temperature gradients at most sites were significantly affected by either short- or long-term changes in discharge operations from Hells Canyon Dam. Only 2 out of 14 study sites exhibited acute flux reversals between the river and riverbed resulting from short-term, large magnitude changes in discharge. At all sites temperature increased with depth into the riverbed, including significant differences ($p<0.05$) in mean water temperature of up to 3.8°C between the river and the riverbed among all the sites. During each of the three water years studied, river and riverbed temperatures varied significantly among all the study sites, among the study sites within each reach, and between sites located in the two reaches. Considerable variability in riverbed temperatures among the sites resulted in fall Chinook salmon emergence timing estimates that varied by as much as 55 days. By incorporating the knowledge of channel morphology, hydrologic exchange processes and incubation environment characteristics in fall Chinook salmon spawning habitat into recovery activities and water management planning, regional agencies will be better prepared to make science-based water management decisions within the Snake River basin.

TABLE OF CONTENTS

INTRODUCTION

Populations of salmon (*Oncorhynchus* spp.) and steelhead (*O. mykiss*) in the Snake River have declined during the past 30 years, leading to their protection under the U. S. Endangered Species Act (ESA). In 1991 Snake River sockeye salmon (*O. nerka*) were listed under the ESA as endangered. In 1992 Snake River spring and fall Chinook salmon *(O. tshawytscha*) were listed as threatened. In 1998 Snake River steelhead were listed as threatened. These listing prompted management agencies, regulatory agencies, and researchers to initiate activities aimed at restoring these fish populations and the ecological functions that support them (ISG 1996).

Fall Chinook salmon historically spawned in the mainstem of the Snake River as far upstream as Salmon Falls at river kilometer (rkm) 925 (Dauble et al., 2003). Access to the upper river was blocked in the late 19th and early 20th century by the construction of a series of hydroelectric dams. Swan Falls Dam (rkm 737) was constructed in 1901 and was the upstream terminus for Chinook salmon until the construction of Brownlee Dam (rkm 459) in 1958. Shortly after Brownlee Dam was built, construction was completed on Oxbow Dam (rkm 439) in 1961 and Hells Canyon Dam (rkm 399) in 1967. Brownlee, Oxbow and Hells Canyon dams form what is now referred to as the Hells Canyon Complex, operated by the Idaho Power Company (IPC).

Current fall Chinook salmon spawning areas in the Snake River occur downstream from Hells Canyon Dam, which is now the upstream terminus for anadromous fish migration in the Snake River Basin. The decline of fall Chinook salmon has prompted management and regulatory agencies to consider actions directed at recovering lost salmon spawning areas, including dam removal, reservoir drawdown, reintroduction into blocked historic habitat, and expanding existing salmon spawning areas (Dauble et al., 2003; Hanrahan et al., 2004; Groves and Chandler, 2005; Hanrahan et al., 2005). A key component to evaluating these actions is quantifying the salmon spawning habitat potential of a given river reach so that realistic recovery goals for salmon abundance can be developed (ISG, 1996). Previous research has identified associations between salmon spawning and geomorphic characteristics (Payne and Lapointe, 1997; Geist and Dauble, 1998; Montgomery et al., 1999; Dauble and Geist, 2000; Moir et al. 2004), yet incorporating these associations into estimates of salmon spawning habitat potential has remained elusive. Quantifying the relationships between channel morphology and fall Chinook salmon spawning habitat will provide information that will be useful for directing recovery efforts for this imperiled salmon population.

Like many other river systems throughout the world where salmon populations are imperiled (e.g., Pacific salmon in western North America, and Atlantic salmon (*Salmo salar*) in eastern North America and Europe), the flow magnitude and timing from hydroelectric dams in the Snake River basin is managed in part for the benefit of salmon (Groves and Chandler, 1999; Gibbins and Acornley, 2000; Gibbins et al., 2002; Hendry et al., 2003; Berland et al., 2004). The management of discharge operations from Hells Canyon Dam takes on a variety of forms, but always involves water policy tradeoffs among multiple competing uses, including salmon recovery, flood control, irrigation supply, hydropower production, and recreation. One discharge management option under consideration by regional agencies is the manipulation of discharge operations during some portions of the fall Chinook salmon incubation period (October–June) in order to improve the riverbed incubation environment through alteration of the hyporheic exchange between the river and riverbed (i.e., interaction between river water and ground water). Another discharge management option involves the establishment of a minimum discharge during the fall Chinook salmon spawning period (early-October to early-December), which must be maintained through the period of salmon fry emergence (early-June of the following year) to protect embryos that are incubating in the riverbed (Groves and Chandler, 1999). Therefore, there is a need for a better understanding of the hyporheic exchange and incubation environment characteristics within Snake River fall Chinook salmon spawning habitat. By incorporating the knowledge of hyporheic exchange processes and incubation environment characteristics into water management planning, regional agencies will be better prepared to manage the limited water resources among competing priorities within the Snake River basin.

The objective of this research was to improve upon the understanding of physical habitat characteristics (channel morphology, hyporheic exchange, temperature gradients) affecting Snake River fall Chinook salmon spawning and incubation environments. The research was conducted in a section of the Snake River extending from Hells Canyon Dam (rkm 399) downstream to near the confluence with Asotin Creek (rkm 240). The studies evaluated the relationships among channel morphology, river discharge, hyporheic exchange, and egg pocket water temperature in Snake River fall Chinook salmon spawning areas. The dissertation is comprised of three manuscripts, organized under the general themes: 1) bed form morphology of fall Chinook salmon spawning areas, 2) effects of river discharge on the hyporheic exchange between the river and riverbed, and 3) spatial variability of riverbed temperature gradients in fall Chinook salmon spawning areas. The first manuscript (formatted for the journal *Geomorphology*) characterizes the longitudinal bed form profile, which is thought to control the hydrologic exchange between the river and riverbed. The second manuscript (formatted for the journal *Hydrological Processes*) uses this characterization as a foundation for investigating the hyporheic exchange under varying river discharge at the pool-riffle scale. The third manuscript (formatted for the journal *River Research and Applications*) quantifies the variability of riverbed temperature gradients to evaluate the implications for incubation and emergence timing of fall Chinook salmon.

This research was focused on physical habitat characteristics that affect the life-cycle of Snake River fall Chinook salmon; however, the studies were conducted in the context of enhancing and restoring the physical processes of gravel-bed rivers in general. The expected value of the research includes:

- A better understanding of the physical riverine processes affecting the habitats that support Snake River fall Chinook salmon, which will foster science-based water management planning and recovery activities for this imperiled salmon population
- A better understanding of the spatial and temporal patterns and physical processes of riverbed temperature gradients in gravel-bed rivers
- Knowledge of riverbed temperature gradient patterns and processes that may be applied to understanding and predictive modeling in other gravel-bed rivers
- A better understanding of the implications of riverbed temperature gradient variability on the incubation period of salmonid embryos in gravel-bed rivers

References

Berland, G., Nickelsen, T., Heggenes, J., Okland, F., Thorstad, E. B., and Halleraker, J. 2004. Movements of wild Atlantic salmon parr in relation to peaking flows below a hydropower station. River Research and Applications 20, 957–966.

Dauble, D. D., Geist, D. R., 2000. Comparison of mainstem spawning habitats for two populations of fall chinook salmon in the Columbia River Basin. Regulated Rivers: Research and Management 16, 345–361.

Dauble, D. D., Hanrahan, T. P., Geist, D. R., Parsley, M. J., 2003. Impacts of the Columbia River hydroelectric system on main-stem habitats of fall chinook salmon. North American Journal of Fisheries Management 23, 641–659.

Geist, D. R., Dauble, D. D., 1998. Redd site selection and spawning habitat use by fall chinook salmon: the importance of geomorphic features in large rivers. Environmental Management 22, 655–669.

Gibbins, C. N. and Acornley, R. M. 2000. Salmonid habitat modelling studies and their contribution to the development of an ecologically acceptable release policy for Kielder Reservoir, north-east England. Regulated Rivers: Research and Management 16, 203–224.

Gibbins, C. N., Moir, H. J., Webb, J. H., and Soulsby, C. 2002. Assessing discharge use by spawning Atlantic salmon: A comparison of discharge electivity indices and PHABSIM simulations. River Research and Applications 18, 383–395.

Groves, P. A., Chandler, J. A., 2005. Habitat quality of historic Snake River fall Chinook salmon spawning locations and implications for incubation survival: part 2, intra-gravel water quality. River Research and Applications 21, 469–483.

Hanrahan, T. P., Dauble, D. D., Geist, D. R., 2004. An estimate of chinook salmon (*Oncorhynchus tshawytscha*) spawning habitat and redd capacity upstream of a migration barrier in the upper Columbia River. Canadian Journal of Fisheries and Aquatic Sciences 61, 23–33.

Hanrahan, T. P., Geist, D. R., Arntzen, E. V., 2005. Habitat quality of historic Snake River fall Chinook salmon spawning locations and implications for incubation survival: part 1, substrate quality. River Research and Applications 25, 455–467.

Hendry, K., Cragg-Hine, D., O'Grady, M., Sambrook, H., and Stephen, A. 2003. Management of habitat for rehabilitation and enhancement of salmonid stocks. Fisheries Research 62, 171–192.

Independent Scientific Group, 1996. Return to the river: Restoration of salmonid fishes in the Columbia River ecosystem. Northwest Power Planning Council, Portland, OR.

Moir, H. J., Gibbins, C. N., Soulsby, C., Webb, J., 2004. Linking geomorphic characteristics to spatial patterns of spawning activity and discharge use by Atlantic salmon (*Salmo salar* L.). Geomorphology 60, 21–35.

Montgomery, D. R., Beamer, E. M., Pess, G. R., Quinn, T. P., 1999. Channel type and salmonid spawning distribution and abundance. Canadian Journal of Fisheries and Aquatic Sciences 56, 377–387.

Payne, B. A., LaPointe, M. F., 1997. Channel morphology and lateral stability: effects on distribution of spawning and rearing habitat for Atlantic salmon in a wandering cobble-bed river. Canadian Journal of Fisheries and Aquatic Sciences 54, 2627–2636.

MANUSCRIPT ONE

Short Communication

Title:

Bed form morphology of salmon spawning areas in a large gravel-bed river

Author:

Timothy P. Hanrahan

Pacific Northwest National Laboratory

P.O. Box 999 MS K6-85

Richland, WA 99354 USA

Tel. 509 376 0972

tim.hanrahan@pnl.gov

Abstract

While the importance of river channel morphology to salmon spawning habitat is increasingly recognized, quantitative measures of the relationships between channel morphology and habitat use are lacking. Such quantitative measures are necessary as management and regulatory agencies within the Pacific Northwestern region of the USA, and elsewhere, seek to quantify potential spawning habitat and develop recovery goals for declining salmon populations. The objective of this study was to determine if fall Chinook salmon (*Oncorhynchus tshawytscha*) spawning areas in the Snake River, Idaho, USA, were correlated with specific bed form types at the pool-riffle scale. A bed form differencing technique was used to objectively quantify the longitudinal riverbed profile into four distinct pool-riffle units that were independent of discharge. The vertical location of thalweg points within these units was quantified with a riffle proximity index. Chinook salmon spawning areas were mapped and correlated with the pool-riffle units through the use of cross-tabulation tables. The results indicate that 84% of fall Chinook salmon spawning areas were correlated with riffles (Chi-square=152.1, df=3, $p<0.001$), with 53% of those areas located on the upstream side of riffle crests. The majority of Snake River fall Chinook salmon spawning occurred at a vertical location within 80% of the nearest riffle crest elevation. The analyses of bed form morphology will assist regional fish mangers in quantifying existing and potential fall Chinook salmon spawning habitat, and will provide a quantitative framework for evaluating general ecological implications of channel morphology in large gravel-bed rivers.

Keywords: Channel morphology; Chinook salmon; river bed form

1. Introduction

Development of hydroelectric dams in the Columbia River basin of the United States has contributed to the declining abundance of fall Chinook salmon (*Oncorhynchus tshawytscha*) through conversion of rivers to reservoirs and blocked access to historic spawning areas (Dauble et al., 2003). Populations of Snake River fall Chinook salmon have declined to the point that they are now protected under the U.S. Endangered Species Act (NMFS, 1992). The decline of fall Chinook salmon has prompted management and regulatory agencies to consider actions directed at recovering lost salmon spawning areas, including dam removal, reservoir drawdown, and reintroduction into blocked historic habitat (Dauble et al., 2003; Hanrahan et al., 2004; Groves and Chandler, 2005; Hanrahan et al., 2005), as well as expanding existing salmon spawning areas. A key component to evaluating these actions is quantifying, through modeling, the salmon spawning habitat potential of a given river reach so that realistic recovery goals for salmon abundance can be developed (ISG, 1996).

Fish biologists are increasingly recognizing the importance of geomorphic characteristics of rivers to salmon spawning habitat, however little effort has been directed at incorporating quantitative measures of these characteristics into habitat modeling. The typical approach to habitat modeling is based on depth, velocity, substrate, and channelbed slope characteristics, an approach that often overestimates the amount of available habitat (Geist and Dauble, 1998). Channel morphology influences these and other microhabitat variables (e.g., hydrologic exchange between the river and riverbed), and previous researchers have investigated the association of salmon spawning with specific geomorphic characteristics (Payne and Lapointe, 1997; Geist and Dauble, 1998; Montgomery et al., 1999; Dauble and Geist, 2000; Moir et al. 2004). What these studies lacked was a quantification of the bed form geomorphic characteristic(s) at the pool-riffle scale to which salmon spawning was being associated. For example, salmon spawning was identified to have occurred near geomorphic features such as islands and alternate bars, and in ‘response’ type reaches, but identification of these features and reaches was qualitative (Geist and Dauble, 1998; Moir et al., 2004). Similarly, a recurring issue in the study of riffles and pools is their reliable and objective identification (O’Neill and Abrahams, 1984; Carling and Orr, 2000). Despite the importance of riffle-pool structure on channel morphology adjustments, hydrologic exchange between the river and riverbed, and the provision of habitat, most investigators identify pool-riffle structure through qualitative visual delineation in the field or though methods that depend on discharge (O’Neill and Abrahams, 1984; Carling and Orr, 2000). While these qualitative approaches are easy to apply, they are not conducive to quantifying riverine processes or estimating the salmon spawning habitat potential of a river reach.

This paper reports on a study that addressed the research hypothesis that fall Chinook salmon spawning locations in the Hells Canyon reach of the Snake River, Idaho, USA, are correlated with specific bed form types at the pool-riffle scale. Specific objectives of the study were to: 1) quantify the longitudinal riverbed profile of the Hells Canyon reach of the Snake River into distinct bed form types at the pool-riffle scale, and 2) correlate fall Chinook salmon spawning locations with identified bed form types.

2. Study area and methods

2.1 Study area

This research was conducted throughout 160 km of the Hells Canyon reach (HCR) of the Snake River, located in western Idaho, U.S. The HCR extends from Hells Canyon Dam (river kilometer (rkm) 399) downstream to Asotin Creek near rkm 240 (Figure 1). This entire reach of the Snake River is narrowly confined by valley walls, and is generally controlled by large-scale geologic and geomorphic features, resulting in a lack of floodplain development. The upper section of the HCR (rkm 399−306; hereafter upper reach) is situated in a deep and narrow gorge entrenched in erosion-resistant basalt and metamorphic bedrock. Although when viewed in planform the HCR exhibits a meandering course, geomorphically it is a straight or slightly sinuous river. The river possesses the characteristics of passive meandering, where the planform pattern is imposed by the local landform. While large alluvial terraces exist along the river, they are remnant deposits of the Pleistocene Lake Bonneville Floods, and are located tens of meters above contemporary flood stages (O'Connor, 1993). Alluvial deposits within the bankfull channel from these and other flood events have been reworked by the contemporary flow regime, resulting in a longitudinal pool-riffle bed form morphology, despite the valley confinement. Due to the lack of floodplain development, interactions between the river and its banks are limited to near-river areas (small lateral bars, terraces, fans) inundated by contemporary flow regimes. The lower HCR (rkm 306−240; hereafter lower reach) exhibits a lower slope and more floodplain development than the upper reach, owing mostly to a geologic fault zone near rkm 306 and the influence from three major tributaries – the Imnaha River at rkm 307, the Salmon River at rkm 300 and the Grande Ronde River at rkm 269. However, even the lower reach is considered narrowly confined within the valley walls. Average bankfull channel widths range from approximately 100 m in the upper reach to 150 m in the lower reach (Miller et al., 2002).

The Hells Canyon Complex (Hells Canyon, Oxbow, and Brownlee dams) controls nearly all of the flow through the upper reach, and just over 50% of the flow in the lower reach. Immediately downstream from Hells Canyon Dam at U. S. Geological Survey (USGS) gage 13290450, mean daily discharge has averaged 589 $m^3 s^{-1}$ since 1965. Over this same time period, mean daily discharge in the lower reach has averaged 1035 $m^3 s^{-1}$ (USGS gage 13334300, rkm 269). Inputs from the Imnaha, Salmon and Grande Ronde rivers (USGS gages 13292000, 13317000, and 13333000, respectively) during this period make up a mean daily discharge of 426 $m^3 s^{-1}$, resulting in a residual input of approximately 20 $m^3 s^{-1}$ from tributaries between Hells Canyon Dam (rkm 399) and the Imnaha River confluence (rkm 307).

2.2 *Bed form analysis*

A quantitative analysis of the longitudinal bed form profile was completed using sequential bed elevation data from the thalweg of the river. A total of 5573 thalweg points (*x*-coordinate, *y*-coordinate, *z*-elevation) spaced no more than 50 m apart were imported into a geographic information system (GIS) database from a comprehensive bathymetry dataset for the entire 160 km of the HCR (Butler, 2002). The vertical accuracy of the thalweg points was estimated to be ±10–0 cm (Butler, 2002). The thalweg points were used in a bed form differencing technique to identify pools and riffles (O'Neill and Abrahams, 1984). The technique involves differencing successive bed elevations in a downstream direction, and then calculating the standard deviation of the resulting difference values. The standard deviation of bed elevation differences is used to set a threshold value that filters out pool-riffle bed forms from the undulating longitudinal riverbed profile. In this study, the threshold value was set at 2.5 times the standard deviation of bed elevation differences. Based on guidance in O'Neill and Abrahams (1984) the threshold value was the inverse of the ratio of the average distance between sampled thalweg points to average channel widths, which was approximately 0.4. Details of the bed form differencing technique are available in O'Neill and Abrahams (1984). Application of the technique resulted in identification of the thalweg points that were either riffle crests or pool bottoms.

After riffle crests and pool bottoms were identified, two additional analyses were completed in order to classify where the remaining thalweg points were located relative to the riffle crests and pool bottoms. First, the thalweg points were determined to be in riffles or pools based on their riffle proximity index (*RPI*)

$$RPI = 1 - \frac{rcelev - tpelev}{rcelev - pbelev}$$

where *rcelev* = nearest riffle crest elevation, *tpelev* = thalweg point elevation, and *pbelev* = nearest pool bottom elevation. The *RPI* ranges from 0.0 to 1.0, where thalweg points with a *RPI* > 0.50 were categorized as being in riffles, while the remaining points were categorized as being in pools. Second, all thalweg points were categorized as being located in one of four areas along the longitudinal profile: (1) upstream side of riffle crests, (2) downstream side of riffle crests, (3) upstream side of pool bottoms, (4) downstream side of pool bottoms.

Fall Chinook salmon spawning locations were incorporated into the GIS database for an analysis of their spatial relationship with bed form types. Fall Chinook salmon spawning areas have been monitored and mapped annually since 1991, including observations from helicopter and underwater video surveys (Phil Groves, Idaho Power Company, personal communications). The fall Chinook salmon spawning areas were mapped in the GIS as point features that represented individual redds (salmon spawning nests) for all years of observation. GIS overlay techniques were used to code all thalweg points as spawning or non-spawning depending on their proximity to the observed spawning locations. In all cases, the mapped redds were considered the upstream and downstream extent of the spawning habitat used at a given site. Thalweg points within the spawning habitat were coded as spawning, while thalweg points outside of the spawning habitat were coded as non-spawning.

Cross-tabulation tables and Pearson's Chi-square (χ^2) test statistic were used to test the null hypothesis that spawning habitat use was independent of bed form category (α=0.05). Welch's t-test for unbalanced sample sizes and separate variances was used to test the null hypothesis that thalweg points in spawning and non-spawning areas had the same mean RPI (α=0.05) (Zar, 1999).

3. Results

A total of 209 riffles were identified, with 134 located in the upper reach and 75 located in the lower reach. The spacing between riffles was similar for both reaches, averaging

7.1±0.64 (95% confidence interval) and 6.9±1.53 (95% confidence interval) channel widths apart for the upper and lower reach, respectively. Exclusive of outliers, the variability in riffle crest spacing was larger in the upper reach (inter-quartile range (IQR)=5.1) than in the lower reach (IQR=3.9) (Figure 2).

Results from the analyses of all thalweg points indicated that spawning areas were more likely to occur near riffle crests than elsewhere along the longitudinal profile (Figure 3). The median riffle proximity index (*RPI*) for spawning areas was larger (0.82) and less variable (IQR=0.18) than the *RPI* for non-spawning areas (median=0.65, IQR=0.25, Figure 4). More than 50% of the spawning areas had an *RPI* larger than 0.80 (Figure 5). Results from the t-test indicated that the mean *RPI* in spawning areas was significantly larger than the mean *RPI* in non-spawning areas (t=-10.25, df=441, p<<0.001).

Results from the cross-tabulation analysis indicated that spawning habitat use was dependent on bed form type (χ^2=152.1, df=3, p<<0.001). The upstream and downstream sides of riffle crests contained 53% and 31% of the spawning habitat use, respectively (Table 1). The remaining spawning habitat use occurred on the upstream (6%) and downstream (10%) ends of pools (Figure 6).

4. Discussion

Application of the bed form differencing technique resulted in quantifying discharge-independent pool-riffle bed forms in the Snake River, which matched well with both theory and the results from other empirical studies. The average riffle spacing reported in this paper (6.9–7.1 channel widths) is similar to the often cited spacing of five to seven channel widths in self-formed and geomorphically-forced rivers, hypothesized to result from velocity reversals between riffles and pools, kinematic wave propagation, longitudinal oscillations in macroturbulent flow, and non-rhythmic distributions of channel obstructions (Langbein and Leopold, 1968; Keller, 1971; Hey and Thorne, 1986; Yalin, 1992; Knighton, 1998; Thompson, 2001). Beginning with

Leopold et al. (1964), research in many different river environments and using many different methods has documented pool-riffle spacing to average approximately five to seven channel widths, while also including a large amount of variability (Keller and Melhorn, 1978; Gregory et al., 1994; Knighton, 1998; Carling and Orr, 2000; Thompson, 2001). The location and spacing of identified bed forms reported in this paper matched well with visually mapped geomorphic units (including pools and riffles) in the Snake River and their calculated spacing (average of 5.9 channel widths) (Miller et al., 2002). Similarly, the average riffle spacing reported in this paper matches well with previous work that used the bed form differencing technique, including the average riffle spacing of 4.7–7.3 channel widths in small rivers (O'Neill and Abrahams, 1984; Jurmu, 2002) and the average riffle spacing of 5.5–8.8 channel widths in the much larger lower Mississippi River (Harmar et al. 2005). The differences in average riffle spacing among these studies that applied the bed form differencing technique likely result from the inherent variability in channel morphology within and among different rivers, and the method used for selecting the threshold value that delineates bed forms.

The findings reported in this paper provide a quantitative association between salmon spawning habitat and geomorphic features, an association that previous research has documented in qualitative terms. The results indicate that most Snake River fall Chinook salmon spawning occurs in riffles, and at a vertical location within 80% of the riffle crest elevation. In addition to specific requirements for water depth, velocity, and substrate size, many salmon species tend to prefer to spawn in the transitional areas between pools and riffles (Bjornn and Reiser, 1991). Owing to localized variations in sediment transport rates, these transitional areas are depositional zones that are often associated with the formation of bars (lateral, mid-channel, point) and islands. Previous researchers have observed salmon spawning locations to be associated with depositional 'response' reaches (Montgomery et al., 1999; Moir et al., 2004), especially near the upstream end of bars and islands (Dauble and

Watson, 1997; Geist and Dauble, 1998; Coulombre-Pontbriand and Lapointe, 2004). The results reported in this paper corroborate these earlier findings, and quantify the location along the longitudinal profile where Chinook salmon spawning occurs. By quantifying the two-dimensional location (vertical and longitudinal) of salmon spawning areas, these findings complement previous planform mapping of Snake River fall Chinook salmon spawning areas. Dauble and Geist (2000) reported that Chinook salmon spawning in the Hells Canyon Reach of the Snake River was associated with the presence of bars that were mapped along 1.6 km river segments. Based on planform mapping of morphological channel types (bar, fan, glide, pool, rapid, riffle) Groves and Chandler (2002) observed that most fall Chinook salmon spawning occurred in riffles.

The findings reported in this paper provide an important context for estimating the spawning habitat potential of Snake River fall Chinook salmon and other salmon populations. The objective identification and quantification of stage-independent pool-riffle bed forms will result in more accurate estimates of salmon spawning habitat potential, as microhabitat characteristics (e.g., depth, velocity, substrate size) in salmon spawning areas encompass such a large range that their predictive potential is often limited. For example, incorporating the quantitative association between salmon spawning habitat and riffles into habitat modeling will improve the predictive potential of such models by providing a quantitative means of identifying the suitable microhabitat located in riffles, and not elsewhere along the longitudinal profile. Such an approach is not possible through visual planform mapping of pools and riffles, as the identified geomorphic units are stage-dependent, subject to individual interpretation, and provide no quantitative metric that can be incorporated into habitat models. Results from previous research has suggested that geomorphic characteristics at the pool-riffle scale may also be important controlling factors of other microhabitat variables (e.g., substrate quality, hyporheic exchange, hydraulic habitat complexity) important to spawning salmon and other fish

(Geist and Dauble, 1998; Baxter and Hauer, 2000; Geist, 2000; Moir et al., 2002; Coulombre-Pontbriand and Lapointe, 2004; Crowder and Diplas, 2006). Incorporating the quantitative linkages between bed forms and these other microhabitat variables when predicting habitat potential will also result in more accurate estimates of suitable habitat. Improvements to the predictive potential of habitat models will help management and regulatory agencies in the Snake River basin and elsewhere to develop realistic recovery goals for salmon abundance.

While pool-riffle bed forms may be controlling factors of fish habitat, quantifying their location in the longitudinal profile also provides a useful framework for evaluating general ecological implications of riverine processes in large gravel-bed rivers. The identification of bed forms and application of the *RPI* provide a quantitative framework for testing hypotheses regarding the associations between riverine processes and ecological function (e.g., benthic macroinvertebrate habitat, nutrient cycling, biofilm development). This may include using the location along the longitudinal profile as an independent variable to evaluate the magnitude of hydrologic exchange between the river and riverbed, the local turbulence characteristics of the flow field, and the local bedload sediment transport capacity as it affects bed material grain size distributions. Using hydrologic exchange as an example, our ability to understand patterns and develop predictive models of hydrologic exchange within large rivers depends on the extent to which we can objectively and quantitatively identify the controlling factors of the exchange. Exchange flows at larger scales (e.g., reaches of multiple pool-riffle sequences) are controlled by valley morphology and physiography (Larkin and Sharp, 1992; Stanford and Ward, 1993; Fernald et al., 2001), characteristics that are easily observed and measured. At the scale of pool-riffle sequences, changes in the longitudinal bed profile control exchange flows through the riverbed and banks (Harvey and Bencala, 1993; Hill et al., 1998; Kasahara and Wondzell, 2003). The objective identification of bed forms at this scale is much more tenuous (Carling and Orr, 2000), especially in large rivers. Thus, identification of bed forms with the differencing technique and application of the *RPI* will foster a quantitative understanding of hydrologic exchange at the pool-riffle scale.

5. Acknowledgements

This research was funded by the U. S. Department of Energy Bonneville Power Administration under the Northwest Power and Conservation Council's Fish and Wildlife Program. Co-funding was provided by Idaho Power Company. I extend my gratitude to Brad Alcorn, Mike Butler, and Phil Groves of Idaho Power Company for contributing data. The Pacific Northwest National Laboratory is operated by Battelle Memorial Institute for the U. S. Department of Energy under contract DE-AC06-76RLO-1830.

6. References

Baxter, C. V., Hauer, F. R., 2000. Geomorphology, hyporheic exchange, and selection of spawning habitat by bull trout (*Salvelinus confluentus*). Canadian Journal of Fisheries and Aquatic Sciences 57, 1470–1481.

Bjornn, T. C. and Reiser, D. W., 1991. Habitat requirements of salmonids in streams. In: Meehan, W. R. (Ed.), Influences of forest and rangeland management on salmonid fishes and their habitats, AFS Special Publication 19. American Fisheries Society, Bethesda, MD.

Butler, M., 2002. Topographic integration for the Hells Canyon studies. Technical Report Appendix E.1.3 to FERC Relicensing Application. Idaho Power Company, Boise, ID.

Carling, P. A., Orr, H. G., 2000. Morphology of riffle-pool sequences in the River Severn, England. Earth Surface Processes and Landforms 25, 369–384.

Coulombe-Pontbriand, M., Lapointe, M., 2004. Geomorphic controls, riffle substrate quality, and spawning site selection in two semi-alluvial salmon rivers in the Gaspe Peninsula, Canada. River Research and Applications 577–590.

Crowder, D. W., Diplas, P., 2006. Applying spatial hydraulic principles to quantify stream habitat. River Research and Applications 22, 79–89.

Dauble, D. D., Hanrahan, T. P., Geist, D. R., Parsley, M. J., 2003. Impacts of the Columbia River hydroelectric system on main-stem habitats of fall chinook salmon. North American Journal of Fisheries Management 23, 641–659.

Dauble, D. D., Watson, D. G., 1997. Status of fall chinook salmon populations in the mid-Columbia River, 1948-1992. North American Journal of Fisheries Management 17, 283–300.

Dauble, D. D., Geist, D. R., 2000. Comparison of mainstem spawning habitats for two populations of fall chinook salmon in the Columbia River Basin. Regulated Rivers:

Research and Management 16, 345–361.

Fernald, A. G., Winington Jr., P. J., Landers, D. H., 2001. Transient storage and hyporheic flow along the Willamette River, Oregon: field measurements and model estimates. Water Resources Research 37, 1681–1694.

Geist, D. R., 2000. Hyporheic discharge of river water into fall chinook salmon (*Oncorhynchus tshawytscha*) spawning areas in the Hanford Reach, Columbia River. Canadian Journal of Fisheries and Aquatic Sciences 57, 1647–1656.

Geist, D. R., Dauble, D. D., 1998. Redd site selection and spawning habitat use by fall chinook salmon: the importance of geomorphic features in large rivers. Environmental Management 22, 655–669.

Gregory, K. J., Gurnell, A. M., Hill, C. T., Tooth, S., 1994. Stability of the pool-riffle sequence in changing river channels. Regulated Rivers: Research and Management 9, 35–43.

Groves, P. A., Chandler, J. A., 2002. The quality and availability of fall Chinook salmon spawning and incubation habitat downstream of the Hells Canyon Complex. Technical Report Appendix E.3.1.3 to FERC Relicensing Application. Idaho Power Company, Boise, ID.

Groves, P. A., Chandler, J. A., 2005. Habitat quality of historic Snake River fall Chinook salmon spawning locations and implications for incubation survival: part 2, intra-gravel water quality. River Research and Applications 21, 469–483.

Hanrahan, T. P., Dauble, D. D., Geist, D. R., 2004. An estimate of chinook salmon (*Oncorhynchus tshawytscha*) spawning habitat and redd capacity upstream of a migration barrier in the upper Columbia River. Canadian Journal of Fisheries and Aquatic Sciences 61, 23–33.

Hanrahan, T. P., Geist, D. R., Arntzen, E. V., 2005. Habitat quality of historic Snake River fall Chinook salmon spawning locations and implications for incubation survival: part 1, substrate quality. River Research and Applications 25, 455–467.

Harmar, O. P., Clifford, N. J., Thorne, C. R., Biedenharn, D. S., 2005 . Morphological changes of the lower Mississippi River: geomorphological response to engineering intervention. River Research and Applications 21, 1107–1131.

Harvey, J. W., Bencala, K. E., 1993. The effect of streambed topography on surface-subsurface water exchange in mountain catchments. Water Resources Research 29, 89–98.

Hey, R. D., Thorne, C. R., 1986. Stable channels with mobile gravel beds. Journal of Hydraulic Engineering 112, 671–689.

Hill, A. R., Labadia, C. F., Sanmugadas, K., 1998. Hyporheic zone hydrology and nitrate dynamics in relation to the streambed topography of a N-rich stream. Biogeochemistry 42, 285–310.

Independent Scientific Group, 1996. Return to the river: Restoration of salmonid fishes in the Columbia River ecosystem. Northwest Power Planning Council, Portland, OR.

Jurmu, M. C., 2002. A morphological comparison of narrow, low-gradient streams traversing wetland environments to alluvial streams. Environmental Management 30, 831–856.

Kasahara, T., Wondzell, S. M., 2003. Geomorphic controls on hyporheic exchange flow in mountain streams. Water Resources Research 39, 1005, DOI:10.1029/2002WR001386.

Keller, E. A., 1971. Areal sorting of bed load material: the hypothesis of velocity reversal. Bulletin of the Geological Society of America 82, 753–756.

Keller, E. A., Melhorn, W. N., 1978. Rhythmic spacing and origin of pools and riffles. Bulletin of the Geological Society of America 89, 723–730.

Knighton, D., 1998. Fluvial forms and processes: A new perspective. Oxford University Press, New York, NY.

Langbein, W. B., Leopold, L. B., River chanel bars and dunes: theory of kinematic waves. Professional paper 422L. United States Geological Survey.

Larkin, R. G., Sharp, J. M., 1992. On the relationship between river-basin geomorphology, aquifer hydraulics, and ground-water flow direction in alluvial aquifers. Geological Society of America Bulletin 104, 1608–1620.

Leopold, L. B., Wolman, M. G., Miller, J. P., 1964. Fluvial processes in geomorphology. W. H. Freeman and Co., San Francisco, CA.

Miller, S., Glanzman, D., Doran, S., Parkinson, S., Buffington, J., Milligan, J., 2002. Geomorphology of the Hells Canyon Reach of the Snake River. Technical Report Appendix E.1.2 to FERC Relicensing Application. Idaho Power Company, Boise, ID.

Moir, H. J., Gibbins, C. N., Soulsby, C., Webb, J., 2004. Linking geomorphic characteristics to spatial patterns of spawning activity and discharge use by Atlantic salmon (*Salmo salar* L.). Geomorphology 60, 21–35.

Moir, H. J., Soulsby, C., Youngson, A. F., 2002. Hydraulic and sedimentary controls on the availability and use of Atlantic salmon (*Salmo salar*) spawning habitat in the River Dee system, north-east Scotland. Geomorphology 45, 291–308.

Montgomery, D. R., Beamer, E. M., Pess, G. R., Quinn, T. P., 1999. Channel type and salmonid spawning distribution and abundance. Canadian Journal of Fisheries and Aquatic Sciences 56, 377–387.

National Marine Fisheries Service (NMFS), 1992. Threatened status for Snake River spring/summer chinook salmon, threatened status for Snake River fall chinook salmon. Federal Register 57, 14653–14663.

O'Connor, J. E., 1993. Hydrology, hydraulics, and geomorphology of the Bonneville Flood. Special paper 274. Geological Society of America, Boulder, CO.

O'Neill, M. P., Abrahams, A. D., 1984. Objective identification of pools and riffles . Water Resources Research 20, 921–926.

Payne, B. A., LaPointe, M. F., 1997. Channel morphology and lateral stability: effects on distribution of spawning and rearing habitat for Atlantic salmon in a wandering cobble-bed river. Canadian Journal of Fisheries and Aquatic Sciences 54, 2627–2636.

Stanford, J. A., Ward, J. V., 1993. An ecosystem perspective of alluvial rivers: connectivity and the hyporheic zone. Journal of the North American Benthological Society 12, 48–60.

Thompson, D. M., 2001. Random controls on semi-rhythmic spacing of pools and riffles in constriction-dominated rivers. Earth Surface Processes and Landforms 26, 1195–1212.

Yalin, M. S., 1992. River mechanics. Pergamon, Oxford, England.

Zar, J. H., 1999. Biostatistical analysis. 4th ed. Prentice Hall, Upper Saddle River, NJ, USA.

7. Tables

Table 1. Summary frequency table of four bed form types in fall Chinook salmon spawning and non-spawning areas. Points along the longitudinal profile were categorized as being on the upstream (proximal) or downstream (distal) side of a riffle crest or pool ogee.

	Riffle proximal	Riffle distal	Pool proximal	Pool distal
Spawning				
count	196	115	24	36
frequency	53%	31%	6%	10%
Non-spawning				
count	1276	2042	941	943
frequency	25%	39%	18%	18%

8. List of figures

Figure 1. The study area encompassed the Snake River from Hells Canyon Dam downstream to near the confluence with the Asotin Creek, including the upper reach (river kilometer 399 – 306) and lower reach (river kilometer 306 – 240). The numbers along the Snake River indicate the approximate river kilometer location.

Figure 2. Riffle crest spacing (in channel widths) for the upper and lower reaches of the Snake River study area. The boxplots indicate the median (small box), surrounded by the 25th and 75th percentiles (large box), and extend to the 10th and 90th percentiles (whiskers) of observed values.

Figure 3. Sample planview map indicating the correlation of fall Chinook salmon spawning areas (○) with identified riffle crests (large ▲) and pool bottoms (large ●). The longitudinal extent of riffles (small ▲) and pools (small •) is also indicated. Within channel and near-shore elevation contour lines are mapped at 2 m intervals.

Figure 4. Riffle proximity index for Snake River fall Chinook salmon spawning and non-spawning locations. The boxplots indicate the median (small box), surrounded by the 25th and 75th percentiles (large box), and extend to the 10th and 90th percentiles (whiskers) of observed values.

Figure 5. Cumulative frequency of riffle proximity index *RPI* values for thalweg points (n=371) within fall Chinook salmon spawning areas.

Figure 6. Sample of the Snake River longitudinal profile indicating the percentage of fall Chinook salmon spawning areas located in pool and riffle bed forms (■).

9. Figures

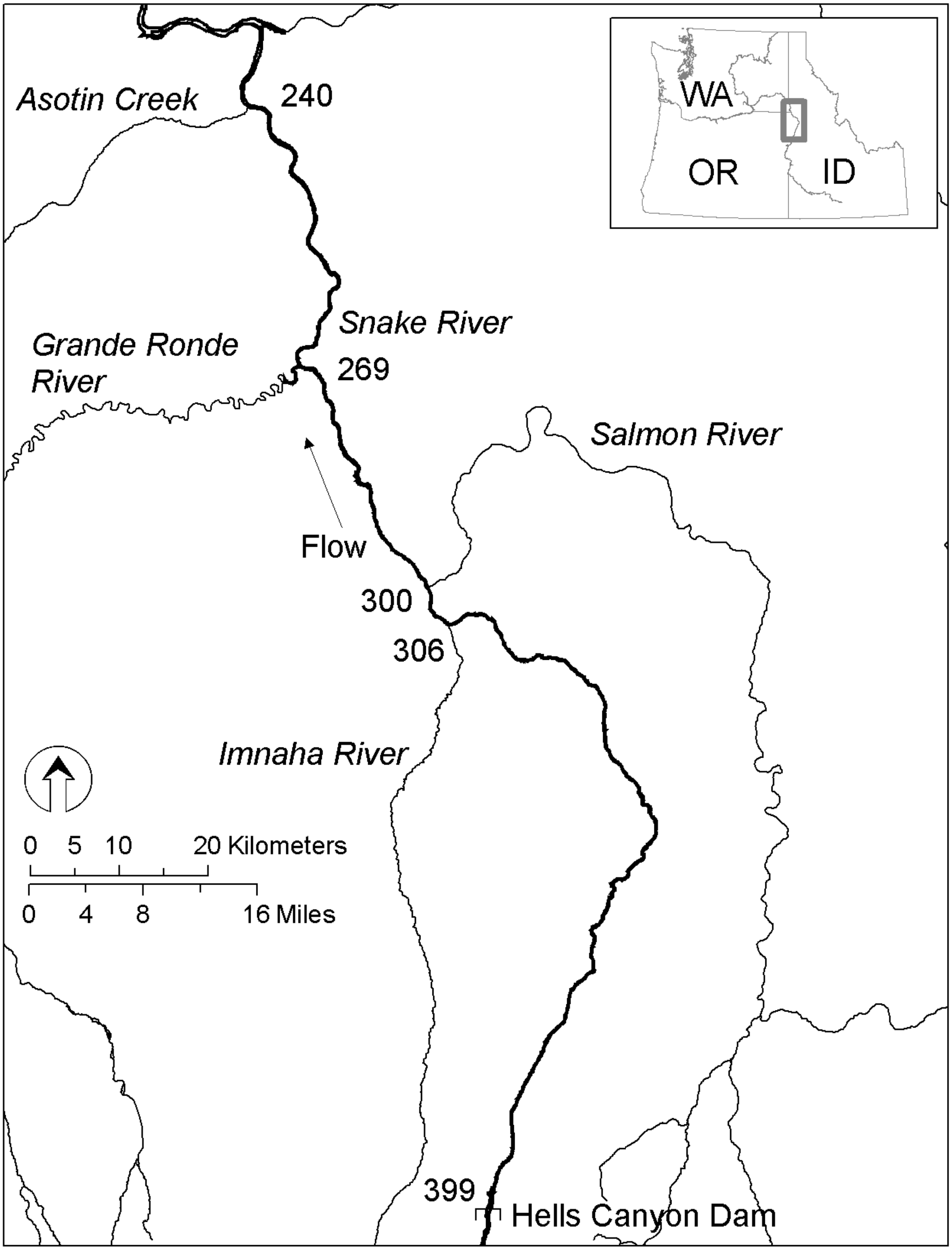

Figure 1

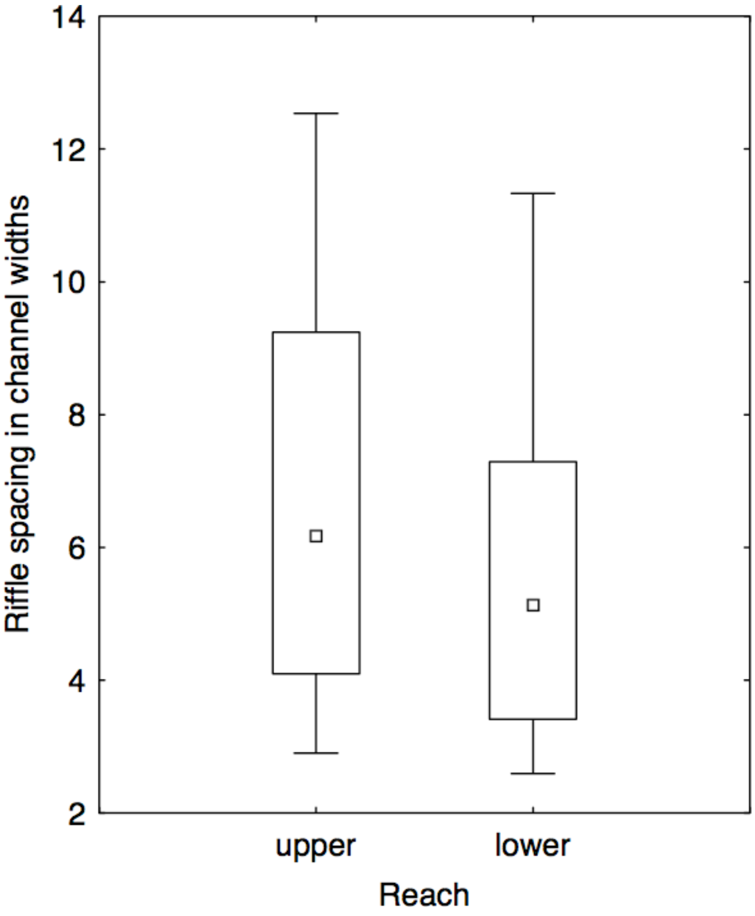
14
12
10
8
6
4
2
Riffle spacing in channel widths
upper
lower
Reach

Figure 2

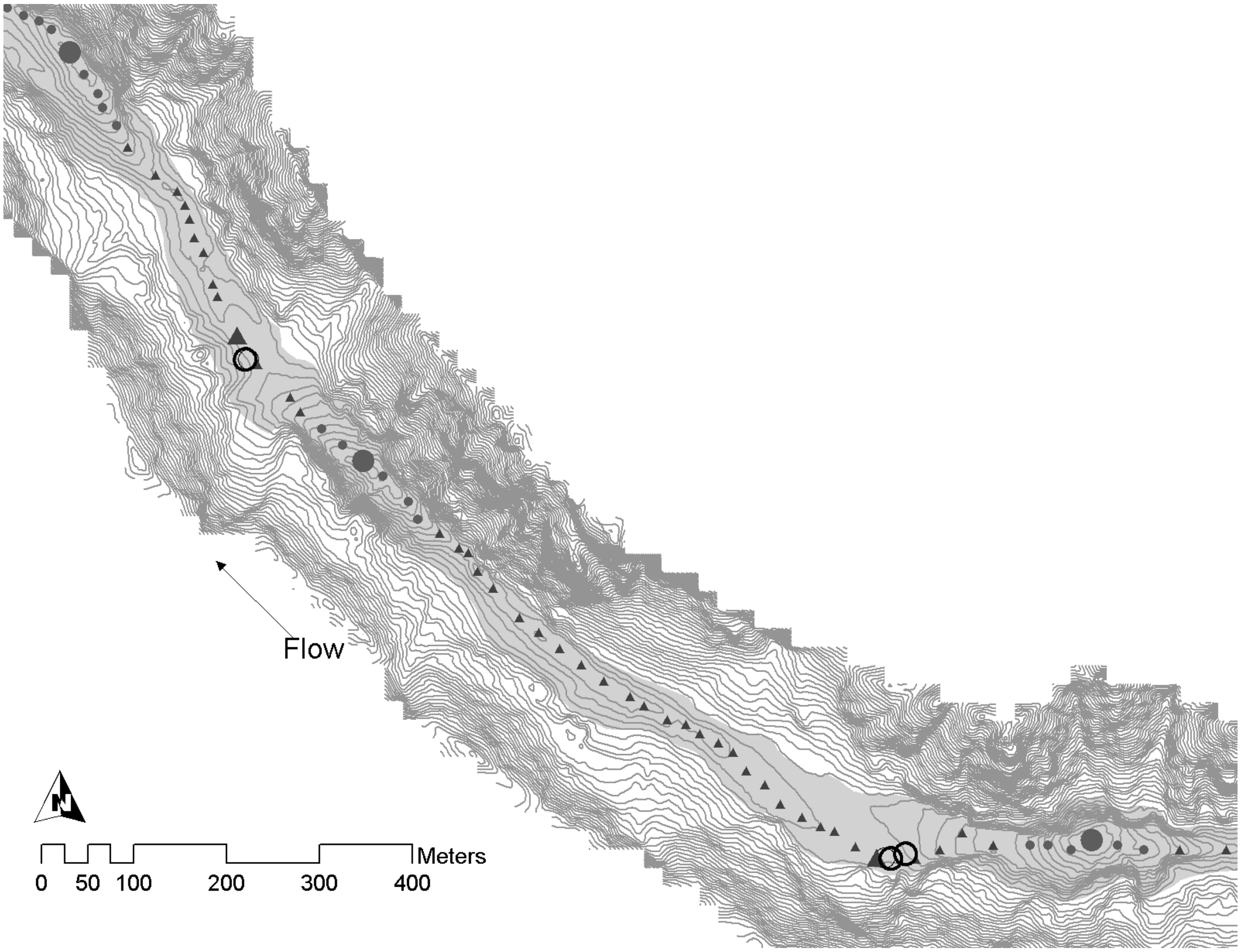

Figure 3

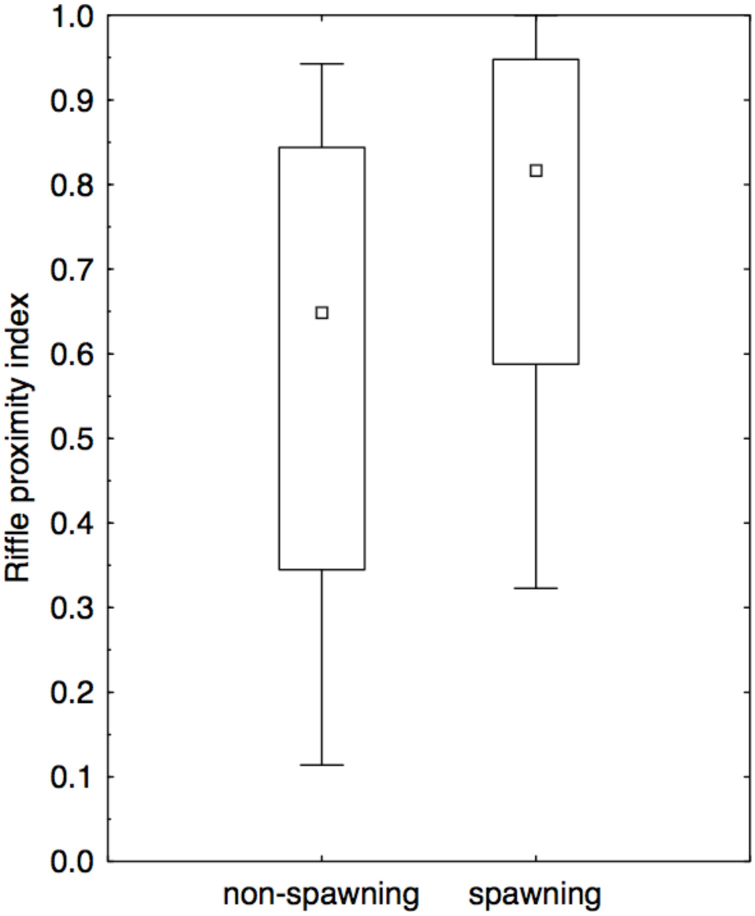
1.0
0.9
0.8
0.7
0.6
0.5
0.4
0.3
0.2
0.1
0.0
Riffle proximity index
non-spawning
spawning

Figure 4

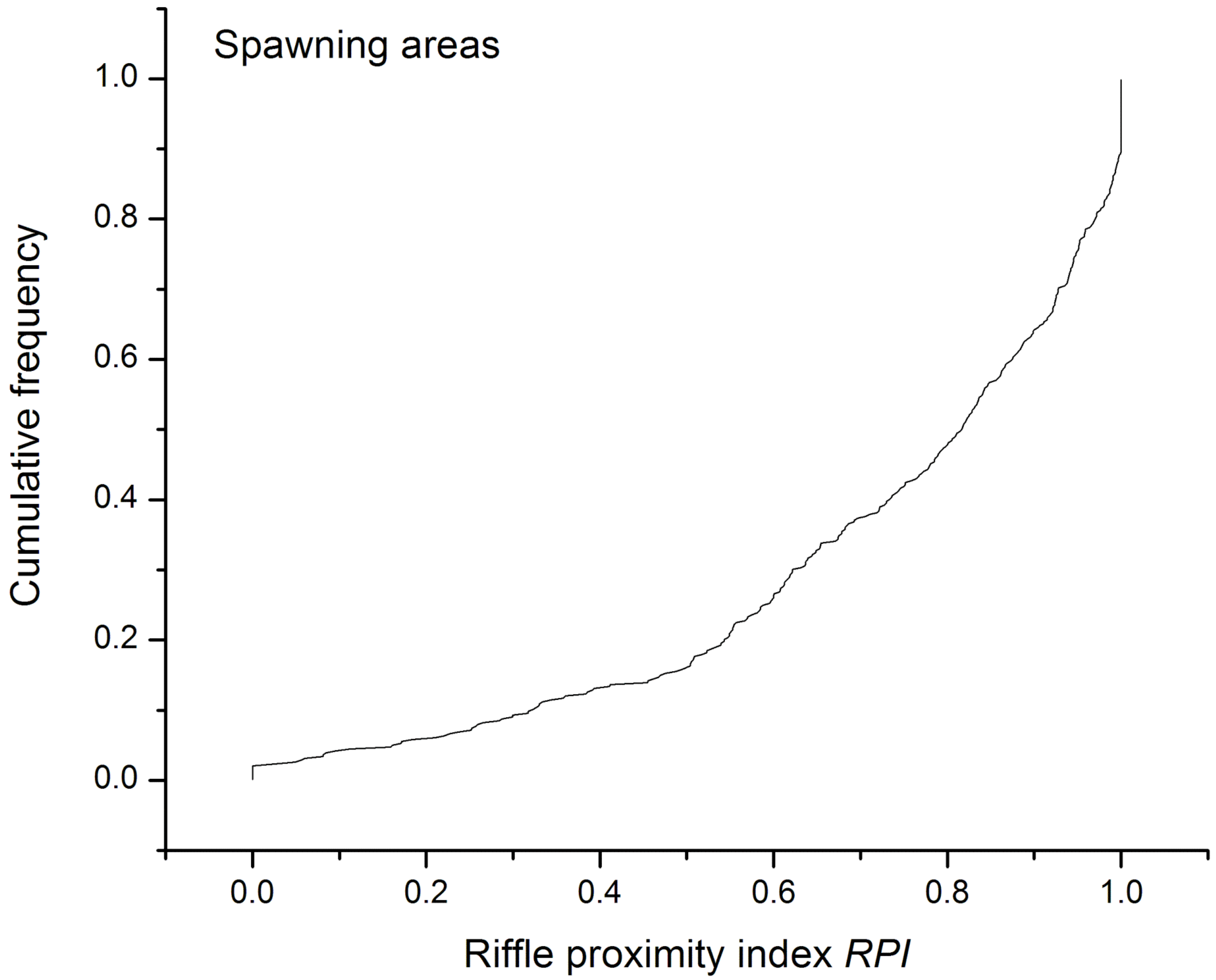
Spawning areas
Cumulative frequency
0.0
0.2
0.4
0.6
0.8
1.0
0.0
0.2
0.4
0.6
0.8
1.0
Riffle proximity index *RPI*

Figure 5

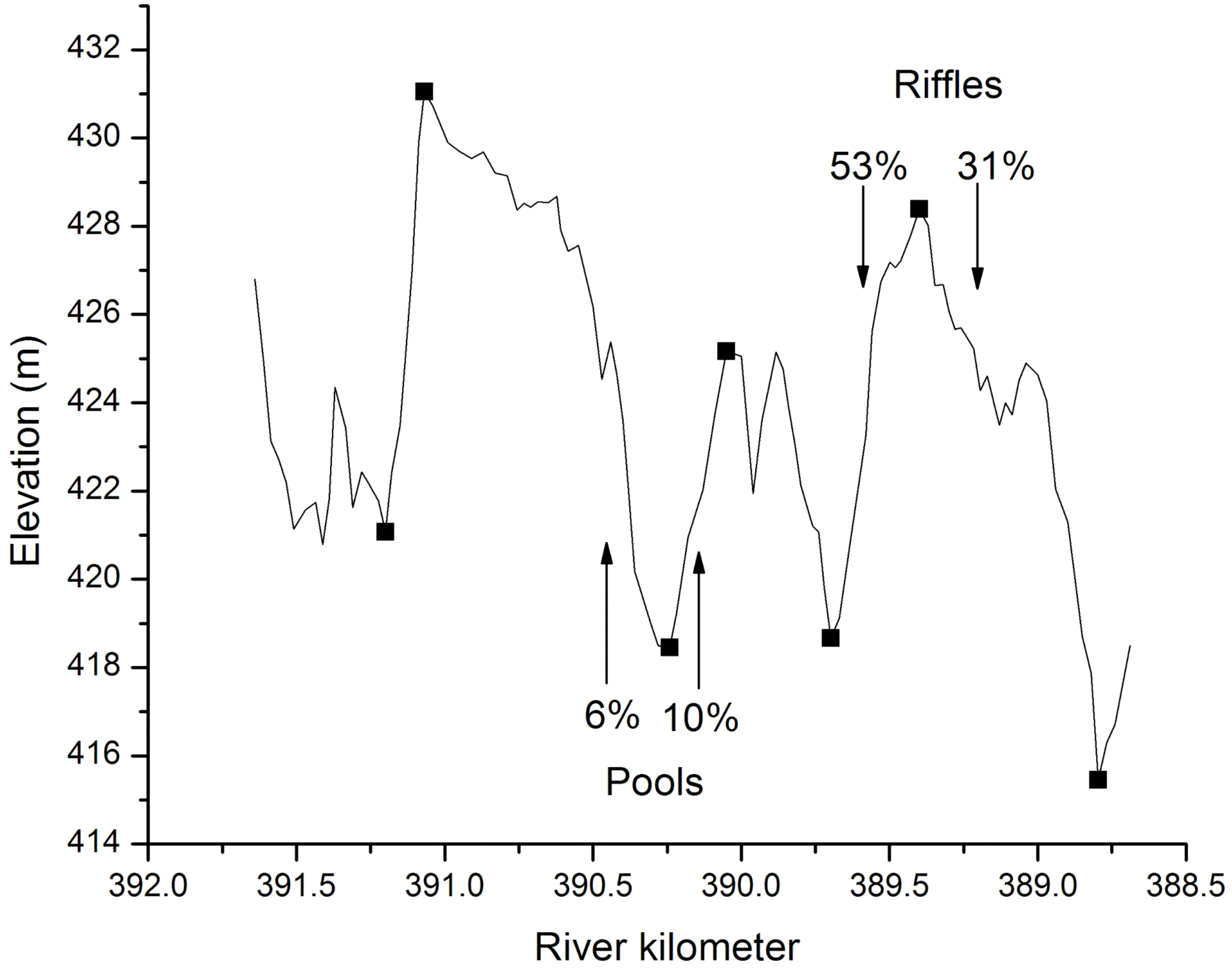

Riffles
53%
31%
6%
10%
Pools
Elevation (m)
432
430
428
426
424
422
420
418
416
414
392.0
391.5
391.0
390.5
390.0
389.5
389.0
388.5
River kilometer

Figure 6

MANUSCRIPT TWO

Full title:

Effects of river discharge on hyporheic exchange flows in a large gravel-bed river

Short title:

Hyporheic exchange flows

Author:

Timothy P. Hanrahan

Pacific Northwest National Laboratory

P.O. Box 999 MS K6-85

Richland, WA 99352

ph. 509.376.0972

tim.hanrahan@pnl.gov

Research sponsors:

U.S. Department of Energy and Idaho Power Company

Keywords:

hyporheic exchange; gravel-bed rivers; temperature

Abstract

The flow magnitude and timing from hydroelectric dams in the Snake River basin of the Pacific northwestern United States is managed in part for the benefit of salmon. The objective of this research was to evaluate the effects of current Hells Canyon Dam discharge operations on hydrologic exchange flows between the river and riverbed in Snake River fall Chinook salmon spawning areas. Interactions between river water and pore water within the upper 1 m of the riverbed were quantified through the use of self-contained temperature and water level data loggers suspended inside of piezometers. The data were recorded at 20 min intervals over a period of 200 days when the mean daily discharge was 218–605 $m^3 s^{-1}$, with hourly stage changes as large as 1.9 m. Differences in head pressure between the river and riverbed were small, often within ±2 cm. Measured temperature gradients in the riverbed indicated significant interactions between the surface and subsurface water. Neither hydraulic nor temperature gradients at most sites were significantly affected by either short- or long-term changes in discharge operations from Hells Canyon Dam. Only 2 out of 14 study sites exhibited acute flux reversals between the river and riverbed resulting from short-term, large magnitude changes in discharge. The findings suggest small-scale piezometric head differences play a minor role in the hydrologic exchange between the river and riverbed at the study sites. The processes controlling hydrologic exchange at the study sites are likely to be bedform-induced advective pumping, turbulence at the riverbed surface, and large-scale hydraulic gradients along the longitudinal profile of the riverbed. By incorporating the knowledge of hydrologic exchange processes into water management planning, regional agencies will be better prepared to manage the limited water resources among competing priorities that include salmon recovery, flood control, irrigation supply, hydropower production, and recreation.

Introduction

Like many other river systems throughout the world where salmon populations are imperiled (e.g., Pacific salmon (*Oncorhynchus* spp.) in western North America, and Atlantic salmon (*Salmo salar*) in eastern North America and Europe), the flow magnitude and timing from hydroelectric dams in the Snake River basin of the Pacific northwestern United States is managed in part for the benefit of salmon (Groves and Chandler, 1999; Gibbins and Acornley, 2000; Gibbins *et al.,* 2002; Hendry *et al.,* 2003; Berland *et al.,* 2004). One management tool under consideration by regional agencies in the Snake River basin is the manipulation of discharge operations from the Hells Canyon Complex of dams during some portions of the fall Chinook salmon (*O. tshawytscha*) incubation period (October – May). Under current dam operations, and beginning in mid-October, the discharge from Hells Canyon Dam is lowered and daily fluctuations are minimized to benefit spawning fall Chinook salmon within the mainstem Snake River. The period of low, stable discharge from Hells Canyon Dam terminates at the end of the fall Chinook salmon spawning period (early-December) and the discharge pattern reverts to large and variable discharge operations at an hourly time scale.

It has been hypothesized that modifying the current discharge operations of Hells Canyon Dam to include selective releases of upstream reservoir water may accelerate fall Chinook salmon egg incubation and growth (Connor *et al*., 2002). One potential mechanism for this effect of discharge operations on accelerated egg incubation and growth derives from ground water and surface water interactions observed in other salmon spawning areas. Previous research from salmon spawning areas indicated that decreases in river discharge may cause the hydrologic exchange between the river and riverbed to change from downwelling to upwelling (Geist, 2000; Soulsby *et al*., 2001; Malcolm *et al*., 2004). Assuming that the upwelling ground water is warmer than the river water during the egg incubation period, egg development and growth may be accelerated as a result of these hyporheic zone interactions.

Riverbed temperatures are a complex function of water and heat transfer processes at multiple spatial and temporal scales (Clark *et al.*, 1999; Brown *et al.*, 2005). The exchange of water between the open channel and the bed is ultimately controlled by potential hydraulic gradients and the hydraulic conductivity of the bed (Freeze and Cherry, 1979). At a small scale (e.g., several meters) these gradients may be created by small changes in bedform (Vittal *et al.*, 1977; Savant *et al.*, 1987; Thibodeaux and Boyle, 1987; Marion *et al.*, 2002). At the scale of pool-riffle sequences, changes in the longitudinal bed profile control exchange flows through the riverbed and banks (Harvey and Bencala, 1993; Hill *et al.*, 1998; Kasahara and Wondzell, 2003). Exchange flows at larger scales (e.g., reaches of multiple pool-riffle sequences) are controlled by valley morphology and physiography (Larkin and Sharp, 1992; Stanford and Ward, 1993; Fernald *et al.*, 2001). Heat transfer between surface water and the riverbed is realized through these exchange flows (i.e., advection) and in the absence of exchange flows through molecular diffusion processes (i.e., conduction) (Comer and Grenney, 1977; Sinokrot and Stefan, 1993; Hondzo and Stefan, 1994; Evans *et al.*, 1995; Clark *et al.*, 1999). Heat transfer through both advection and conduction is controlled by sedimentological properties of the riverbed material, including hydraulic conductivity, thermal conductivity, heat capacity, and thermal diffusivity (Stallman, 1965; Lapham, 1989; Silliman *et al.*, 1995).

While hydrological processes within riverbeds have become the subject of much research in recent years (White, 1993; Brunke and Gonser, 1997; Boulton *et al.* 1998; Jones and Mulholland, 2000), little effort has been directed at evaluating the effects of river discharge on the hydrologic exchange between the open channel and the riverbed. Some of the previous work has focused on the relationships between river discharge and storage zones (pools, eddies, hyporheic zones) in streams, including the extent and the rate of exchange between the open channel and these zones (Legrand-Marcq and Laudelot, 1985; D'Angelo *et al.*, 1993; Morrice *et al.*, 1997; Hart *et al.*, 1999; Wondzell, 2006). These efforts quantified the storage zone dynamics through the application of tracer injection experiments combined with solute transport models. These tracer methods result in estimates of reach-scale exchange rates between the open channel and storage zones, but are considered to be crude approximations of the mechanisms of hyporheic exchange, especially at finer scales (Worman *et al.*, 2002). Process based evaluations of the effects of river discharge on hydrologic exchange have been completed using ground-water flow models, wherein the focus has been on quantifying the reach-scale water budget components under changes in discharge (Wondzell and Swanson, 1996; Wroblicky *et al.*, 1998; Storey *et al.*, 2003). A limited number of empirical studies have evaluated the effects of river discharge on hydrologic exchange at finer scales, including at the scale of individual salmon redds, which are excavations of the riverbed surface by spawning salmon, wherein eggs are deposited in small depressions that are backfilled to protect incubating embryos. At the scale of individual salmon redds, reversals in hydraulic head gradients resulting from changes in discharge have been observed through physicochemical and hydraulic measurements in artificial redds and piezometers (Geist, 2000; Soulsby *et al.*, 2001; Malcolm *et al.*, 2004).

Because of the changes in Hells Canyon Dam discharge operations being considered by regional agencies in the Snake River basin, there is a need to evaluate the effects of river discharge on hydrologic exchange in Snake River fall Chinook salmon spawning areas. There are currently no empirical data quantifying the hydrologic exchange occurring during the fall Chinook salmon spawning and incubation periods within Hells Canyon. The limited number of empirical studies that evaluated the effects of river discharge on hydrologic exchange in salmon spawning areas were conducted in much different physical settings than the Snake River, encompassed just a few sites over a small longitudinal scale, and were based on discrete sampling events rather than continuous, long-term sampling (Geist, 2000; Soulsby *et al.*, 2001; Malcolm *et al.*, 2004). Therefore, it is unknown to what extent the findings from those studies can be used as analogues to predict the hydrologic exchange characteristics in Snake River fall Chinook salmon spawning areas. In general, the effects of hydrological variability on the dynamic nature of the hyporheic zone must be quantified if the controls on egg development and growth are to be fully understood (Soulsby *et al.*, 2001).

The purpose of this research was to evaluate the effects of current Hells Canyon Dam discharge operations on hydrologic exchange flows in Snake River fall Chinook salmon spawning areas. The research hypothesis was that hydrologic exchange, as indicated by temperature and hydraulic gradients, would be inversely related to river discharge. Specific objectives were to: (1) quantify the vertical hydraulic and temperature gradients within the upper 1 m of the riverbed, and (2) quantify the relationship between river discharge and the vertical hydraulic and temperature gradients.

Methods

Study area

This research was conducted throughout 160 km of the Hells Canyon reach (HCR) of the Snake River, located in the Pacific Northwest United States of America. The HCR extends from Hells Canyon Dam (river kilometer (rkm) 399) downstream to Asotin Creek near rkm 240 (Figure 1). This reach of the Snake River is narrowly confined by valley walls, and is generally controlled by large-scale geologic and geomorphic controls, resulting in a lack of floodplain development. The upper section of the HCR (rkm 399–306) is situated in a deep and narrow gorge entrenched in erosion-resistant basalt and metamorphic bedrock. Although when viewed in planform the HCR exhibits a meandering course, geomorphically it is a straight or slightly sinuous river. The river possesses the characteristics of passive meandering, where the planform pattern is imposed by the local landform. While large alluvial terraces exist along the river, they are remnant deposits of the Pleistocene Lake Bonneville Floods, and are located tens of meters above contemporary flood stages (O’Connor, 1993). Alluvial deposits within the bankfull channel from these and other flood events are actively reworked by the contemporary flow regime, resulting in a longitudinal pool-riffle bedform morphology, despite the valley confinement. Due to the lack of floodplain development, interactions between the river and its banks are limited to small lateral bars, terraces, and fans inundated by contemporary flow regimes. The lower HCR (rkm 306–240) exhibits more floodplain development than the upper HCR, owing mostly to a geologic fault zone near rkm 306 and the influence from three major tributaries – the Imnaha River at rkm 307, the Salmon River at rkm 300 and the Grande Ronde River at rkm 269. However, even the lower HCR is considered narrowly confined within the valley walls.

The Hells Canyon Complex (Hells Canyon, Oxbow, and Brownlee dams) controls nearly all of the flow through the upper HCR, and just over 50% of the flow in the lower HCR. Immediately downstream from Hells Canyon Dam at U. S. Geological Survey (USGS) gage 13290450, mean daily discharge has averaged 589 $m^3 s^{-1}$ since 1965. Over this same time period, mean daily discharge in the lower HCR has averaged 1035 $m^3 s^{-1}$ (USGS gage 13334300, rkm 269). Inputs from the Imnaha, Salmon and Grande Ronde rivers (USGS gages 13292000, 13317000, and 13333000, respectively) during this period make up a mean daily discharge of 426 $m^3 s^{-1}$, resulting in a residual input of approximately 20 $m^3 s^{-1}$ from tributaries between Hells Canyon Dam (rkm 399) and the Imnaha River confluence (rkm 307). From mid-October to early-December, the Hells Canyon Complex maintains low and stable hourly discharges (e.g., 255 $m^3 s^{-1}$) for the benefit of spawning fall Chinook salmon. During the remainder of the year, power peaking operations cause large daily fluctuations in discharge (240–800 $m^3 s^{-1}$), resulting in stage changes of over 2.0 m in the upper HCR.

Study sites were selected by stratified random sampling of fall Chinook salmon spawning locations. The HCR was stratified into three segments based on longitudinal valley slope and the confluence with major tributaries. The upper segment extends from Hells Canyon Dam (rkm

399) downstream to a fault zone near Pine Bar (rkm 364), and has a longitudinal slope of 0.002. The middle and lower segments are separated just downstream of the Salmon River confluence (near rkm 298), where the longitudinal gradient changes from 0.001 (middle segment) to 0.0007 (lower segment). Fall Chinook salmon redd counts from 1997 to 2001 were used to identify the 56 most used spawning sites (Garcia *et al.*, 2003). Of the 56 spawning sites, 20% were in the upper segment, 48% in the middle segment, and 32% in the lower segment. Fourteen study sites (25% of the total) were randomly selected, with the number in each segment corresponding to the proportion of spawning sites within each segment (Figure 1). The physical characteristics at each site include channel widths ranging from 70 to 270 m, depths ranging from 0.3 to 2.5 m, velocities ranging from 0.5 to 1.5 m s^{-1}, and median riverbed surface grain sizes ranging from 32 to 60 mm (TP Hanrahan, unpublished data; Miller *et al.*, 2002). Despite the variability in physical characteristics among the study sites, all the sites were located in areas of the channel characterized as pool tailouts, wherein the riverbed elevation is locally increasing in the downstream direction (Hanrahan, in review a).

Site-scale study design

Hyporheic exchange at each site was quantified through the use of self-contained temperature and water level data loggers (Solinst model 3001 mini LT Levelogger M10) suspended inside of piezometers. Each site contained one cluster of two piezometers and one river standpipe spaced within 1.0 m of one another. One piezometer monitored the shallow hyporheic zone (30 cm) while the other monitored the deeper hyporheic zone (60 cm). Each piezometer consisted of a 31.0 cm length of well screen with a 3.2 cm inside diameter. The screen was welded on one end to a 12.0 cm solid drive point and welded on the other end to a variable length section of unscreened stainless steel pipe. The river standpipe was constructed from an unscreened section of galvanized pipe threaded at one end onto a solid drive point and on the other end to an 18.0 cm section of PVC screen open to the river. The piezometers were driven into the riverbed until the top of one piezometer screen reached approximately 30.0 cm below the riverbed surface (average 30.5 cm) and the other piezometer screen reached approximately 60.0 cm below the riverbed surface (average 60.4 cm). The river standpipe was driven into the riverbed until the top of the PVC screen was approximately 20.0 cm above the riverbed surface (average 20.9 cm). The elevations of the piezometers and the standpipe were surveyed relative to local arbitrary benchmarks using differential leveling. Relative elevations were surveyed from multiple stations until the differences among the results from three stations did not exceed 0.2 cm.

Data loggers were suspended inside the pipes by non-stretch stainless steel cable attached to a water-tight cap at the top of the pipe. The temperature and pressure sensor end of the data loggers was placed near the top of the piezometer screens. Data loggers were programmed to record temperature and absolute pressure (cm of water) every 20 min. Four additional Solinst data loggers were distributed throughout the entire study area to record atmospheric pressure at the same time intervals. Atmospheric pressure was subtracted from the absolute pressure readings in the piezometers to determine the gage pressure (cm of water) due to river stage changes every 20 min. According to calibration certificates provided by the data logger manufacturer, the instruments are accurate to ± 0.1 °C and ± 0.7 cm of water. The data loggers were deployed in October 2002 and retrieved in March 2003.

Additional temperature data were acquired from each site through placement of self-contained temperature data loggers (Onset Water Temp Pro) in artificial egg pockets. Three artificial egg pockets, spaced 3–5 m apart, were created at each site. Each egg pocket was dug within a 1.0 m diameter PVC standardizing template using a hydraulic pump and hand tools. Egg pockets were excavated until the bottom of the egg pocket was approximately 25.0 cm (average 23.0 cm) beneath the riverbed surface, which is within the range (19–37 cm) of Chinook salmon egg pocket depths in the Columbia River (Chapman, 1988). On 18 November

2002, near the peak of fall Chinook salmon spawning activity, one self-contained temperature data logger was placed inside of a perforated PVC tube (30.0 cm length x 3.2 cm i.d.) and buried within each egg pocket. Temperature data loggers were programmed to record at 20 min time intervals until they were retrieved near the end of the egg incubation period in March 2003. According to calibration certificates provided by the temperature data logger manufacturer, the instruments are accurate to ±0.17°C. The methods used to deploy the egg pocket temperature loggers precluded surveying their relative elevation. Data from these instruments were not used in the numerical modeling described below.

The vertical hydraulic gradient (*VHG*) at each site was determined from the gage pressure readings as

$$VHG = \frac{dh}{L} \qquad (1)$$

where *dh* is the hydraulic head (cm) inside the piezometer minus the hydraulic head (cm) of the river, and *L* is the distance (cm) from the top of the piezometer screen to the riverbed surface. The *VHG* represents a potential for upwelling from the hyporheic zone (positive *VHG*) or downwelling into the hyporheic zone (negative *VHG*). Analyses of hydraulic gradients between the river and riverbed were primarily based on *dh* values. The *dh* values were used so that hydraulic gradients could be evaluated relative to the uncertainty error of the instruments (±1.4 cm), which does not vary over the range of depths for which they were used in this study.

The effects of discharge on vertical hydrologic exchange between the river and riverbed were evaluated through measured temperature gradients between the river and riverbed, and the application of a numerical model. Lapham (1989) presented an explicit finite-difference approximation to Stallman's (1965) equation describing the steady, one-dimensional, vertical flow of fluid and heat through homogenous, porous media. Lapham's equation was used in the software Mathcad to model the shallow hyporheic zone temperature as

$$T_{i,n+1} = \frac{k\Delta t}{\rho c \Delta z^2}\left(1 + \frac{\rho_w c_w v_z \Delta z}{2k}\right)T_{i-1,n} + \frac{k\Delta t}{\rho c \Delta z^2}\left(1 - \frac{\rho_w c_w v_z \Delta z}{2k}\right)T_{i+1,n} + \left(1 - \frac{2k\Delta t}{\rho c \Delta z^2}\right)T_{i,n} \qquad (2)$$

where $T_{i,n+1}$ = temperature at node i (shallow hyporheic zone) at time step n+1; $T_{i-1,n}$ = temperature at node i-1 (river) at time step n; $T_{i+1,n}$ = temperature at node i+1 (deep hyporheic zone) at time step n; $T_{i,n}$ = temperature at node i at time step n; Δt = time increment (s) between steps; Δz = spacing (cm) between nodes; k = thermal conductivity (cal s^{-1} cm °C) of the rock-water matrix; ρ = wet bulk density (g cm^{-3}) of the rock-water matrix; ρ_w = density of water (g cm^{-3}); c = specific heat capacity (cal cm^{-3} °C) of the rock-water matrix; c_w = specific heat capacity (cal cm^{-3} °C) of the water; v_z = vertical component of Darcian water velocity (cm s^{-1}).

At every 20-min time step, equation (2) was used to estimate the temperature in the shallow hyporheic zone given the time-varying upper thermal boundary condition of the river temperature and the lower thermal boundary condition of the deep hyporheic zone temperature (Lapham, 1989; Hunt *et al.*, 1996; Anderson, 2005). The magnitude and direction of vertical flux (i.e., apparent Darcy velocity v_z) between the river and the riverbed was determined by adjusting v_z until the model-simulated shallow hyporheic zone temperature matched the observed temperature at the same depth and over time. Because this model assumes that water flow occurs under steady-state conditions, the v_z value was not adjusted at every time step. Rather, the v_z was held constant for periods of days to weeks until there was a relatively large deviation between modeled and observed temperatures. At that point, v_z was adjusted until modeled temperatures again closely matched observed temperatures. The matching of modeled and observed temperature was done by trial-and-error, using time-series plots of the two temperatures and minimizing the mean absolute error (*MAE*) over time. The root mean-squared error (*RMSE*) was used to identify model runs where the average prediction error was especially large at some time steps.

The application of equation (2) required estimates of the physical and thermal properties of the riverbed materials. Estimates of the grain size distribution of the riverbed material were derived from the results of freeze coring at sites 152.3 and 222.7 (Arntzen *et al.*, 2001), which represent the range of grain sizes at all the study sites. Characteristic particle sizes (d_i) from these distributions were a d_{10} range of 0.5–3.0mm and a d_{60} range of 40.0–95.0mm (where d_i is the grain size in mm at which i% of the sample is finer than). The porosity λ of the riverbed was estimated using the empirical relation (Schalchli, 1995)

$$\lambda = 0.486 \cdot \left(\frac{d_{60}}{d_{10}} \right)^{-0.20} \tag{3}$$

Particle densities ρ_p ranging from 2.65 g cm^{-3} to 2.80 g cm^{-3} were used in the following relation to estimate dry bulk density ρ_b (Fetter, 1994)

$$\lambda = 100\left[1 - \left(\frac{\rho_b}{\rho_p} \right)\right] \tag{4}$$

The resulting dry bulk densities ranged from 2.01 g cm^{-3} to 2.23 g cm^{-3}. Using Figure 2 in Lapham (1989) these dry bulk densities correspond to thermal conductivity *k* values of 0.007–0.0088 cal s^{-1} cm °C and volumetric heat capacity (*cρ*) values of 0.53–0.56 cal cm^{-3} °C. Initial model runs were insensitive to this small range in *k* and *cρ*, so constant values were chosen. Because the *k* and *cρ* values in Lapham (1989) are based on empirical relationships with reconstituted mixtures of much smaller grain sizes (Lunardini, 1981) than the present study, it was necessary to adjust the k and $c\rho$ values to correspond to a higher dry bulk density. The final values used for all model runs include k = 0.0112 cal s^{-1} cm °C, ρ = 2.9 g cm^{-3}, ρ_w = 1.0 g cm^{-3}, $c\rho$ = 0.51 cal cm^{-3} °C, and c_w = 1.0 cal cm^{-3} °C.

For those sites where the solution to equation (2) resulted in large estimates of downward flux (positive v_z), the solutions were compared with those obtained from an alternative procedure. Stallman's (1965) equation describing the steady, one-dimensional, vertical flow of fluid and heat through homogenous, porous media can be approximated as a travel time model:

$$v_z = V_T\left(\frac{\rho \cdot c}{\rho_w \cdot c_w}\right) \tag{5}$$

where V_T is the measured vertical velocity of the temperature peak (Constantz and Thomas, 1996). Application of equation (5) requires meeting the assumption of nonisothermal, downward flow of water into the streambed at a sufficient velocity such that conductive heat transport is negligible relative to advective heat transport. Thus, equation (5) was only applied to the sites meeting this assumption.

Results

The hydrologic regime during the 2002–2003 sampling period exhibited one of the lowest, most stable daily discharge patterns of any of the previous twelve water years (Figure 2). The median daily discharge (Q50) during this period was 310 m^3 s^{-1}, which was 210 m^3 s^{-1} lower (or 40% less) than the mean Q50 of the twelve previous water years. The hydrographs indicate two distinct discharge regimes during this time of the water-year, including stable and variable discharge periods. The stable discharge period extended from 20 October 2002 – 7

January 2003, while the variable discharge period extended from 8 January 2003 – 2 March 2003 (Figure 2).

Large temporal scale hydraulic gradients

The hydraulic gradients between the river and the riverbed (shallow hyporheic zone) suggested the potential for predominantly small magnitude upwelling and downwelling vertical exchange. During the stable discharge period, 10 of the 14 sites had a mean hourly difference in head pressure (*dh* in cm; hyporheic - river) within a ± 2.0 cm range. During the variable discharge period, 9 of the 14 sites had a mean *dh* within a ± 2.0 cm range (Figure 3). Within each site there was little change in mean *dh* between time periods. Between the stable and variable discharge periods the difference in mean *dh* was less than 1.0 cm at 11 of the 14 sites, with an average change of 0.4 cm for those sites. Study sites 149.2, 156.8, and 198.8 exhibited a change in mean *dh* of 1.7 cm, 2.1 cm, and 1.5 cm, respectively, between the stable and variable discharge periods. While mean *dh* did not change much between time periods, the range in *dh* changed between the low, stable discharge period and the variable discharge period (Figure 3).

The vertical hydraulic gradients (VHG) between the river and shallow hyporheic zone, as well as between the river and deep hyporheic zone, showed little relationship to changes in river discharge at most sites. At the large temporal scale, most sites exhibited small effects of river discharge on VHG between the low, stable discharge period and the variable discharge period (Figure 4). Sites 149.2, 156.8, and 198.8 indicated marked changes in shallow hyporheic zone VHG between the low, stable discharge period and the variable discharge period. At all three sites, the upwelling potential increased. During the low, stable discharge period, 12 of the 14 study sites indicated small upwelling potential between the river and deep hyporheic zone (Figure 4). As discharge increased and became more variable, only site 156.8 showed a marked change (increase) in VHG between the river and deep hyporheic zone.

Small temporal scale temperature and hydraulic gradients

At a finer temporal scale (3–4 days), vertical temperature and hydraulic gradients also suggest small effects of changes in river discharge on vertical hydrologic exchange. During the low, stable discharge period, sites with relatively larger upwelling potential (Figure 4) also had larger vertical temperature gradients. For example, site 149.2 had a vertical temperature gradient of nearly 1.8 °C between the river and deep hyporheic zone (Figure 5), while the temperature gradient at site 196.0 was approximately 0.3°C (Figure 6). The difference in head pressure (*dh*) between the river and shallow hyporheic zone varied over a range of several centimeters even during this period of low, stable discharge (Figures 5 and 6). During the period of increased magnitude and variation in discharge, sites with relatively larger upwelling potential (especially from the deep hyporheic zone, Figure 4) retained larger vertical temperature gradients. For example, all of the sites in the lower segment (148.5–156.8) had an upwelling potential from the deep hyporheic zone, and maximum temperature gradients greater than 2°C during the 4 day period of fluctuating discharge (e.g., 152.3, Figure 7). In contrast, sites with a strong downwelling potential (e.g., 196.0 and 244.5, Figure 4) had maximum temperature gradients of 0.3–0.5°C during the 4 day period of fluctuating discharge (e.g., 196.0, Figure 8). At all sites, there was a small temperature gradient between the river water and the artificial egg pocket.

During the period of increased magnitude and variation in discharge, only 3 of the 14 sites (198.8, 211.9, and 218.7) exhibited a pronounced effect of changing river stage on hydraulic and temperature gradients. At site 198.8, as river stage increased upwelling potential increased, resulting in a slight increase in hyporheic zone temperatures (Figure 9). At site 211.9, an increase in river stage caused downwelling hydraulic gradients, resulting in a marked decrease in hyporheic zone temperatures (Figure 10). Site 218.7 exhibited a pronounced effect of changing river stage on hyporheic zone temperatures (Figure 11). As river stage increased at site 218.7, hyporheic zone temperatures decreased. Egg pocket temperatures were unaffected by the increased magnitude and variation in discharge, as the temperature gradient between the river and artificial egg pocket remained small during this period.

Numerical modeling of apparent velocity

Despite the relatively small vertical hydraulic gradients at most sites, the results from the numerical modeling of apparent velocity (v_z) and hyporheic zone temperatures suggest that there was significant vertical hydrologic exchange during all time periods. During the period of low, stable discharge 12 of the 14 study sites exhibited a downward flux of surface water entering the riverbed. The apparent velocity of pore water at these sites was 0.2–5.4 cm h^{-1} (Table 1). During the period of increased magnitude and variability of discharge, the apparent velocity at 8 of the 14 sites was a downward flux of 0.2–2.9 cm h^{-1} (Table 1).

The results from the numerical model suggest that the hydrologic interactions between the river and the riverbed at most sites was largely unaffected by changes in hydrologic regime. At the large temporal scale (i.e., weeks to months) only 3 of the 14 sites (196.0, 211.9 and 219.3) displayed a reversal in flux direction resulting from the change in hydrologic regime (i.e., when the discharge pattern changed from low and stable to high and variable) (Table 1). Sites 211.9 and 219.3 displayed a change in flux from slight downwelling to stronger upwelling as a result of the increased magnitude and variability in discharge (Table 1). Site 218.7 experienced acute changes (i.e., hourly) in flux direction resulting from the change in hydrologic regime. However, at the large temporal scale the shallow hyporheic zone temperatures suggested a trend toward a constant upward flux of 0.9 cm h^{-1} (Table 1). An additional 2 of the 14 sites (156.8 and 198.2) displayed small changes in the magnitude of flux as a result of the change in hydrologic regime (Table 1). During the period of increased discharge the downward flux increased slightly at site 156.8 and decreased slightly at site 198.2. For the remaining 7 of the

14 study sites shallow hyporheic zone temperatures were accurately predicted by using a constant value of apparent velocity for the entire study period (Table 1).

The accuracy of the model predictions were evidenced by the average prediction error (*MAE*), which was within the accuracy of the temperature sensor (±0.1 °C) for all sites and time periods, except one (Table 2). Estimates of apparent velocity from the numerical model matched well with those from the time travel model (Table 2). Time-series plots of observed and predicted temperatures also suggest that the numerical model adequately characterized the hydrologic exchange at most sites. At 12 of the 14 study sites, predicted shallow hyporheic zone temperature closely matched the observed temperature (e.g., site 222.7, Figure 12). At the remaining two sites (211.9 and 218.7), the numerical model accurately predicted the average temperature trend of the shallow hyporheic zone, but did not account for the rapid changes in shallow hyporheic zone temperature that were clearly a result of short-term changes in river stage (Figures 13 and 14, respectively). For example, at site 211.9 the long-term temperature trend of the shallow hyporheic zone reflects a change in apparent velocity from downwelling to upwelling as the hydrologic regime changes from low and stable to high and variable. However, at the hourly time scale, acute increases in river stage clearly cause the flux direction to reverse to downwelling (Figure 10). A similar acute flux reversal from upwelling to downwelling is also evident at site 218.7 (Figure 11). The combined results of temperature monitoring and numerical modeling indicate that only two sites (211.9 and 218.7) are significantly affected by short-term (hourly to daily) large magnitude changes in discharge.

Discussion

The results from this study suggest that at most Snake River fall Chinook salmon spawning areas there is a negligible effect of Hells Canyon Dam discharge operations on vertical hydrologic exchange. At both the large and small temporal scales, the *VHG* between the river and shallow hyporheic zone, as well as between the river and deep hyporheic zone, showed little relationship to changes in river discharge at most sites. At only two sites (211.9 and 218.7) was the vertical hydrologic exchange significantly affected by short-term (hourly to daily) large magnitude changes in discharge. At both these sites the hydrologic exchange was inversely related to river discharge, as large changes in river stage caused the exchange flux to reverse from upwelling to downwelling. The flux reversals at these two sites resulted in significant short-term changes in hyporheic zone temperatures, whereas at the remaining sites hyporheic zone temperatures were largely unaffected by changes in river discharge.

Two factors may cast uncertainty on the conclusion of negligible effects of river discharge on vertical hydrologic exchange at most study sites. The first is that the measured *dh* at most sites was small in magnitude, approaching the measurement error of the pressure transducers in the instruments (approximately ±1.4 cm). Thus, it is possible that I was unable to detect the effects of river discharge on hydraulic gradients at those sites where the measured *dh* was within the range of the instrument measurement error. However, because the measured vertical temperature gradients at most sites also showed negligible effects of changing river discharge, I am confident in concluding that the vertical hydraulic gradients at most sites were also minimally affected by changing river discharge. The second factor of uncertainty regarding this conclusion is that the empirical data used in this study were collected during an unusually low water year. Thus, it is possible that any effects of river discharge on hydrologic exchange would be different during more “normal” or high water years. While the magnitude of hydrologic exchange may be different during other water year types, it is unlikely that the relationship between river discharge and hydrologic exchange would be different than the findings presented in this paper. An exception would be during very high water years where the river discharge is large enough to significantly change the hydraulic interactions among the river, riverbed, and river banks at the scale of several pool-riffle sequences. The changes in river stage during the study period were as large as 1.1–1.9 m among the study sites, which was large enough to induce measurable changes in hydraulic gradients were they to occur.

Although the local vertical hydraulic gradients were rather small, the measured temperature gradients in the hyporheic zone indicated significant interactions between surface and subsurface water. This finding suggests that local differences in hydrostatic pressure (i.e., as measured by small-scale piezometric head differences) play a minor role in the hydrologic exchange between the river and riverbed. The processes controlling this hydrologic exchange are likely to be bedform-induced advective pumping, turbulence at the riverbed surface, and large-scale piezometric gradients along the longitudinal profile of the riverbed. The mobile riverbed at all of the study sites allows the development of local undulations of the riverbed surface, including those caused by spawning Chinook salmon (i.e., redd pits and tailspills) as well as by local bed scour and deposition. These bedforms promote advective pumping exchange between the river and riverbed, whereby the acceleration of flow over the bedform and flow separation at the crest create localized pressure variations that induce flow into and out of the bed (Savant *et al*., 1987; Elliott and Brooks, 1997a). Even in the absence of bedforms, exchange between surface water and flat gravel riverbeds has been observed (Nagaoka and Ohgaki, 1990; Shimizu *et al*., 1990). The mechanism of this exchange has been described as turbulent momentum transfer across the river–riverbed interface (Zhou and Mendoza, 1993; Packman *et al*., 2004). Packman *et al*. (2004) also observed advective transport on flat gravel beds, which was induced by bed surface irregularities as small as one grain diameter. The magnitude of exchange with bedforms and flat beds scales with the Reynolds number based on sediment grain diameter (Packman *et al*., 2004). Because all of the study sites have coarse bed surfaces (d_g of 24–80 mm) and high surface water velocities (0.4–1.4 m s^{-1}) (TP Hanrahan, unpublished data), it is likely that advective pumping and turbulent diffusion are major processes controlling hydrologic exchange between the river and the upper

1 m of the riverbed. This is particularly evident at the depth of artificial egg pockets, where the temperatures were nearly isothermal with the river water.

The processes of advective pumping and turbulent diffusion at the study sites are likely complemented by the hydrologic exchange occurring at the larger scale of the pool–riffle sequences. Because of the high longitudinal bed slope at the upper and middle sites, and the geomorphically-confined nature of the river corridor, the upstream–downstream piezometric gradients likely contribute significantly to the surface–subsurface exchange (Castro and Hornberger, 1991; Larkin and Sharp, 1992; Harvey and Bencala, 1993). Similarly, all the sites were located in areas of the channel characterized as pool tailouts or the upstream side of riffles, wherein the riverbed elevation is locally increasing in the downstream direction (Hanrahan, in review). At the scale of pool-riffle sequences, changes in the longitudinal riverbed profile control exchange flows through the riverbed and banks (Larkin and Sharp, 1992; Stanford and Ward, 1993; Fernald *et al.*, 2001), whereby surface water flows into the riverbed along pool tailouts and the upstream face of riffles. These larger-scale piezometric gradients controlled by the channel morphology likely become the dominant exchange process with increasing depth into the riverbed, where the horizontal flow component can be more significant than vertical flow (Saenger, 2002).

Because of the physical characteristics of the Hells Canyon reach of the Snake River, the hydrologic exchange processes observed at the study sites are likely more analogous with high gradient, geomorphically-confined mountain rivers than with lower gradient rivers adjacent to expansive floodplains. In the Hells Canyon reach of the Snake River, and in other rivers within similar physical settings, the ground water component of the hydrologic exchange likely derives largely from an alluvial aquifer beneath the riverbed. In large gravel-bed rivers with adjacent floodplains, the ground water component of the hydrologic exchange derives largely from an adjacent floodplain aquifer (Triska *et al.*, 1989; Larkin and Sharp, 1992; Winter *et al.*, 1998). The high longitudinal riverbed gradient of the Hells Canyon reach of the Snake River, and the pool-riffle morphology, dictates that hydrologic exchange in fall Chinook salmon spawning areas is controlled longitudinally and is much less susceptible to flux reversals resulting from discharge changes. This is because the longitudinal hydraulic gradients are likely always larger than the lateral hydraulic gradients in the riverbanks. It is likely that salmon spawning areas in low-gradient, floodplain rivers are more susceptible to flux reversals resulting from discharge changes because the floodplain aquifer exerts a lateral control on the hydrologic exchange, wherein the lateral hydraulic gradient may be greater than the longitudinal hydraulic gradient. Given the context of these hydrologic controls, the findings reported in this paper are more comparable with other gravel-bed rivers in similar physical settings regardless of river size, than with other large gravel-bed rivers in different physical settings.

The results reported in this paper suggest that at most of the study sites there is a negligible effect of river discharge on vertical hydrologic exchange. During the periods of low, stable discharge and high, variable discharge the measured shallow hyporheic zone temperatures at most sites could be accurately modeled with a constant estimate of apparent velocity. At most sites, acute changes in river discharge had a small effect on measured *VHG*. In many cases, the measured head differences approached the measurement error of the equipment (approximately ±1.4cm). At most of the sites with a measurable relationship (positive or negative) between river stage and *VHG*, the resulting effect was a very small or nonexistent change in bed temperature. Similar observations of the negligible effect of river stage on exchange flux have resulted from modeling (Storey *et al*., 2003) and field studies (Lenk and Saenger, 2000; Wondzell, 2006).

The combined results of temperature monitoring and numerical modeling indicated that at only two sites (211.9 and 218.7) was the vertical hydrologic exchange significantly affected by short-term (hourly to daily) large magnitude changes in discharge. At both of these sites, a large increase in river stage caused the exchange flux to reverse from upwelling to downwelling. Similar observations have been made within fall Chinook salmon spawning areas in the Columbia River (Geist, 2000). The exact mechanism for this flux reversal has not been fully explored, although it may result from the proximity of piezometers located in highly permeable substrate adjacent to riverbanks with significant storage capacity (Geist, 2000). The physical characteristics of sites 211.9 and 218.7 are similar enough to the other upper and middle sites that the hydrologic exchange between the riverbed and banks should be quite similar. Thus it is not likely that bank storage alone explains the observed flux reversals. Another possible reason for the flux reversals may be that sites 211.9 and 218.7 contain shallow riverbed layers of relatively low hydraulic conductivity (*K*), such that advected surface water is not easily entrained into the riverbed. However, permeability alone does not explain the flux reversals observed at sites 211.9 and 218.7 that were not observed at the other sites. The average *K* at 218.7 was estimated from slug tests to be 0.16 cm s^{-1}, which is an order of magnitude higher than the *K* estimate of 0.05 cm s^{-1} at site 196.0 (TP Hanrahan, unpublished data), a site where rapid advection of surface water into the riverbed resulted in near isothermal conditions between the river and riverbed. The *K* estimate of 0.01 cm s^{-1} at site 211.9 is within the same order of magnitude as the *K* estimate at most of the upper and middle sites, and an order of magnitude larger than the *K* estimate at the lower sites. Application of the temperature travel time model to estimate the flux rate at sites 211.9 and 218.7 (just during the periods of acute stage changes and rapid downwelling) resulted in apparent velocity estimates of 3.0 cm h^{-1} and 5.7 cm h^{-1}, respectively, which is near the upper end of the range among all sites. Based on the temperature monitoring and numerical modeling at sites 211.9 and 218.7, it appears that at low river discharge the riverbed at these sites is dominated by horizontal/longitudinal flow that has a relatively long residence time in the bed, thus being considerably warmer than the river; when the stage increases, the local hydraulics (e.g., water surface slope) change such that advective processes dominate the exchange, even to a depth of 60 cm below the riverbed surface. This explanation is qualitatively supported by the model results from Storey *et al*. (2003).

The numerical model used to estimate the vertical apparent velocity (v_z) in the hyporheic zone has some limitations, but the results indicate that the model performed well. Application of the model assumes that 1) v_z is constant over time and depth within the riverbed and 2) flux occurs only in the vertical direction. These assumptions are likely violated, as hyporheic flow is often observed to be unsteady and three-dimensional (Worman *et al*., 2002; Storey *et al*., 2003). Estimates of v_z from the numerical model match well with those based on other methods. At four of the study sites (152.3, 198.8, 222.7, and 240.6) previous investigations estimated v_z as the product of vertical hydraulic gradients (*VHG*) measured in standpipes and hydraulic conductivity (*K*) estimated with slug tests (Arntzen *et al*., 2001). At sites 152.3 and 222.7 the v_z estimate from the numerical model was within the same order of magnitude as the average v_z from the empirical data. At sites 198.8 and 240.6 v_z estimates from the numerical model and empirical data differed by two orders of magnitude. It is likely that the differences are due to methodological issues and small-scale variability in hyporheic zone characteristics, as both *VHG* and *K* varied by one to three orders of magnitude within the same site (Arntzen *et al*., 2001). At other contemporary and historic fall Chinook salmon spawning locations in the Columbia and Snake rivers, application of similar empirical methods resulted in v_z estimates of comparable magnitude to the numerical estimates of v_z reported in this paper (Geist, 2000; Hanrahan *et al*., 2005). Estimates of v_z from the numerical model also match well with v_z estimates based on similar numerical models from other gravel-bed rivers (Silliman *et al*., 1995; Constantz and Thomas, 1996; Lenk and Saenger, 2000; Saenger, 2002). The evaluation of model performance by comparing modeled and measured bed temperatures indicated that the model was fairly robust over long time periods. While the numerical model does not predict total flux rates (owing to the one-dimensional solution), it is a tool that provides a good means of comparing the relative apparent velocity in the hyporheic zones among different locations.

The results indicate that hyporheic water at the study sites has the potential to simultaneously flow in multiple directions from the same location within the hyporheic zone. These seemingly contradictory results may be caused by the difficulty in measuring small hydraulic gradients. It is more likely that the observations reflect the complex nature of the hydraulic interactions between the river and riverbed. Hyporheic flow in the vertical (both upward and downward) and horizontal direction at the same location has been modeled (Elliott and Brooks, 1997b; Worman *et al*., 2002) and observed in the laboratory (Thibodeaux and Boyle, 1987; Elliott and Brooks, 1997b; Packman *et al*., 2004), but has not been widely observed in riverbeds. Using tracer injections and piezometric potential measurements in multilevel probes placed in the riverbed, Saenger (2002) was able to divide the apparent velocity vector into its vertical and horizontal components. She found that vertical flow dominated in the upper 20 cm of the riverbed, while horizontal flow dominated in the sediments deeper than 20 cm. The findings reported in this paper seem to correlate well with those of Saenger (2002), and with the model and laboratory observations cited above. For example, at 13 of the 14 study sites the average *VHG* between the shallow hyporheic zone and the river was greater than the *VHG* between the deep hyporheic zone and the river. This finding implies that at some area of the riverbed near the shallow hyporheic zone, pore water had the potential for both upwelling and downwelling. Results from the numerical model and temperature monitoring support this finding. For example, at site 198.8 the positive *VHG* potential (upwelling) from the shallow hyporheic zone was larger than the positive *VHG* potential (upwelling) from the deep hyporheic zone, resulting in a small downwelling potential from the shallow to the deep hyporheic zone. Results from the numerical model suggested an average downward flux of 0.4 cm h^{-1} from the river to the riverbed. The temperature monitoring indicated that this advective infiltration from the river must be tempered by horizontal and/or vertical flux (advective or diffusive) from deeper within the riverbed, as in the absence of these secondary processes the temperature gradient between the river and the hyporheic zone would be much smaller than observed. This finding of three-dimensional flow at the same point within a riverbed matches very well with recent laboratory observations. Packman *et al*. (2004) injected dye at 3 cm below a gravel bed surface in a flume, and observed the dye moving upward, downward and horizontally from the same injection point.

The findings regarding the hydraulic interactions between the river and riverbed illustrate both the difficulty of measuring surface–subsurface exchange and the complexity of that exchange. Elliott and Brooks (1997a) noted that the spatial and temporal complexity of the hyporheic zone makes modeling (or observing) the fluid mechanics a formidable task. Indeed, it is in the different treatment of the basic fluid mechanics of the system under investigation that contributes to the difficulty in discerning the dominant hydraulic process of the system. When considering the advection and turbulent diffusion of surface water into the riverbed, the interface zone is treated similar to open channel problems, wherein the energy due to the velocity head is explicitly considered. These processes are most important over small temporal and spatial scales (Elliott and Brooks, 1997b), especially where the hydraulic conductivity of the shallow subsurface is much higher than deeper within the riverbed. When considering hydrostatic head differences between surface and subsurface water, the interface zone is treated as a groundwater system wherein the kinetic energy (i.e., the velocity head) is excluded from the solution. These processes are most important over larger temporal and spatial scales (Elliott and Brooks, 1997b). It is likely that both advective and diffusive processes were observed over small and large temporal and spatial scales, all of which are important to the riverbed incubation environment of Chinook salmon.

Regional management agencies in the Snake River basin of the Pacific northwestern United States are considering modifications to the discharge operations of Hells Canyon Dam as part of recovery efforts for imperiled fall Chinook salmon populations. Before modifications to discharge operations are implemented, additional information regarding the effects of river discharge on hydrologic exchange between the river and riverbed in fall Chinook salmon spawning areas is necessary. The results from this study suggest that manipulated variations of river discharge from Hells Canyon Dam have a negligible effect on vertical hydrologic exchange. Because variation in river discharge have a negligible effect on riverbed temperature gradients, manipulations of river discharge from Hells Canyon Dam would likely have a negligible effect on accelerating fall Chinook salmon egg incubation and growth (Hanrahan *et al.*, 2004). Nevertheless, the large variability in riverbed temperatures within and among the study sites suggests the need to better understand this variability in order to better manage the limited water resources in the highly-regulated Snake River basin (Hanrahan, in review b). By incorporating the knowledge of hydrologic exchange processes into water management planning, regional agencies will be better prepared to manage the limited water resources among competing priorities that include salmon recovery, flood control, irrigation supply, hydropower production, and recreation.

Acknowledgments

This research was funded by the U.S. Department of Energy Bonneville Power Administration (BPA) under the Northwest Power and Conservation Council's Fish and Wildlife Program. Co-funding was provided by Idaho Power Company (IPC). I extend my gratitude to Brad Alcorn, Jim Chandler and Phil Groves at IPC, and Scott Abernethy, Evan Arntzen, and David Geist the Pacific Northwest National Laboratory (PNNL) for their cooperation and collaboration on the research project. Some of the data presented in this paper are included in PNNL Report 14850, a contract report to BPA. PNNL is operated by Battelle Memorial Institute for the U.S. Department of Energy under contract DE-AC06-76RLO-1830.

References

Anderson MP. 2005. Heat as a ground water tracer. *Ground Water* **43**: 951–968.

Arntzen EV, Geist DR, and Hanrahan TP. 2001. *Substrate quality of fall chinook salmon spawning habitat, Hells Canyon Reach, Snake River, Idaho*. Final report to Idaho Power Company, PNWD-3114. Battelle Pacific Northwest Division, Richland, WA.

Berland G, Nickelsen T, Heggenes J, Okland F, Thorstad EB, and Halleraker J. 2004. Movements of wild Atlantic salmon parr in relation to peaking flows below a hydropower station. *River Research and Applications* **20**: 957–966.

Boulton AJ, Findlay S, Marmonier P, Stanley EH, and Valett HM. 1998. The functional significance of the hyporheic zone in streams and rivers. *Annual Review of Ecological Systems* **29**: 59–81.

Brown LE, Hannah DM, and Milner AM. 2005. Spatial and temporal water column and streambed temperature dynamics within an alpine catchment: implications for benthic communities. *Hydrological Processes* **19**: 1585–1610.

Brunke M and Gonser T. 1997. The ecological significance of exchange processes between rivers and groundwater. *Freshwater Biology* **37**: 1–33.

Castro NM and Hornberger GM. 1991. Surface-subsurface water interactions in an alluviated mountain stream channel. *Water Resources Research* **27**: 1613–1621.

Chapman DW. 1988. Critical review of variables used to define effects of fines in redds of large salmonids. *Transactions of the American Fisheries Society* **117**: 1–21.

Clark E, Webb BW, and Ladle M. 1999. Microthermal gradients and ecological implications in Dorset rivers. *Hydrologic Processes* **13**: 423–438.

Comer LE and Grenney WJ. 1977. Heat transfer processes in the bed of a small stream. *Water Research* **11**: 743–744.

Connor WP, Burge HL, Waitt R, and Bjornn TC. 2002. Juvenile life history of wild fall chinook salmon in the Snake and Clearwater rivers. *North American Journal of Fisheries Management* **22**: 703–712.

Constantz J and Thomas CL. 1996. The use of streambed temperature profiles to estimate the depth, duration, and rate of percolation beneath arroyos. *Water Resources Research* **32**: 3597–3602.

D'Angelo DJ, Webster JR, Gregory SV, and Meyer JL. 1993. Transient storage in Appalachian and Cascade mountain streams as related to hydraulic characteristics. *Journal of the North American Benthological Society* **12**: 223–235.

Elliott AH and Brooks NH. 1997a. Transfer of nonsorbing solutes to a streambed with bed forms: theory. *Water Resources Research* **33**: 123–136.

Elliott AH and Brooks NH. 1997b. Transfer of nonsorbing solutes to a streambed with bed forms: laboratory experiments. *Water Resources Research* **33**: 137–151.

Evans EC, Greenwood MT, and Petts GE. 1995. Thermal profiles within river beds. *Hydrological Processes* **9**: 19–25.

Fernald AG, Winington Jr. PJ, and Landers DH. 2001. Transient storage and hyporheic flow along the Willamette River, Oregon: field measurements and model estimates. *Water Resources Research* **37**: 1681–1694.

Fetter CW. 1994. *Applied hydrogeology*. 3rd.458 pp., Merrill Publishing Company, Upper Saddle River, NJ.

Freeze RA and Cherry JA. 1979. *Groundwater*. 604 pp., Prentice-Hall, Inc., Englewood Cliffs, NJ.

Garcia A, Bradbury S, Arnsberg B, Rocklage S, and Groves P. 2003. *Fall Chinook salmon spawning ground surveys in the Snake River basin upriver of Lower Granite Dam*. BPA Report DOE/BP-00004700-2. Bonneville Power Administration, Portland, OR.

Geist DR. 2000. Hyporheic discharge of river water into fall chinook salmon (*Oncorhynchus tshawytscha*) spawning areas in the Hanford Reach, Columbia River. *Canadian Journal of Fisheries and Aquatic Sciences* **57**: 1647–1656.

Gibbins CN and Acornley RM. 2000. Salmonid habitat modelling studies and their contribution to the development of an ecologically acceptable release policy for Kielder Reservoir, north-east England. *Regulated Rivers: Research and Management* **16**: 203–224.

Gibbins CN, Moir HJ, Webb JH, and Soulsby C. 2002. Assessing discharge use by spawning Atlantic salmon: A comparison of discharge electivity indices and PHABSIM simulations. *River Research and Applications* **18**: 383–395.

Groves PA and Chandler JA. 1999. Spawning habitat used by fall chinook salmon in the Snake River. *North American Journal of Fisheries Management* **19**: 912–922.

Hanrahan TP, Geist DR, and Arntzen EV. 2005. Habitat quality of historic Snake River fall Chinook salmon spawning locations and implications for incubation survival: part 1, substrate quality. *River Research and Applications* **25**: 455–467.

Hanrahan TP, Geist DR, Arntzen EV, and Abernethy CS. 2004. *Effects of hyporheic exchange flows on egg pocket water temperature in Snake River fall Chinook salmon spawning areas*. PNNL–14850: Pacific Northwest National Laboratory, Richland, WA.

Hanrahan TP. In review a. Bed form morphology of salmon spawning areas in a large gravel-bed river. To be submitted to *Geomorphology*.

Hanrahan TP. In review b. Large-scale spatial variability of riverbed temperature gradients in Snake River fall Chinook salmon spawning areas. To be submitted to *River Research and Applications*.

Hart DR, Mulholland PJ, Marzolf ER, DeAngelis DL, and Hendricks SP. 1999. Relationships between hydraulic parameters in a small stream under varying flow and seasonal conditions. *Hydrological Processes* **13**: 1497–1510.

Harvey JW and Bencala KE. 1993. The effect of streambed topography on surface-subsurface water exchange in mountain catchments. *Water Resources Research* **29**: 89–98.

Hendry K, Cragg-Hine D, O'Grady M, Sambrook H, and Stephen A. 2003 . Management of habitat for rehabilitation and enhancement of salmonid stocks. *Fisheries Research* **62**: 171–192.

Hill AR, Labadia CF, and Sanmugadas K. 1998. Hyporheic zone hydrology and nitrate dynamics in relation to the streambed topography of a N-rich stream. *Biogeochemistry* **42**: 285–310.

Hondzo M and Stefan HG. 1994. Riverbed heat conduction prediction. *Water Resources Research* **30**: 1503–1513.

Hunt RJ, Krabbenhoft DP, and Anderson MP. 1996. Groundwater inflow measurements in wetland systems. *Water Resources Research* **32**: 495–507.

Johnson SL. 2003. Stream temperature: scaling of observations and issues for modelling. *Hydrological Processes* **17**: 497–499.

Jones JA and Mulholland P. 2000. *Streams and ground waters*. Academic Press, Orlando, FL.

Kasahara T and Wondzell SM. 2003. Geomorphic controls on hyporheic exchange flow in mountain streams. *Water Resources Research* **39**: 1005, DOI:10.1029/2002WR001386.

Lapham WW. 1989. *Use of temperature profiles beneath streams to determine rates of vertical ground-water flow and vertical hydraulic conductivity*. Water-Supply Paper 2337. U. S. Geological Survey, Denver, CO.

Larkin RG and Sharp JM. 1992. On the relationship between river-basin geomorphology, aquifer hydraulics, and ground-water flow direction in alluvial aquifers. *Geological Society of America Bulletin* **104**: 1608–1620.

Legrad-Marcq C and Laudelout H. 1985. Longitudinal dispersion in a forest stream. *Journal of Hydrology* **78**: 317v324.

Lenk M and Saenger N. 2000 . Exchange processes in the river bed and their influence on temperature variations. *Verh. Internat. Verein. Limnol.* **27**: 427–430.

Lunardini VJ. 1981. *Heat transfer in cold climates*. 731 pp., Van Nostrand Reinhold Company, New York.

Malcolm IA, Soulsby C, Youngson AF, Hannah DM, McLaren IS, and Thorne A. 2004. Hydrological influences on hyporheic water quality: implications for salmon egg survival. *Hydrologic Processes* **18**: 1543–1560.

Malcolm IA, Soulsby C, Youngson AF, and Petry J. 2003. Heterogeneity in ground water-surface water interactions in the hyporheic zone of a salmonid spawning stream. *Hydrological Processes* **17**: 601–617.

Marion A, Bellinello M, Guymer I, and Packman A. 2002. Effect of bed form geometry on the penetration of nonreactive solutes into a streambed. *Water Resources Research* **38**: 1209, DOI:10.1029/2001WR000264.

Miller S, Glanzman D, Doran S, Parkinson S, Buffington J, and Milligan J. 2002. *Geomorphology of the Hells Canyon Reach of the Snake River*. Technical Report Appendix E.1.2 to FERC Relicensing Application. Idaho Power Company, Boise, ID.

Morrice JA, Valett HM, Dahm CN, and Campana ME. 1997. Alluvial characteristics, groundwater-surface water exchange and hydrological retention in headwater streams. *Hydrological Processes* **11**: 253–267.

Nagaoka H and Ohgaki AJ. 1990. Mass transfer mechanism in a porous riverbed. *Water Research* **24**: 417–425.

O'Connor JE. 1993. *Hydrology, hydraulics, and geomorphology of the Bonneville Flood*. Special paper 274. Geological Society of America, Boulder, CO.

Packman AI, Salehin M, and Zaramella M. 2004. Hyporheic exchange with gravel beds: Basic hydrodynamic interactions and bedform-induced advective flows. *Journal of Hydraulic Engineering* **130**: 647–656.

Saenger N. 2002. Estimation of flow velocities within the hyporheic zone. *Verh. Internat. Verein. Limnol.* **28**: 1790–1795.

Savant SA, Reible DD, and Thibodeaux LJ. 1987. Convective transport within stable river sediments. *Water Resources Research* **23**: 1763–1768.

Schalchli U. 1995. Basic equations for siltation of riverbeds. *Journal of Hydraulic Engineering* **121**: 274–287.

Shimizu Y, Tsujimoto T, and Nakagawa H. 1990. Experiment and macroscopic modelling of flow in highly permeable porous medium under free-surface flow. *Journal of Hydroscience and Hydraulic Engineering* **8**: 69–78.

Silliman SE, Ramirez J, and McCabe RL. 1995. Quantifying downflow through creek sediments using temperature time series: one-dimensional solution incorporating measured surface temperature. *Journal of Hydrology* **167**: 99–119.

Sinokrot BA and Stefan HG. 1993. Stream temperature dynamics: measurements and modeling. *Water Resources Research* **29**: 2299–2312.

Soulsby C, Malcolm IA, and Youngson AF. 2001. Hydrochemistry of the hyporheic zone in salmon spawning gravels: a preliminary assessment in a degraded agricultural stream. *Regulated Rivers: Research and Management* **17**: 651–665.

Stallman RW. 1965. Steady one-dimensional fluid flow in a semi-infinite porous medium with sinusoidal surface temperature. *Journal of Geophysical Research* **70**: 2821–2827.

Stanford JA and Ward JV. 1993. An ecosystem perspective of alluvial rivers: connectivity and the hyporheic zone. *Journal of the North American Benthological Society* **12**: 48–60.

Storey RG, Howard KWF, and Williams DD. 2003. Factors controlling riffle-scale hyporheic exchange flows and their seasonal changes in a gaining stream: A three-dimensional groundwater flow model. *Water Resources Research* **39**: 1034, DOI:10.1029/2002WR001367.

Stream Solute Workshop. 1990. Concepts and methods for assessing solute dynamics in stream ecosystems. *Journal of the North American Benthological Society* **9**: 95–119.

Thibodeaux LJ and Boyle JD. 1987. Bedform-generated convective transport in bottom sediment. *Nature* **325**: 341–343.

Triska FT, Kennedy VC, Avanzino RJ, Zellweger GW, and Bencala KE. 1989. Retention and transport of nutrients in a third-order stream in northwestern California: hyporheic processes. *Ecology* **70**: 1893–1905.

Vittal N, Ranga Raju KG, and Garde RJ. 1977. Resistance of two dimensional triangular roughness. *Journal of Hydraulic Research* **15**: 19–36.

White DS. 1993. Perspectives on defining and delineating hyporheic zones. *Journal of the North American Benthological Society* **12**: 61–69.

Winter TC, Harvey JW, Franke OL, and Alley WM. 1998. *Ground water and surface water: a single resource*. Circular 1139. U. S. Geological Survey, Denver, CO.

Wondzell SM. 2006. Effect of morphology and discharge on hyporheic exchange flows in two small streams in the Cascade Mountains of Oregon, USA. *Hydrological Processes* **20**: 267–287.

Wondzell SM and Swanson FJ. 1996. Seasonal and storm dynamics of the hyporheic zone of a 4th-order mountain stream. I: Hydrologic processes. *Journal of the North American Benthological Society* **15**: 3–19.

Worman A, Packman AI, Johansson H, and Jonsson K. 2002. Effect of flow-induced exchange in hyporheic zones on longitudinal transport of solutes in streams and rivers. *Water Resources Research* **38**: 1001, DOI:10.1029/2001WR000769.

Wroblicky GJ, Campana ME, Valett HM, and Dahm CN. 1998. Seasonal variation in surface-subsurface water exchange and lateral hyporheic area of two stream-aquifer systems. *Water Resources Research* **34**: 317–328.

Zhou D and Mendoza C. 1993 . Flow through porous bed of turbulent stream. *Journal of Engineering Mechanics* **119**: 365–383.

Tables

Table 1. Apparent velocity *v_z* of pore water derived from the numerical model of shallow hyporheic zone temperatures at each site. The *v_z* was held constant during the period indicated. Positive *v_z* indicates downward flux; negative *v_z* indicates upward flux. Comparison of modeled and observed shallow hyporheic zone temperatures is provided by the mean absolute error (MAE) and root mean-squared error (RMSE).

Site	Segment	Period	v_z (cm h^{-1})	MAE (°C)	RMSE (°C)
148.5	lower	20 October 2002–2 March 2003	0.2	0.09	0.13
149.2	lower	20 October 2002–2 March 2003	1.3	0.11	0.15
152.3	lower	20 October 2002–2 March 2003	-0.4	0.06	0.08
156.8	lower	20 October 2002–14 January 2003	0.2	0.13	0.17
		15 January 2003–1 February 2003	1.1	0.08	0.09
		2 February 2003–2 March 2003	1.8	0.12	0.14
196.0	middle	20 October 2002–14 January 2003	5.4	0.06	0.09
		15 January 2003–1 March 2003	-0.4	0.05	0.07
198.2	middle	20 October 2002–5 January 2003	2.2	0.11	0.17
	middle	6 January 2003–2 March 2003	1.4	0.06	0.09
198.8	middle	20 October 2002–2 March 2003	0.4	0.07	0.11
211.9	middle	20 October 2002–5 January 2003	0.4	0.12	0.14
		6 January 2003–2 March 2003	-1.8	0.13	0.16
218.7	middle	20 October 2002–5 January 2003	-0.9	0.10	0.13
		6 January 2003–2 March 2003	-0.9†	0.25	0.35
219.3	middle	20 October 2002–7 January 2003	0.4	0.08	0.09
		8 January 2003–2 March 2003	-1.8	0.03	0.04
222.7	middle	20 October 2002–6 November 2002	0.4	0.08	0.09
		7 November 2002–2 March 2003	-1.1	0.10	0.12
238.6	upper	20 October 2002–2 March 2003	0.7	0.09	0.11
240.6	upper	20 October 2002–2 March 2003	0.7	0.04	0.05
244.5	upper	20 October 2002–2 March 2003	2.9	0.06	0.07

†Temperature changes in the shallow hyporheic zone were too large during this period to model the daily change by adjusting v_z.

Table 2. Comparison of apparent velocity of pore water derived from the numerical model v_{zn} and travel time model v_{ztt}. Values of v_z represent the flux rate between the riverbed surface and the shallow hyporheic zone. Positive v_z indicates downward flux; negative v_z indicates upward flux.

Site	Segment	Period	v_{zn} (cm h^{-1})	v_{ztt} (cm h^{-1})
196.0	middle	20 October 2002–14 January 2003	5.4	5.0
		15 January 2003–1 March 2003	-0.4	2.4
198.2	middle	20 October 2002–5 January 2003	2.2	6.1
		6 January 2003–2 March 2003	1.4	4.2
244.5	upper	20 October 2002–2 March 2003	2.9	5.4
		6 January 2003–2 March 2003	2.9	2.9

List of figures

Figure 1. The study area extended from Hells Canyon Dam downstream to near the confluence with Asotin Creek. Study sites (□) are identified by their river mile location.

Figure 2. Mean daily discharge in the Snake River downstream from Hells Canyon Dam (USGS gage 13290450) during the period from 1 October to 1 May for the water years 1990—2003. Discharge during the sampling period (2002—2003) is shown as a solid black line, while all other water years are shown in gray. Time periods used in the analyses include the period with low, stable discharge (20 October 2002 – 7 January 2003), and the period with variable discharge (8 January – 2 March 2003).

Figure 3. Difference in head pressure (*dh*; shallow hyporheic head minus river head) at each site during (a) the low, stable discharge period (20 October 2002 – 7 January 2003), and (b) the variable discharge period (8 January – 2 March 2003). Each boxplot represents a summary of hourly *dh* at each site. The point in the center of the boxplot indicates the mean, the box is equal to the mean ± 1 standard deviation (SD), and the whiskers represent the mean ± 1.96 × SD.

Figure 4. Mean vertical hydraulic gradient (VHG) between the river and shallow hyporheic zone (☐), and between the river and deep hyporheic zone (■) during (a) the low, stable discharge period (20 October 2002 – 7 January 2003), and (b) the variable discharge period (8 January – 2 March 2003). Positive values indicate upwelling potential while negative values indicate downwelling potential.

Figure 5. Time-series summary of water temperature (top panel) and river stage (bottom panel) at site 149.2 during a period of low, stable river discharge (November 28 – 30, 2002). Average hourly water temperature is shown for the river (+), egg pocket (○), shallow hyporheic (●) and deep hyporheic (▲) zones. Average hourly stage (depth) is shown for the river (+), and shallow

hyporheic zone (●). The difference between these two water depths (hyporheic minus river) is plotted on the Y-right axis as *dh* (—), with positive values indicating upwelling potential.

Figure 6. Time-series summary of water temperature (top panel) and river stage (bottom panel) at site 196.0 during a period of low, stable river discharge (November 28 – 30, 2002). Average hourly water temperature is shown for the river (+), egg pocket (○), shallow hyporheic (●) and deep hyporheic (▲) zones. Average hourly stage (depth) is shown for the river (+), and shallow hyporheic zone (●). The difference between these two water depths (hyporheic minus river) is plotted on the Y-right axis as *dh* (—), with positive values indicating upwelling potential.

Figure 7. Time-series summary of water temperature (top panel) and river stage (bottom panel) at site 152.3 during a period of variable river discharge (January 6 – 9, 2003). Average hourly water temperature is shown for the river (+), egg pocket (○), shallow hyporheic (●) and deep hyporheic (▲) zones. Average hourly stage (depth) is shown for the river (+), and shallow hyporheic zone (●). The difference between these two water depths (hyporheic minus river) is plotted on the Y-right axis as *dh* (—), with positive values indicating upwelling potential.

Figure 8. Time-series summary of water temperature (top panel) and river stage (bottom panel) at site 196.0 during a period of variable river discharge (January 6 – 9, 2003). Average hourly water temperature is shown for the river (+), egg pocket (○), shallow hyporheic (●) and deep hyporheic (▲) zones. Average hourly stage (depth) is shown for the river (+), and shallow hyporheic zone (●). The difference between these two water depths (hyporheic minus river) is plotted on the Y-right axis as *dh* (—), with positive values indicating upwelling potential.

Figure 9. Time-series summary of water temperature (top panel) and river stage (bottom panel) at site 198.8 during a period of variable river discharge (January 6 – 9, 2003). Average hourly water temperature is shown for the river (+), egg pocket (○), shallow hyporheic (●) and deep hyporheic (▲) zones. Average hourly stage (depth) is shown for the river (+), and shallow

hyporheic zone (●). The difference between these two water depths (hyporheic minus river) is plotted on the Y-right axis as *dh* (—), with positive values indicating upwelling potential.

Figure 10. Time-series summary of water temperature (top panel) and river stage (bottom panel) at site 211.9 during a period of variable river discharge (January 6 – 9, 2003). Average hourly water temperature is shown for the river (+), egg pocket (○), shallow hyporheic (●) and deep hyporheic (▲) zones. Average hourly stage (depth) is shown for the river (+), and shallow hyporheic zone (●). The difference between these two water depths (hyporheic minus river) is plotted on the Y-right axis as *dh* (—), with positive values indicating upwelling potential.

Figure 11. Time-series summary of water temperature (top panel) and river stage (bottom panel) at site 218.7 during a period of variable river discharge (January 6 – 9, 2003). Average hourly water temperature is shown for the river (+), egg pocket (○), shallow hyporheic (●) and deep hyporheic (▲) zones. Average hourly stage (depth) is shown for the river (+), and shallow hyporheic zone (●). The difference between these two water depths (hyporheic minus river) is plotted on the Y-right axis as *dh* (—), with positive values indicating upwelling potential.

Figure 12. Time-series summary of observed and modeled water temperature (top panel) and river stage (bottom panel) at site 222.7 during the period 1 December 2002 – 2 March 2003. Water temperatures recorded at 20 min intervals in the river (—), shallow hyporheic zone (▬), and deep hyporheic zone (▬) are compared with modeled water temperature at 20 min intervals in the shallow hyporheic zone (—).

Figure 13. Time-series summary of observed and modeled water temperature (top panel) and river stage (bottom panel) at site 211.9 during the period 1 December 2002 – 2 March 2003. Water temperatures recorded at 20 min intervals in the river (—), shallow hyporheic zone (▬), and deep hyporheic zone (▬) are compared with modeled water temperature at 20 min intervals in the shallow hyporheic zone (—).

Figure 14. Time-series summary of observed and modeled water temperature (top panel) and river stage (bottom panel) at site 218.7 during the period 1 December 2002 – 2 March 2003. Water temperatures recorded at 20 min intervals in the river (—), shallow hyporheic zone (▬), and deep hyporheic zone (▬) are compared with modeled water temperature at 20 min intervals in the shallow hyporheic zone (—).

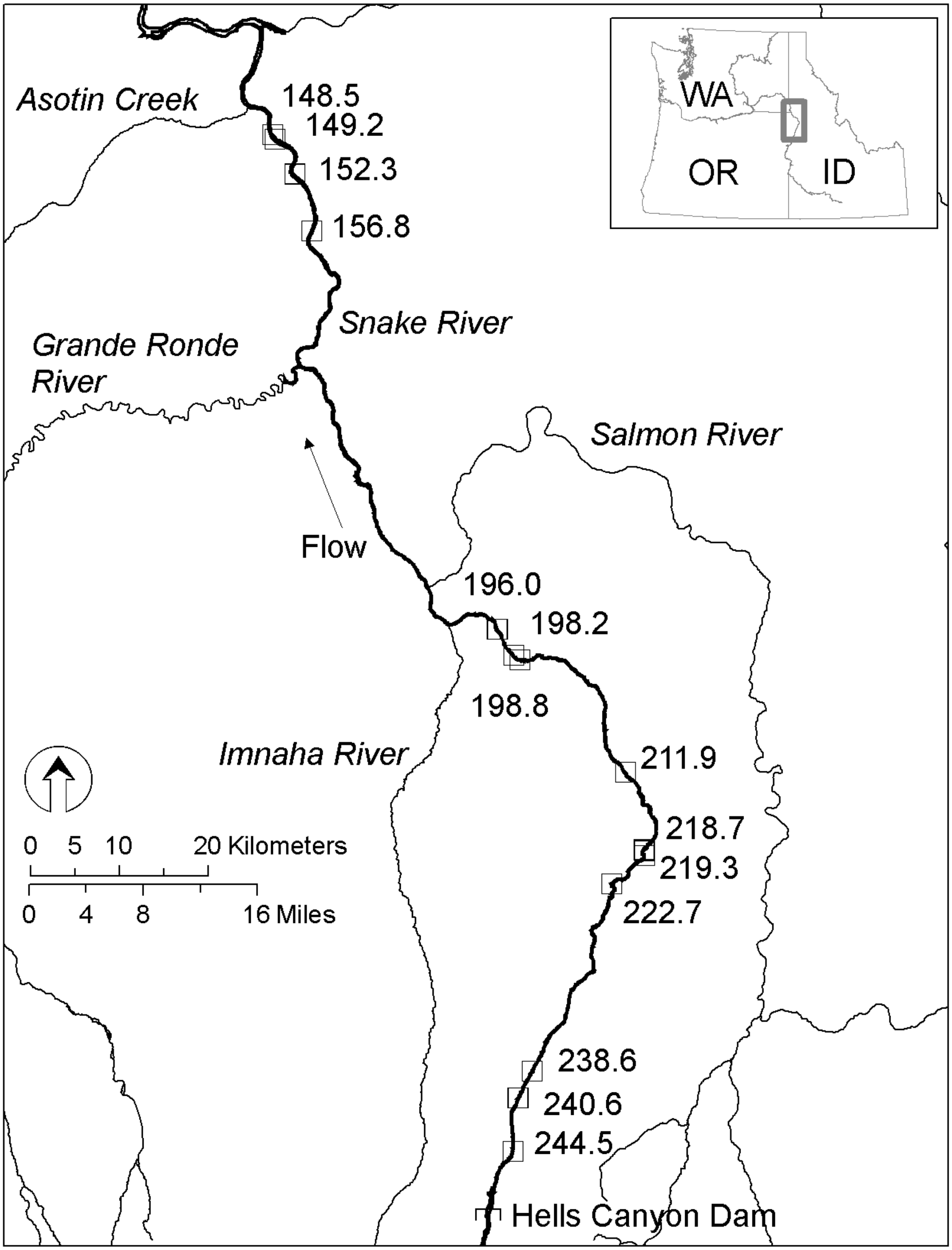
Asotin Creek
148.5
149.2
152.3
156.8
Snake River
Grande Ronde River
Salmon River
Flow
196.0
198.2
198.8
Imnaha River
211.9
218.7
219.3
222.7
238.6
240.6
244.5
Hells Canyon Dam
0 5 10 20 Kilometers
0 4 8 16 Miles
WA
OR
ID

Figure 1

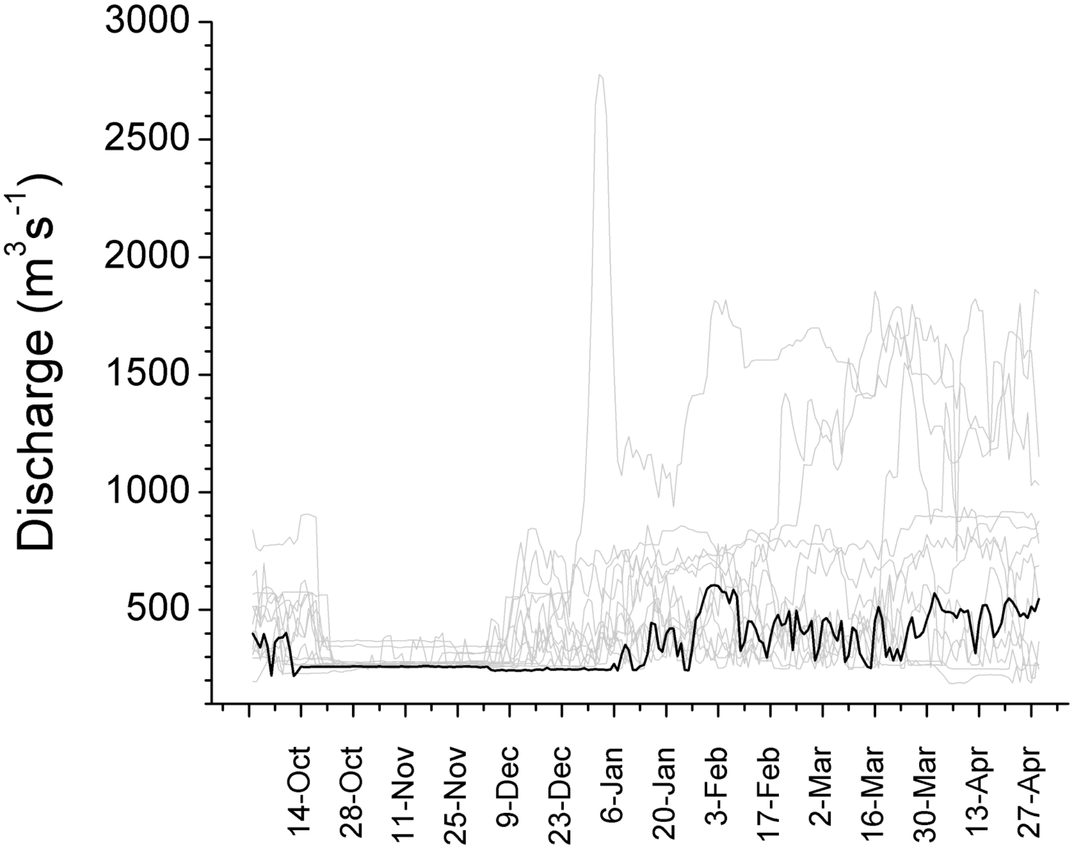

Discharge (m^3s^{-1})
3000
2500
2000
1500
1000
500
14-Oct
28-Oct
11-Nov
25-Nov
9-Dec
23-Dec
6-Jan
20-Jan
3-Feb
17-Feb
2-Mar
16-Mar
30-Mar
13-Apr
27-Apr

Figure 2

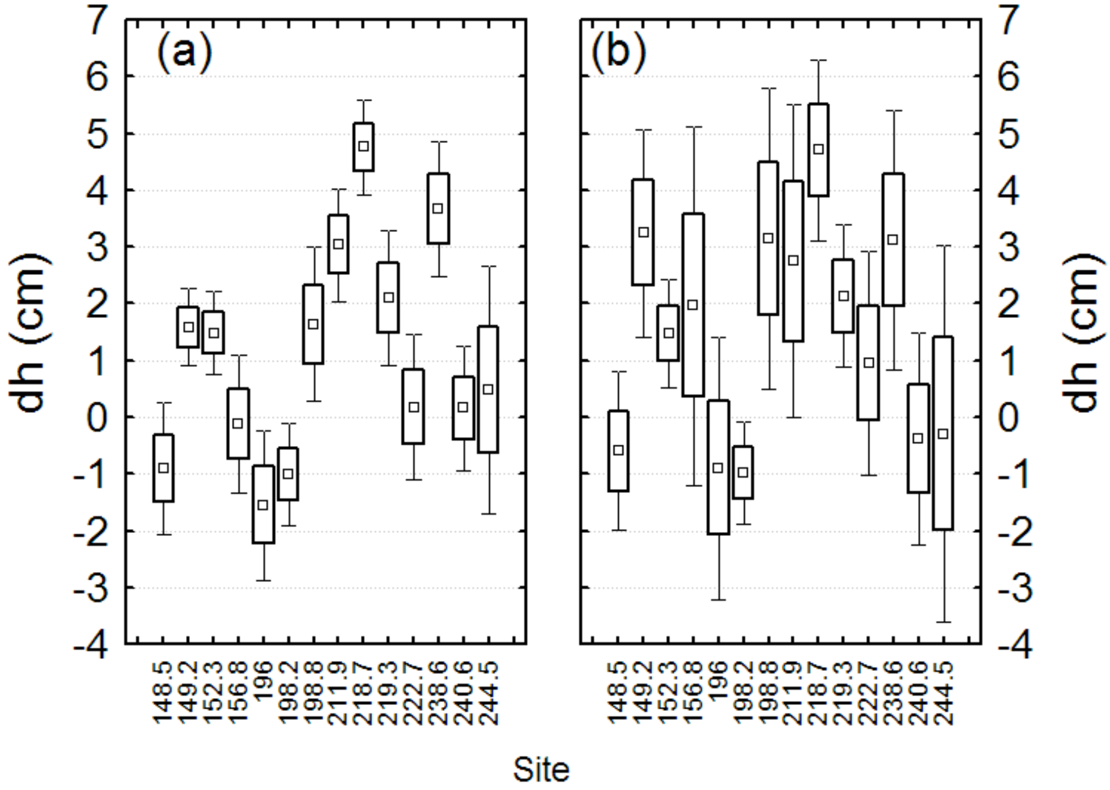
(a)
(b)
dh (cm)
dh (cm)
7
6
5
4
3
2
1
0
-1
-2
-3
-4
148.5
149.2
152.3
156.8
196
198.2
198.8
211.9
218.7
219.3
222.7
238.6
240.6
244.5
Site

Figure 3

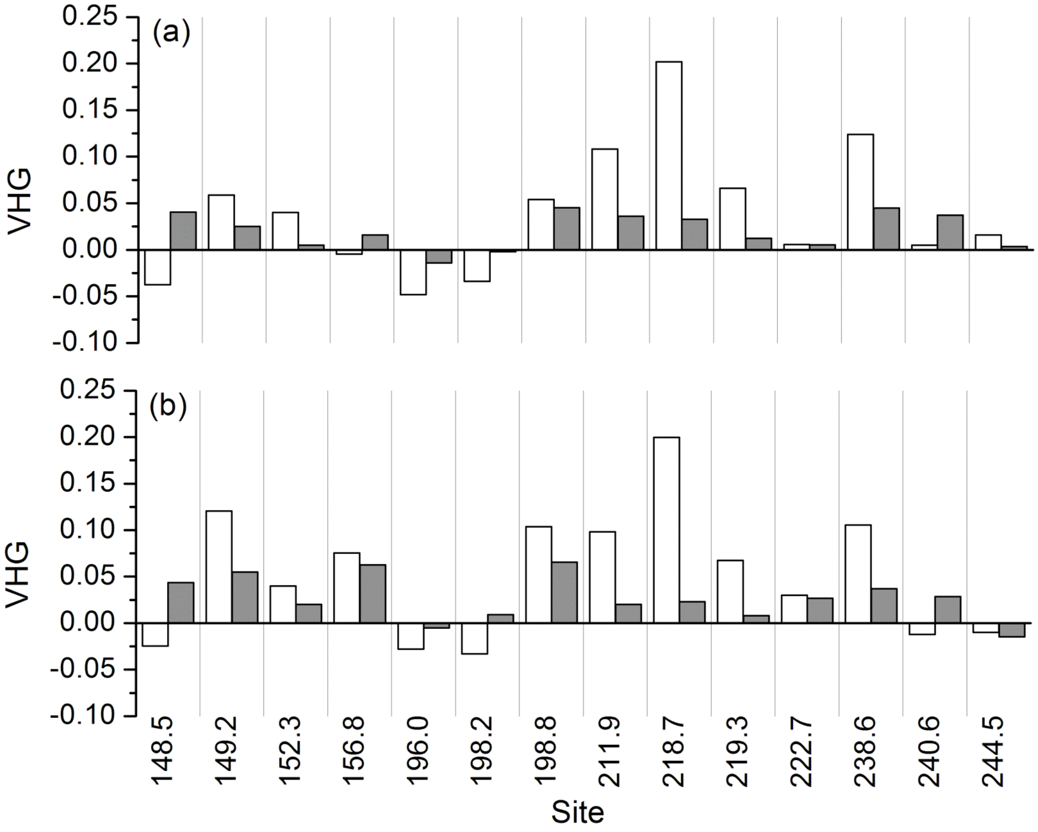
(a)
(b)
VHG
0.25
0.20
0.15
0.10
0.05
0.00
-0.05
-0.10
148.5
149.2
152.3
156.8
196.0
198.2
198.8
211.9
218.7
219.3
222.7
238.6
240.6
244.5
Site

Figure 4

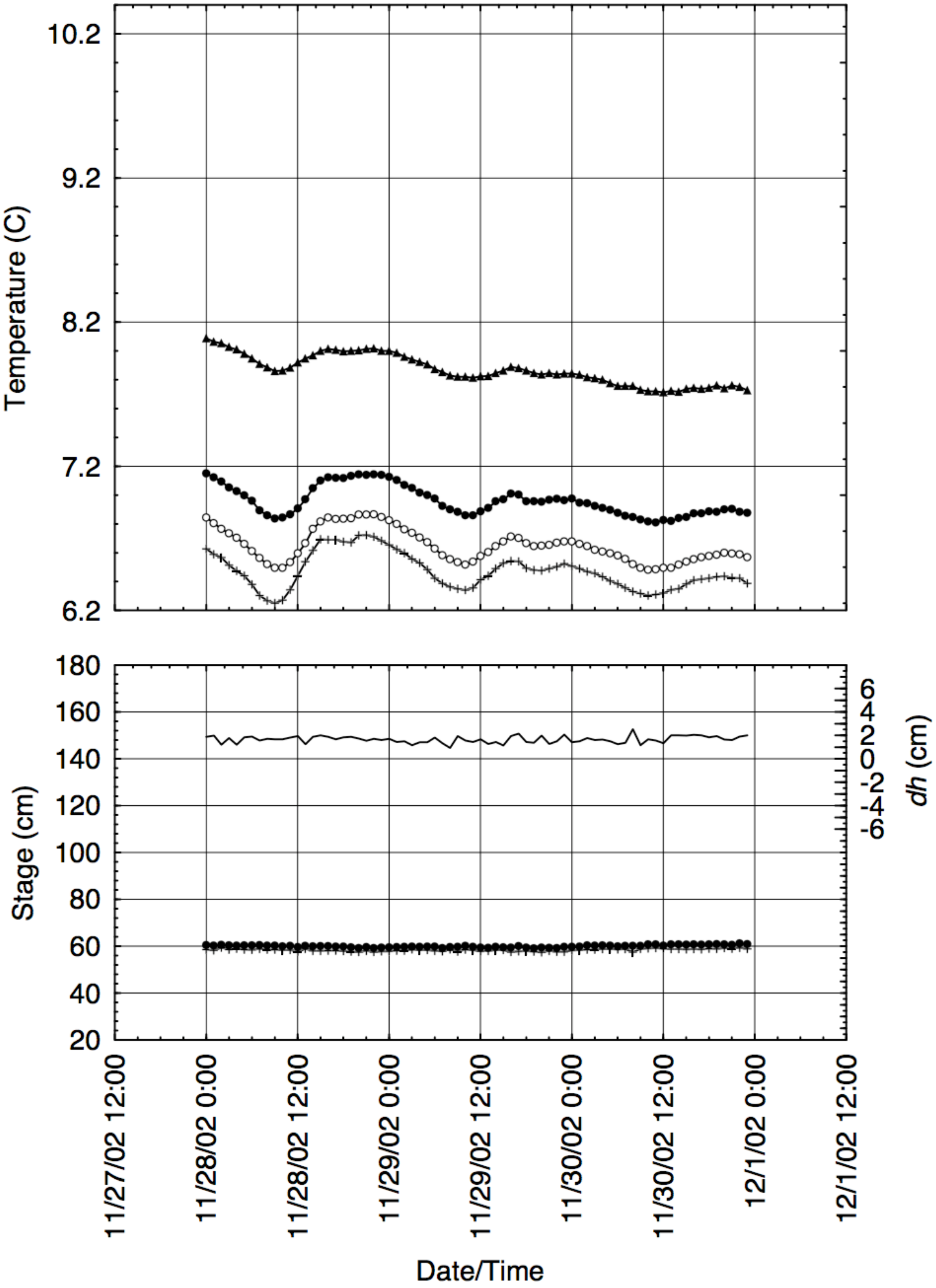
10.2
9.2
8.2
7.2
6.2
Temperature (C)
180
160
140
120
100
80
60
40
20
Stage (cm)
6
4
2
0
-2
-4
-6
dh (cm)
11/27/02 12:00
11/28/02 0:00
11/28/02 12:00
11/29/02 0:00
11/29/02 12:00
11/30/02 0:00
11/30/02 12:00
12/1/02 0:00
12/1/02 12:00
Date/Time

Figure 5

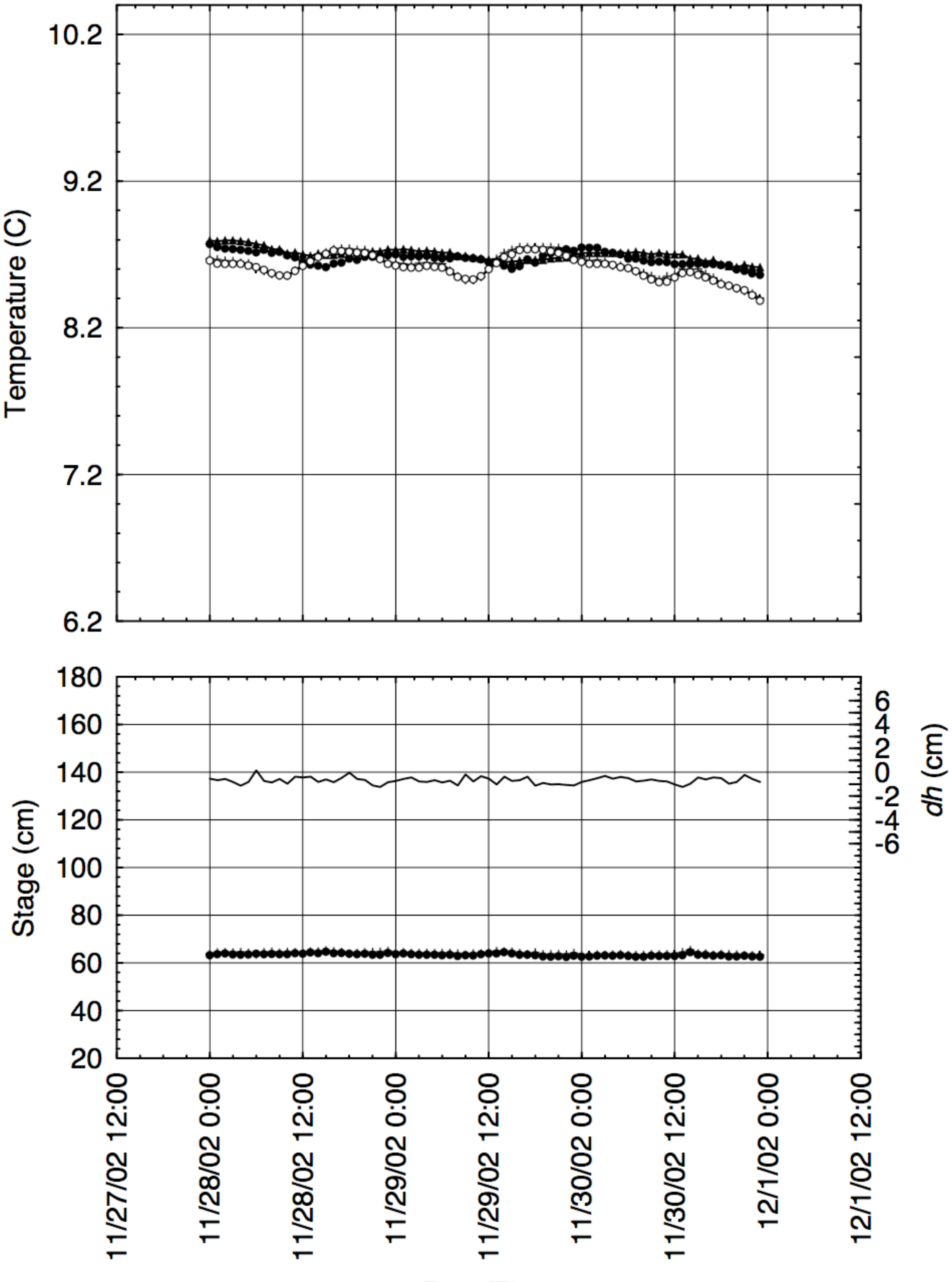
10.2
9.2
8.2
7.2
6.2
Temperature (C)
180
160
140
120
100
80
60
40
20
Stage (cm)
6
4
2
0
-2
-4
-6
dh (cm)
11/27/02 12:00
11/28/02 0:00
11/28/02 12:00
11/29/02 0:00
11/29/02 12:00
11/30/02 0:00
11/30/02 12:00
12/1/02 0:00
12/1/02 12:00
Date/Time

Figure 6

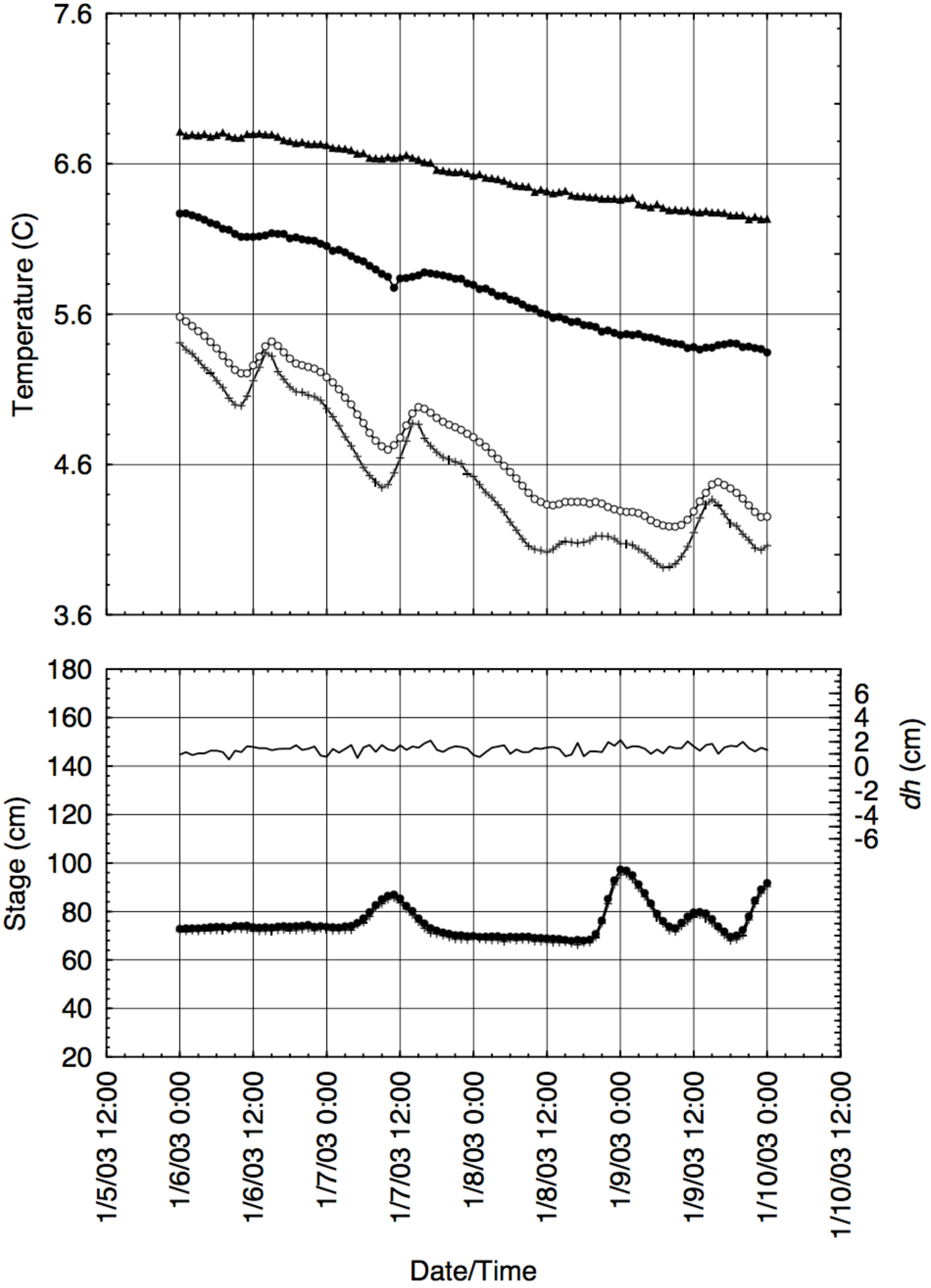

7.6
6.6
5.6
4.6
3.6
Temperature (C)
180
160
140
120
100
80
60
40
20
Stage (cm)
6
4
2
0
-2
-4
-6
dh (cm)
1/5/03 12:00
1/6/03 0:00
1/6/03 12:00
1/7/03 0:00
1/7/03 12:00
1/8/03 0:00
1/8/03 12:00
1/9/03 0:00
1/9/03 12:00
1/10/03 0:00
1/10/03 12:00
Date/Time

Figure 7

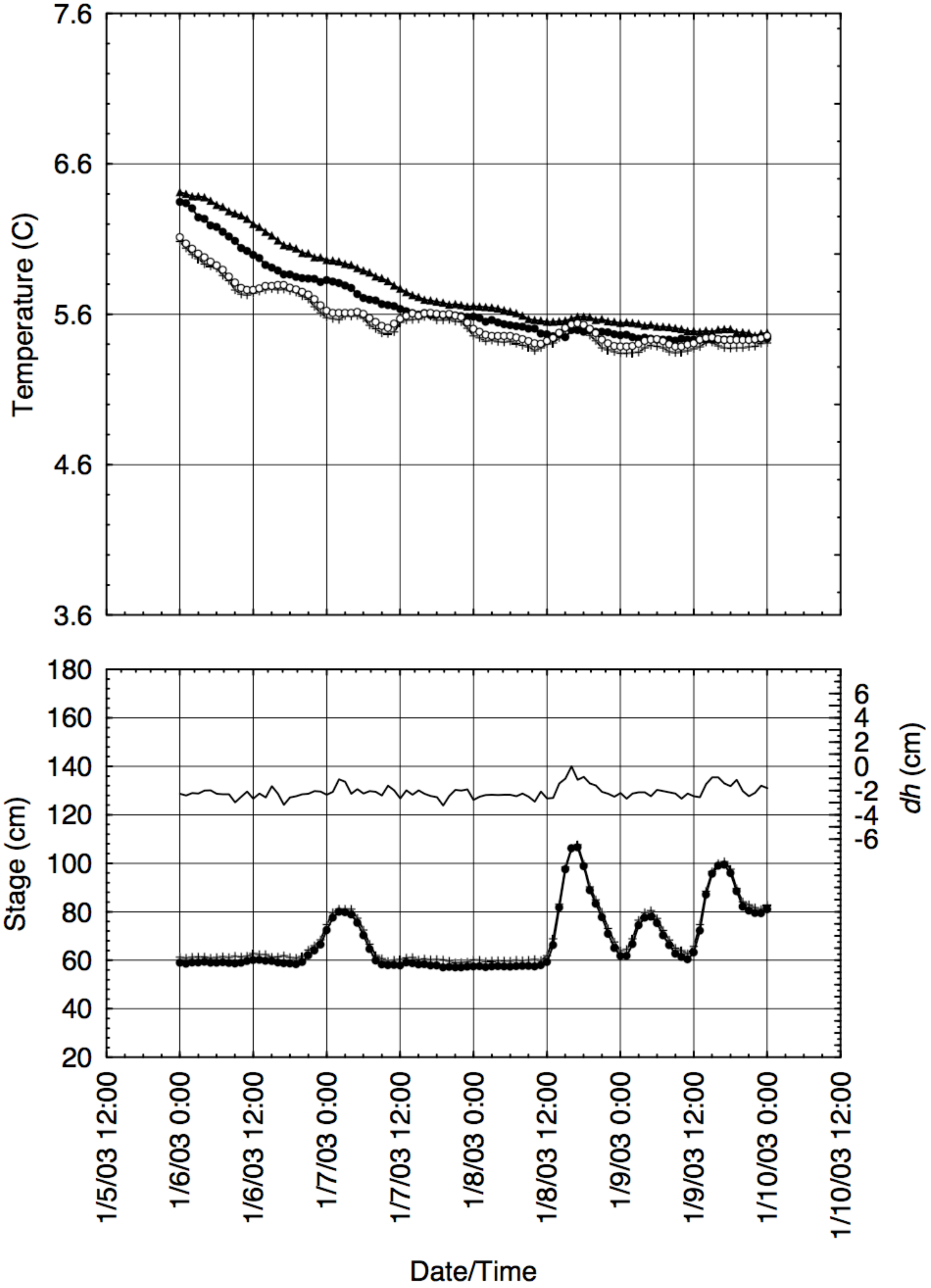

7.6
6.6
5.6
4.6
3.6
Temperature (C)
180
160
140
120
100
80
60
40
20
Stage (cm)
6
4
2
0
-2
-4
-6
dh (cm)
1/5/03 12:00
1/6/03 0:00
1/6/03 12:00
1/7/03 0:00
1/7/03 12:00
1/8/03 0:00
1/8/03 12:00
1/9/03 0:00
1/9/03 12:00
1/10/03 0:00
1/10/03 12:00
Date/Time

Figure 8

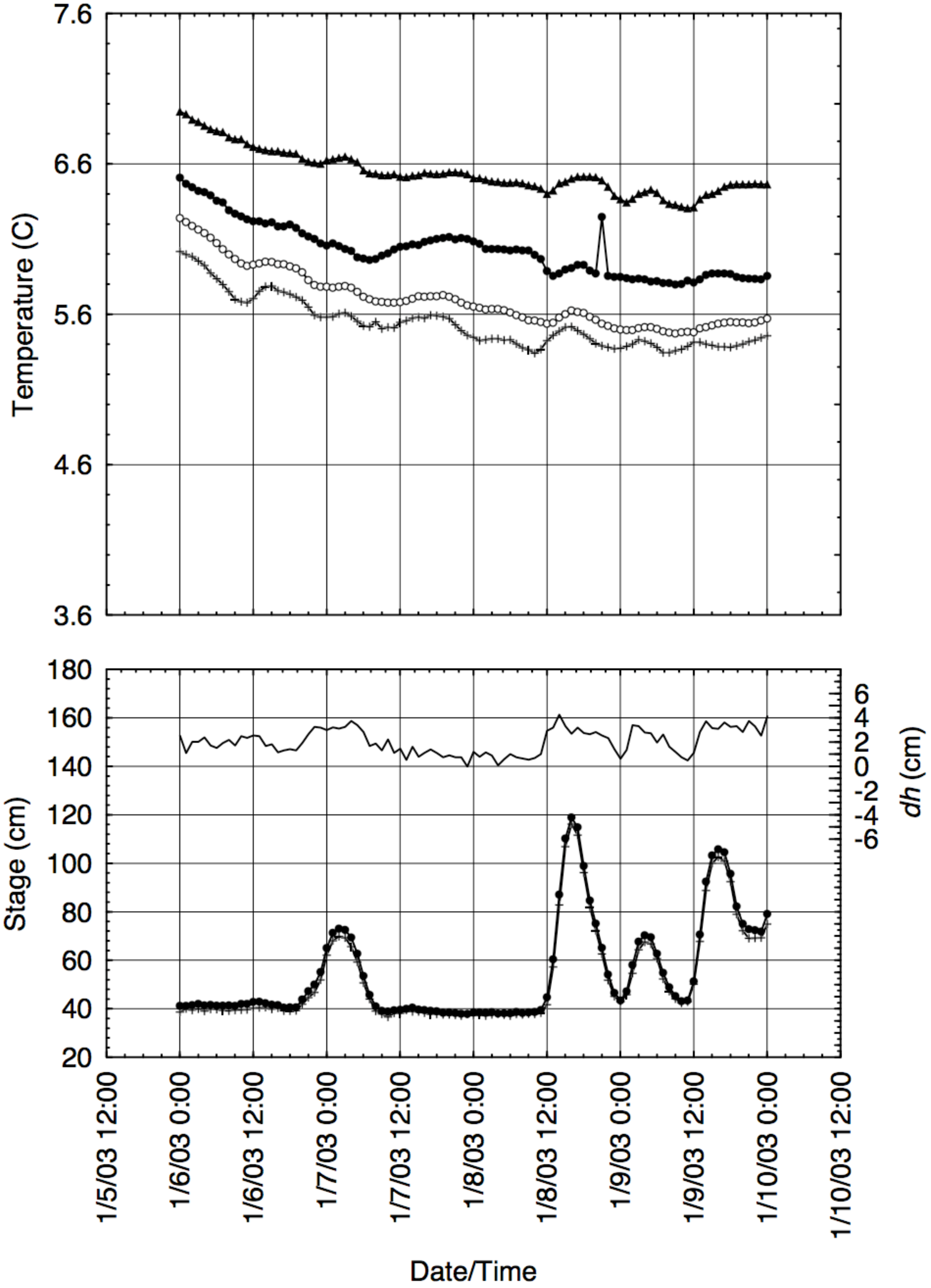
7.6
6.6
5.6
4.6
3.6
Temperature (C)
180
160
140
120
100
80
60
40
20
Stage (cm)
6
4
2
0
-2
-4
-6
dh (cm)
1/5/03 12:00
1/6/03 0:00
1/6/03 12:00
1/7/03 0:00
1/7/03 12:00
1/8/03 0:00
1/8/03 12:00
1/9/03 0:00
1/9/03 12:00
1/10/03 0:00
1/10/03 12:00
Date/Time

Figure 9

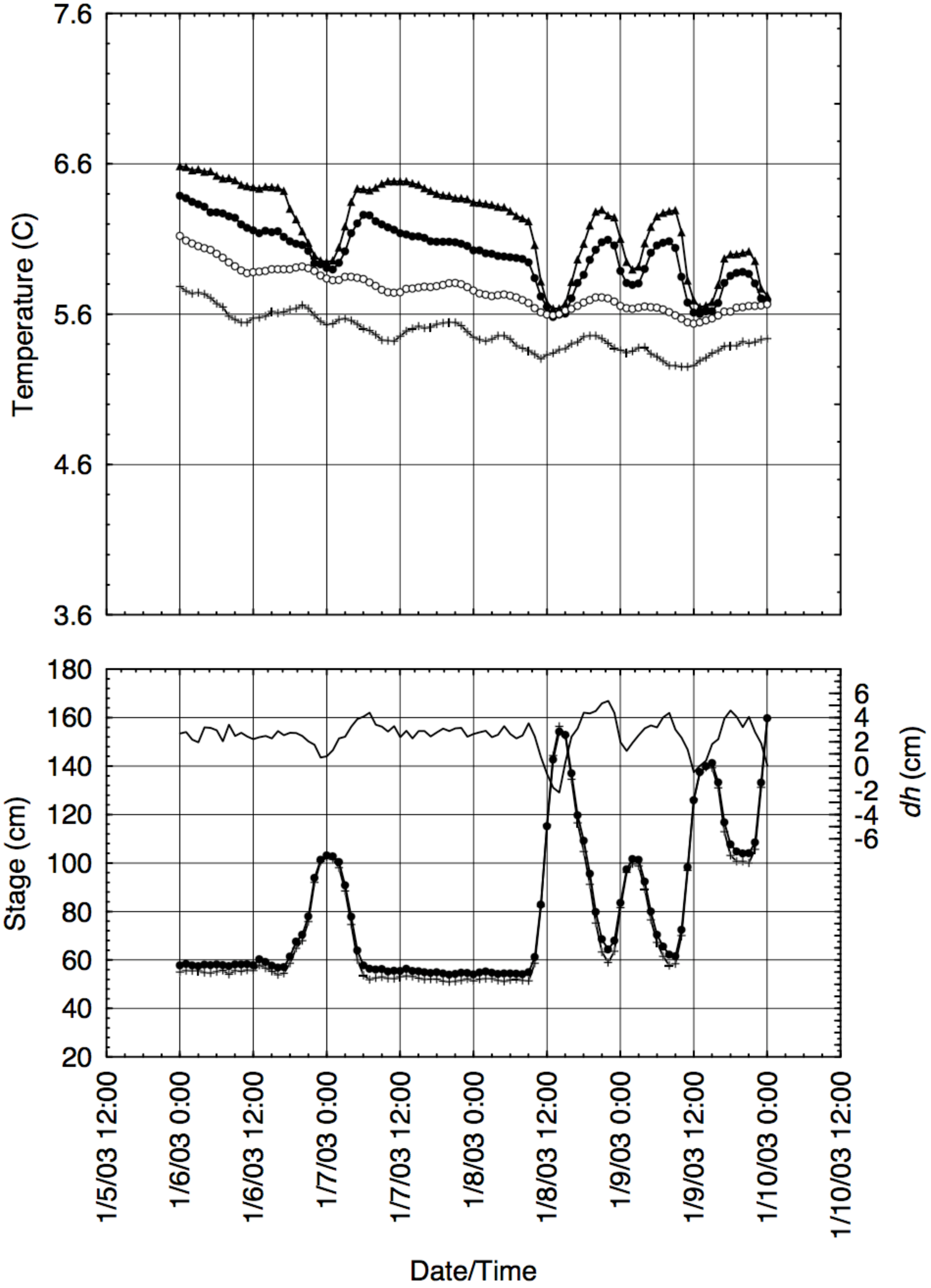
Temperature (C)
7.6
6.6
5.6
4.6
3.6
Stage (cm)
180
160
140
120
100
80
60
40
20
dh (cm)
6
4
2
0
-2
-4
-6
1/5/03 12:00
1/6/03 0:00
1/6/03 12:00
1/7/03 0:00
1/7/03 12:00
1/8/03 0:00
1/8/03 12:00
1/9/03 0:00
1/9/03 12:00
1/10/03 0:00
1/10/03 12:00
Date/Time

Figure 10

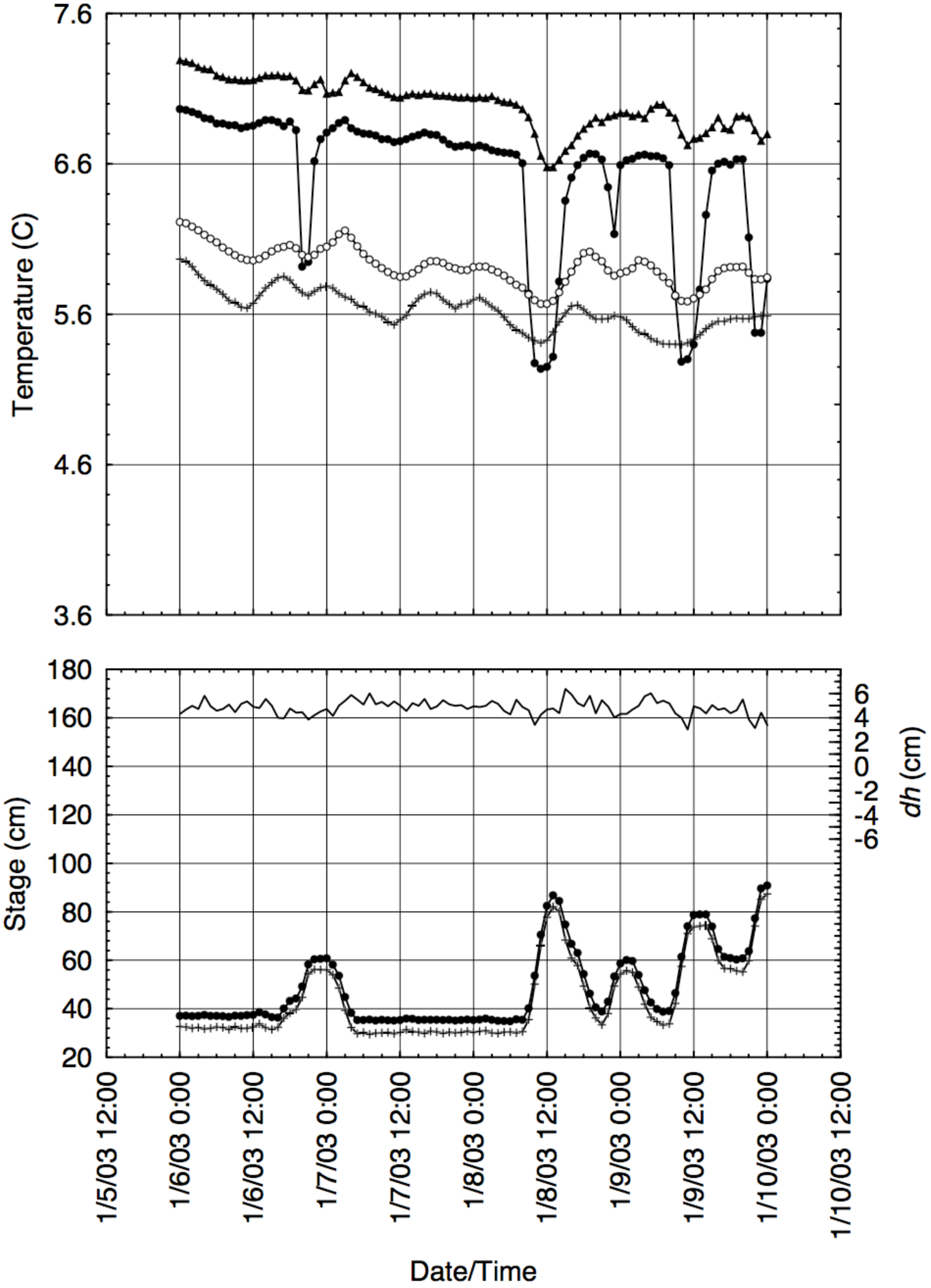
7.6
6.6
5.6
4.6
3.6
Temperature (C)
180
160
140
120
100
80
60
40
20
Stage (cm)
6
4
2
0
-2
-4
-6
dh (cm)
1/5/03 12:00
1/6/03 0:00
1/6/03 12:00
1/7/03 0:00
1/7/03 12:00
1/8/03 0:00
1/8/03 12:00
1/9/03 0:00
1/9/03 12:00
1/10/03 0:00
1/10/03 12:00
Date/Time

Figure 11

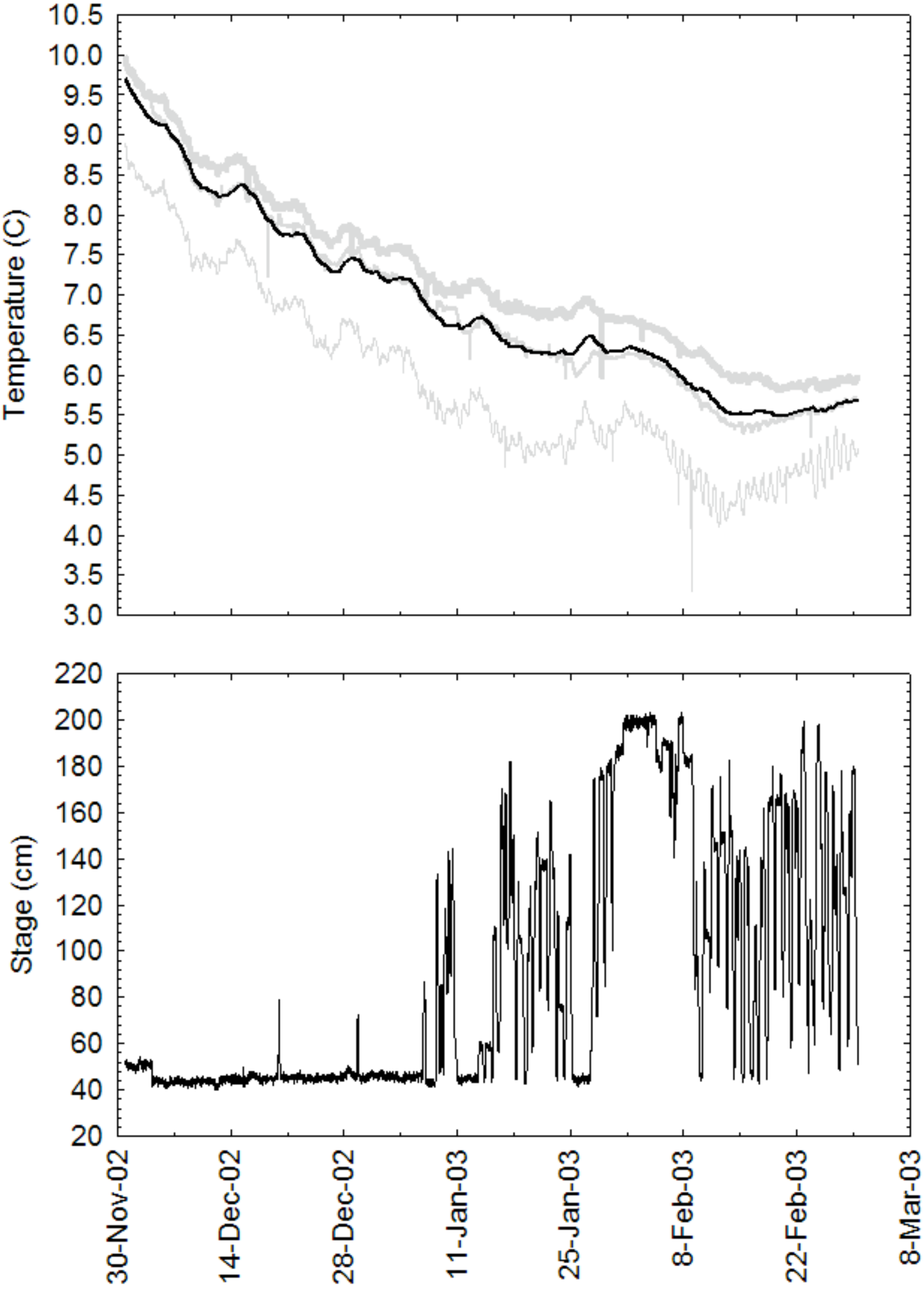
Temperature (C)
10.5
10.0
9.5
9.0
8.5
8.0
7.5
7.0
6.5
6.0
5.5
5.0
4.5
4.0
3.5
3.0
Stage (cm)
220
200
180
160
140
120
100
80
60
40
20
30-Nov-02
14-Dec-02
28-Dec-02
11-Jan-03
25-Jan-03
8-Feb-03
22-Feb-03
8-Mar-03

Figure 12

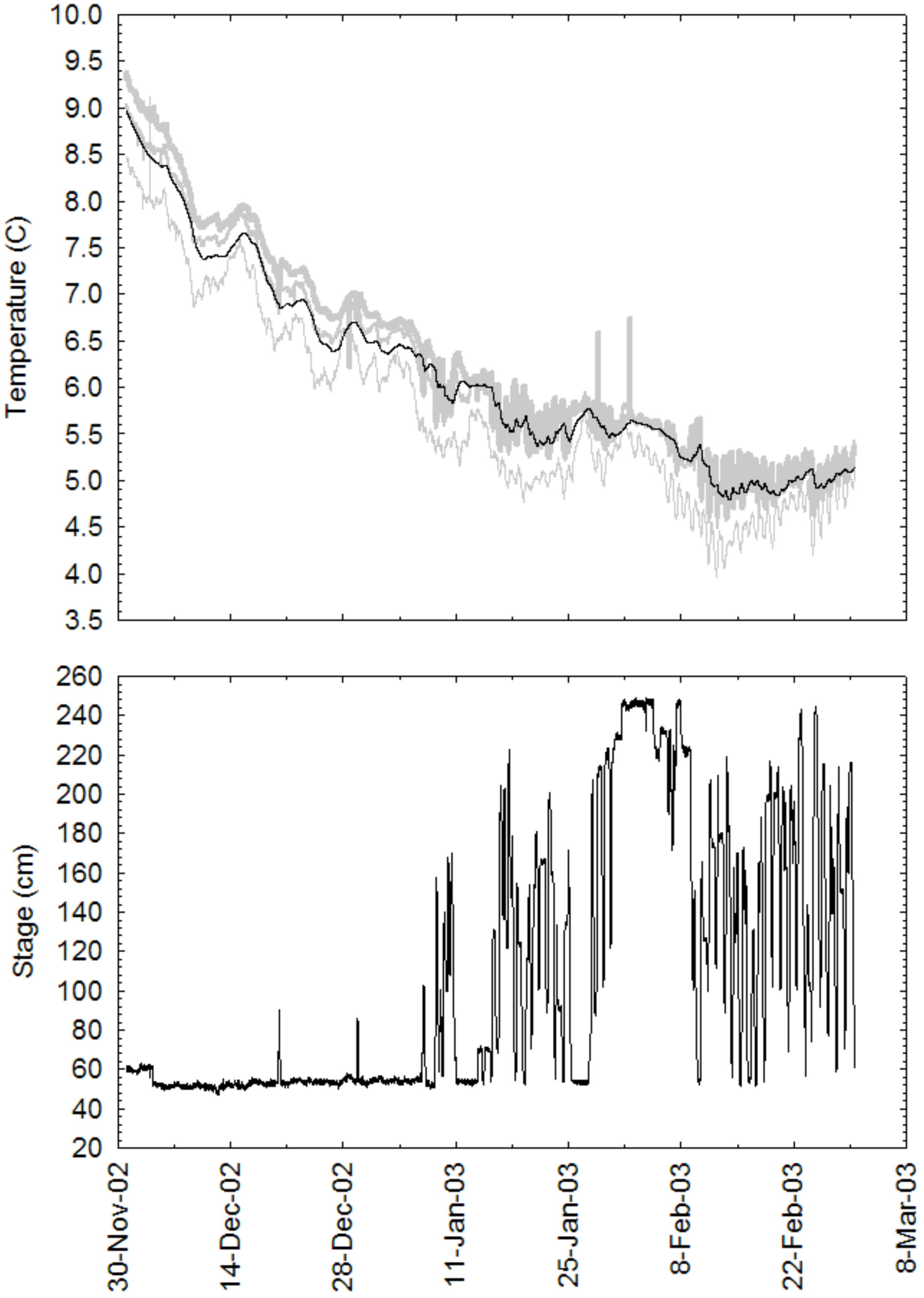
10.0
9.5
9.0
8.5
8.0
7.5
7.0
6.5
6.0
5.5
5.0
4.5
4.0
3.5
Temperature (C)
260
240
220
200
180
160
140
120
100
80
60
40
20
Stage (cm)
30-Nov-02
14-Dec-02
28-Dec-02
11-Jan-03
25-Jan-03
8-Feb-03
22-Feb-03
8-Mar-03

Figure 13

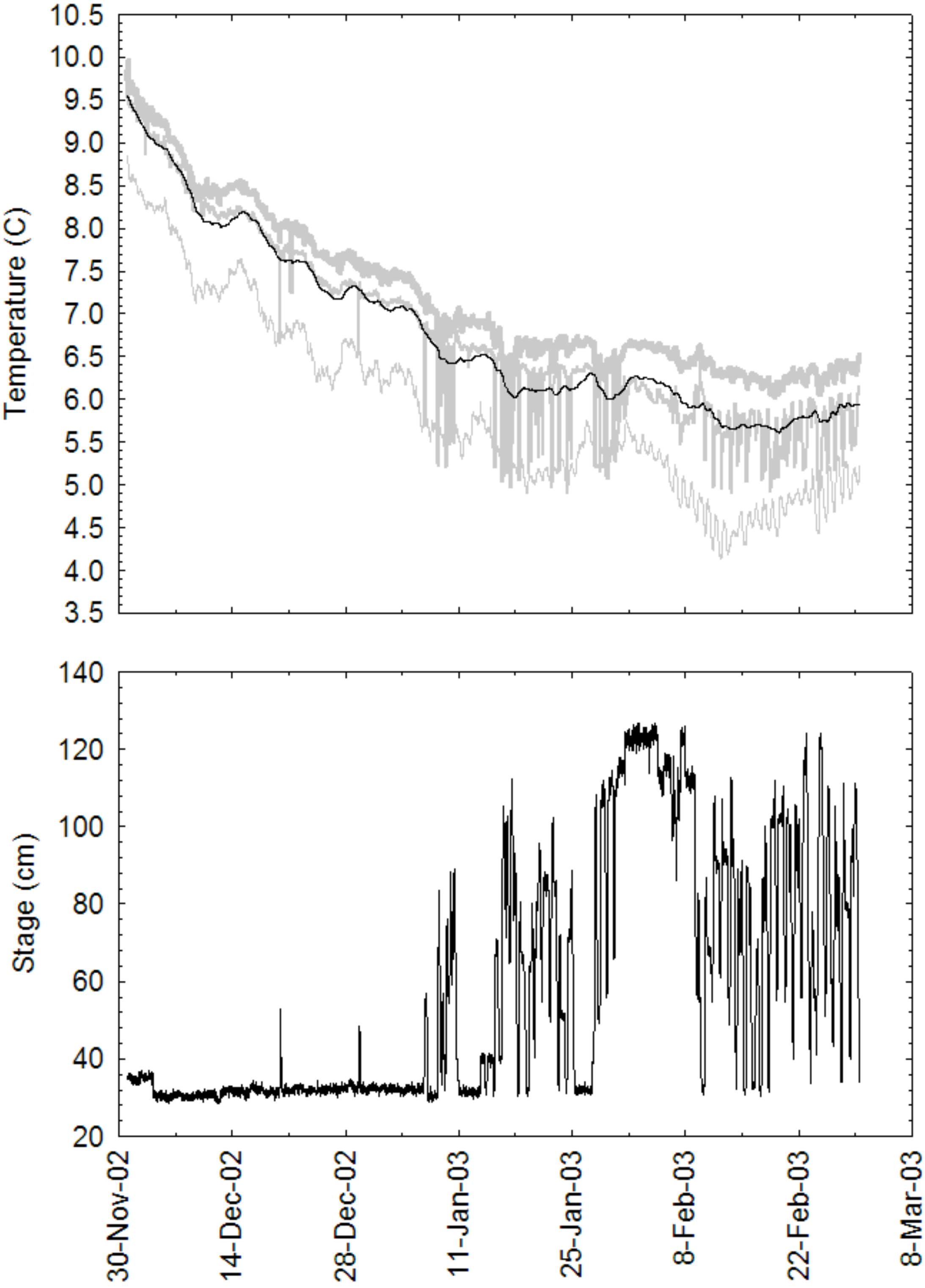
10.5
10.0
9.5
9.0
8.5
8.0
7.5
7.0
6.5
6.0
5.5
5.0
4.5
4.0
3.5
Temperature (C)
140
120
100
80
60
40
20
Stage (cm)
30-Nov-02
14-Dec-02
28-Dec-02
11-Jan-03
25-Jan-03
8-Feb-03
22-Feb-03
8-Mar-03

Figure 14

MANUSCRIPT THREE

Full title:

Large-scale spatial variability of riverbed temperature gradients in Snake River fall Chinook salmon spawning areas

Short title:

Riverbed temperature gradients in the Snake River

Author:

Timothy P. Hanrahan
Pacific Northwest National Laboratory
P.O. Box 999 MS K6-85
Richland, WA 99354
ph. 509 376 0972
tim.hanrahan@pnl.gov

Keywords: temperature; hyporheic; riverbed; salmon

Abstract

In the Snake River basin of the Pacific northwestern United States, hydroelectric dam operations are often based on the predicted emergence timing of salmon fry from the riverbed. The spatial variability and complexity of surface water and riverbed temperature gradients results in emergence timing predictions that are likely to have large errors. The objectives of this study were to quantify the thermal heterogeneity between the river and riverbed in fall Chinook salmon spawning areas and to determine the effects of thermal heterogeneity on fall Chinook salmon emergence timing. This study quantified river and riverbed temperatures at 15 fall Chinook salmon spawning sites distributed in two reaches throughout 160 km of the Snake River in Hells Canyon, Idaho, USA, during three different water years. Temperatures were measured during the fall Chinook salmon incubation period with self-contained data loggers placed in the river and at three different depths below the riverbed surface. At all sites temperature increased with depth into the riverbed, including significant differences ($p<0.05$) in mean water temperature of up to 3.8°C between the river and the riverbed among all the sites. During each of the three water years studied, river and riverbed temperatures varied significantly among all the study sites, among the study sites within each reach, and between sites located in the two reaches. Considerable variability in riverbed temperatures among the sites resulted in fall Chinook salmon emergence timing estimates that varied by as much as 55 days, depending on the source of temperature data used for the estimate. Monitoring of riverbed temperature gradients at a range of spatial scales throughout the Snake River would provide better information for managing hydroelectric dam operations, and would aid in the design and interpretation of future empirical research into the ecological significance of physical riverine processes.

Introduction

Salmon populations in the Snake River basin of the Pacific northwestern United States (U.S.) have declined during the past 30 years, leading to their protection under the U.S. Endangered Species Act (ESA). In 1992, Snake River fall Chinook salmon (*Oncorhynchus tshawytscha*) were listed under the ESA as threatened (NMFS, 1992). This listing prompted management agencies, regulatory agencies, and researchers to initiate activities aimed at restoring these fish populations and the ecological functions that support them (ISG, 1996). Like many other river systems throughout the world where salmon populations are imperiled (e.g., Pacific salmon (*Oncorhynchus* spp.) in western North America, and Atlantic salmon (*Salmo salar*) in eastern North America and Europe), the flow magnitude and timing from hydroelectric dams in the Snake River basin is managed in part for the benefit of salmon (Groves and Chandler, 1999; Gibbins and Acornley, 2000; Gibbins *et al.,* 2002; Hendry *et al.,* 2003; Berland *et al.,* 2004).

In the Snake River basin, and in other regulated river systems, flow regime management operations are often based on the timing of when recently hatched young salmon emerge from their incubation location in the riverbed. For example, downstream from the Hells Canyon Complex of dams on the Snake River a minimum discharge is established during the fall Chinook salmon spawning period (early-October to early-December), which must be maintained through the period of salmon fry emergence (early-June of the following year) to protect embryos that are incubating in the riverbed (Groves and Chandler, 1999). The rate of embryonic development and emergence timing of Chinook salmon is controlled by temperature (Murray and Beacham, 1987; Beer and Anderson, 1997; Beer, 1999; Beer and Anderson, 2001). Because Chinook salmon eggs incubate within the riverbed at depths ranging from 18 to 43 cm beneath the riverbed surface (Chapman, 1988), the water temperature at egg pocket depth may be very different than the surface water temperature. Indeed, previous research from other salmon spawning areas suggests that egg pocket water temperatures during incubation can be considerably warmer than the surface water temperatures (Shepard *et al.,* 1986; Crisp, 1990; Geist *et al.,* 2002). Therefore, the use of surface water temperatures to predict emergence timing, as is common in European and North American rivers (Clark *et al.,* 1999; Beer and Anderson, 2001; Connor *et al.,* 2003), may result in considerable error (Shepard *et al.,* 1986; Acornley, 1999). In a highly regulated river system like the Snake River basin, these errors in predicted emergence timing may have significant implications for water policy decisions in general (e.g., trade-offs between protecting incubating salmon embryos and refilling reservoirs), and for the survival of Snake River fall Chinook salmon in particular. Errors in predicted emergence timing may be compounded by failing to consider the variation in surface water or riverbed temperatures throughout a reach (Clark *et al.,* 1999).

During the past twenty years much effort has been focused on studying temperature gradients within riverbeds. Some of these research efforts have focused on river energy budgets, wherein the primary interest is surface water temperatures, including the energy flux from the bed (Sinokrot and Stefan, 1993; Hondzo and Stefan, 1994; Sinokrot and Stefan, 1994; Webb and Zhang, 1997; Constantz, 1998; Evans *et al.,* 1998; Webb and Zhang, 1999). Other research on temperature gradients within riverbeds has concentrated on the hydrologic exchange between surface and subsurface water (i.e., the hyporheic zone) (Hanrahan, In review), largely in the context of determining water budgets for stream reaches (Lapham, 1989; Silliman and Booth, 1993; Silliman *et al.,* 1995; Harvey *et al.,* 1996). Hyporheic temperature studies have also been completed in the context of ecological implications, including macroinvertebrate distributions (Marmonier and Creuze des Chatelliers, 1991; Dole-Olivier and Marmonier, 1992; Stanley and Boulton, 1993), physicochemical processes (White *et al.*, 1987; Triska *et al.,* 1989; Hendricks and White, 1991), and effects on the life-cycle of fishes (Shepard *et al.,* 1986; Crisp, 1990; Acornley, 1999; Baxter and McPhail, 1999; Hanrahan *et al.*, 2004).

While it is generally recognized that temperature fluctuations within riverbeds become more reduced with depth below the riverbed surface, relative to surface water temperatures, it is equally evident that riverbed temperatures are a complex function of water and heat transfer processes at multiple spatial and temporal scales (Clark *et al.,* 1999; Johnson, 2004; Brown *et al.*, 2005). Therefore, predicting riverbed temperature profiles from surface water temperature alone would likely result in considerable error.

Management agencies in the Snake River basin are tasked with managing the discharge operations of the Hells Canyon Complex of dams for multiple uses, including tradeoffs between providing sufficient downstream flow to protect incubating embryos of imperiled fall Chinook salmon and limiting downstream flow in order to refill reservoirs. Because these water management decisions are based on the emergence timing of fall Chinook salmon, there is a need to quantify the temperature gradient between the river and riverbed in fall Chinook salmon spawning areas, as temperature is the primary basis for emergence timing estimates. There are currently limited published empirical data available quantifying the temperature gradients within Snake River fall Chinook salmon spawning areas (Hanrahan, In review), and there are no empirical data quantifying the variability of temperature gradients among the spawning areas distributed over 160 river kilometers (rkm). Current estimates of Snake River fall Chinook salmon emergence timing are based on surface water temperatures from two locations (Connor *et al.*, 2003), which may result in considerable error. In general, in efforts to link physical habitat characteristics, such as temperature gradients within the riverbed, to the effects on biota, it is important to consider the linkages on a wide range of temporal and spatial scales (Armstrong *et al.,* 1998; Folt *et al.,* 1998).

In this paper I report on river and riverbed temperatures at fifteen fall Chinook salmon spawning sites throughout a 160 rkm reach of the Snake River. The research hypothesis was that river and riverbed temperature differences within and among Snake River fall Chinook salmon spawning areas would be large enough to result in biologically significant differences in emergence timing estimates. Specific objectives of the study were to: (1) quantify the thermal heterogeneity between the river and riverbed within and among fall Chinook salmon spawning areas; and (2) quantify the effects of thermal heterogeneity on fall Chinook salmon emergence timing.

Methods

Study Area

This research was conducted throughout 160 km of the Hells Canyon reach (HCR) of the Snake River, located in western Idaho, U.S. The HCR extends from Hells Canyon Dam (river kilometer (rkm) 399) downstream to Asotin Creek near rkm 240 (Figure 1). The Hells Canyon Complex (Hells Canyon, Oxbow, and Brownlee dams) controls nearly all of the flow through the upper HCR (upstream of the Salmon River; hereafter upper reach), and just over 50% of the flow in the lower HCR (downstream of the Salmon River; hereafter lower reach). Immediately downstream from Hells Canyon Dam at U. S. Geological Survey (USGS) gage 13290450, mean daily discharge has averaged 589 m^3/s since 1965. Over this same time period, mean daily discharge in the lower reach has averaged 1035 m^3/s (USGS gage 13334300, rkm 269). Inputs from the Imnaha, Salmon and Grande Ronde rivers (USGS gages 13292000, 13317000, and 13333000, respectively) during this period make up a mean daily discharge of 426 m^3/s, resulting in a residual input of approximately 20 m^3/s from tributaries between Hells Canyon Dam (rkm 399) and the Imnaha River confluence (rkm 307).

Study sites were selected by stratified random sampling of fall Chinook salmon spawning locations. The HCR was stratified into three segments based on longitudinal valley slope and the confluence with major tributaries. The upper segment extends from Hells Canyon Dam (rkm 399) downstream to a fault zone near Pine Bar (rkm 364), and has a longitudinal slope of 0.002. The middle and lower segments are separated just downstream of the Salmon

River confluence (near rkm 298), where the longitudinal gradient changes from 0.001 (middle segment) to 0.0007 (lower segment). Fall Chinook salmon redd counts from 1997 to 2001 were used to identify the 56 most used spawning sites (Garcia *et al.*, 2003). Of the 56 spawning sites, 20% were in the upper segment, 48% in the middle segment, and 32% in the lower segment. Fourteen study sites (25% of the total) were randomly selected for sampling during the fall Chinook salmon spawning and incubation period of October 2002–March 2003, with the number in each segment corresponding to the proportion of spawning sites within each segment. During the same months of 2003–2004 and 2004–2005, ten and four sites, respectively, were selected for subsequent sampling (Table 1). The physical characteristics at each site include channel widths ranging from 70 to 270 m, depths ranging from 0.3 to 2.5 m, velocities ranging from 0.5 to 1.5 m s^{-1}, and median riverbed surface grain sizes ranging from 32 to 60 mm (TP Hanrahan, unpublished data; Miller *et al.*, 2002).

Site-scale study design

Temperature data were collected through the use of self-contained temperature data loggers placed in piezometers. Each site contained one cluster of two piezometers and one river standpipe spaced within 1 m of one another. One piezometer monitored the shallow hyporheic zone (30 cm) while the other monitored the deeper hyporheic zone (60 cm). One temperature data logger (Solinst model 3001 mini LT Levelogger M10) was placed at the sampling depth within each piezometer and within the river standpipe. According to calibration certificates provided by the data logger manufacturer, the instruments are accurate to ± 0.1°C. The data loggers were programmed to record temperature at 20 min intervals during the fall Chinook salmon spawning and incubation period of the water years 2002–2003, 2003–2004, and 2004–2005. Data loggers were deployed on 20 October 2002, 25 October 2003, and 15 October 2004. During each sampling year the piezometers were installed at different locations within each study site, but the locations were always within 10 m of where they were located during other sampling years. Details on piezometer construction and installation can be found in Hanrahan *et al.* (2004).

Additional temperature data were acquired from each site through placement of self-contained temperature data loggers (Onset Water Temp Pro) in artificial egg pockets (Table 1). The egg pockets were spaced 3–5 m apart at each site, and were created by excavating with a hydraulic pump and hand tools a surface area of approximately 1 m^2. An attempt was made to excavate each egg pocket to the approximate depth of natural fall Chinook salmon egg pockets. While the depth of Snake River fall Chinook salmon egg pockets is unknown, Chinook salmon egg pocket depths in the Columbia River ranged from 19 to 37 cm beneath the riverbed surface (Chapman *et al.*, 1986). Two different containers were used to place the temperature data logger within each artificial egg pocket. One container was a perforated PVC tube 30 cm length and 3 cm inside diameter. The other container was a gravel-filled cylindrical basket (25 cm in length x 15 cm inside diameter) constructed from plastic mesh fabric. Both containers were placed in the artificial egg pockets with the long axis oriented parallel to the riverbed surface and perpendicular to the direction of river flow. Because of the difficulty in excavating the artificial egg pockets to sufficient depth, and the associated concern regarding scouring around the large diameter baskets, the depth during deployment and retrieval was measured for the baskets (Table 1). The temperature data loggers were programmed to record at 20 min intervals beginning in late-October to early-December of each water year (2002, 2003, 2004) until they were retrieved near the end of the egg incubation period during March of the following year. According to calibration certificates provided by the temperature data logger manufacturer, the instruments are accurate to ±0.17°C.

Data analysis

The data were analyzed by calculating average hourly water temperature for the river, egg pocket depth, shallow hyporheic zone (30 cm), and deep hyporheic zone (60 cm) at each site during the period from 18 November through 2 March of each water year sampled. This time period was selected because it begins near the peak of fall Chinook salmon spawning, and because it maximizes the use of available sample data from each site for each water year. Missing egg pocket temperature data during this time period (sites 152.3, 175.2, 198.2, and 238.6 during 2003–2004; site 175.2 during 2004–2005) were estimated based on ordinary least-squares regression with river temperatures. In all cases, missing data were estimated for less than 14 days. The coefficient of determination r^2 was 0.81 for site 152.3, and ranged 0.96–0.99 for all other sites.

Because of non-normality and unequal variances in the sample data, nonparametric statistical tests were used for all analyses. Random samples of approximately 95 were selected from each average hourly water temperature time series (Helsel and Hirsch, 2002), based on the sample size necessary to maintain a statistical power (β) of 0.95 (one-way analysis of variance (ANOVA), α=0.05, 4 treatment groups). Within each site, nonparametric Kruskal-Wallis ANOVA tests (α=0.05) were used to test the null hypothesis that there was no difference in mean temperature (based on ranks) among the river, egg pocket depth, shallow hyporheic zone, and deep hyporheic zone. Within each reach (lower and upper), Kruskal-Wallis ANOVA tests (α=0.05) or Mann-Whitney U tests (α=0.05) were used to test the null hypothesis that there was no difference in mean temperature (based on ranks) among or between the sites, based on river, egg pocket depth, shallow hyporheic zone, and deep hyporheic zone temperatures. Post-hoc multiple comparisons of mean ranks for all pairs of groups were used to identify significant differences among homogeneous groups (α=0.05). Nonparametric Mann-Whitney U tests (α=0.05) were used to evaluate differences between the lower and upper reaches, based on mean temperature of the river, egg pocket depth, shallow hyporheic zone, and deep hyporheic zone.

Accumulated temperature units (ATU) were calculated for the river, egg pocket depth, shallow hyporheic zone, and deep hyporheic zone at each site, where ATU is the sum of the daily average temperatures exceeding 0°C. For each of the three water years, the calculation of ATU began on 20 October 2002, 25 October 2003, and 15 October 2004. Emergence timing comparisons were based on the number of days required to reach 1066 ATU, which is indicative of the median emergence timing for Snake River fall Chinook salmon (Connor *et al.,* 2003).

Results

2002 – 2003 temperature

There was a positive temperature gradient between the river and the riverbed at all sites, with water temperatures increasing with depth into the riverbed. At 11 of the 14 study sites, there was a significant difference ($p<0.05$) in mean water temperature among the river, egg pocket depth, shallow hyporheic zone and deep hyporheic zone. The post-hoc multiple comparison tests indicated that at only one site (156.8) was there a significant difference between the river temperature and egg pocket temperature ($p=0.018$). Seven study sites had a significant temperature difference between the river and shallow hyporheic zone, while eleven sites had a significant temperature difference between the river and deep hyporheic zone (Table 2). The three sites with no significant differences in mean water temperature were all located in the upper reach, including 196.0 ($H=1.81$, $df=3$, $n=391$, $p=0.61$), 240.6 ($H=5.96$, $df=3$, $n=448$, $p=0.11$), and 244.5 ($H=3.13$, $df=3$, $n=434$, $p=0.37$).

At 10 of the 14 study sites, the average egg pocket temperature at each site was within 0.3°C of the river temperature, indicating rapid advection of river water into the egg pockets (Table 2). At the deeper locations within the riverbed, temperature gradients were larger in magnitude than the temperature gradient at egg pocket depth. At sites in the lower reach, the mean temperature gradient between the river and the deep hyporheic zone was 0.9–1.6°C (Table 2). Over the duration of the fall Chinook salmon egg incubation period, this temperature gradient ranged 0.1–2.2°C among sites in the lower reach. The mean temperature gradient between the river and the deep hyporheic zone was similar in the upper reach (0.0–1.6°C, Table 2), ranging 0.0–2.0°C. The mean temperature gradient between the river and the shallow hyporheic zone was 0.3–1.1°C in the lower reach, and 0.0–1.0°C in the upper reach (Table 2). Over the duration of the fall Chinook salmon egg incubation period the temperature gradient between the river and the shallow hyporheic zone ranged 0.0–1.5°C in the lower reach, and 0.0–1.3°C in the upper reach.

Comparisons among sites within the upper reach indicated significant differences in the water temperature of the river, egg pocket depth, shallow hyporheic zone, and deep hyporheic zone. Mean river temperature in the upper reach ranged 6.1–6.7°C, with only sites 244.5 and 198.2 being significantly different from one another (p=0.004). Mean egg pocket temperatures in the upper reach ranged 6.1–6.7°C, with only sites 240.6 and 222.7 being significantly different from one another (p=0.03). As depth within the riverbed increased, differences in water temperature among the sites increased. Mean shallow hyporheic zone temperatures in the upper reach ranged 6.3–7.4°C, with all of the sites being significantly different from at least one other site (H=67.52, df=9, n=1006, p<0.001). Mean deep hyporheic zone temperatures in the upper reach ranged 6.3–8.0°C, with all of the sites being significantly different from at least one other site (H=137.36, df=9, n=962, p<0.001). Comparisons among sites within the lower reach indicated significant differences in the water temperature of the shallow and deep hyporheic zone, but not the river or egg pocket depth. Mean shallow hyporheic zone temperatures in the lower reach ranged 5.7–6.3°C, with all of the sites being significantly different from at least one other site (H=38.79, df=3, n=401, p<0.001). Mean deep hyporheic zone temperatures in the lower reach ranged 6.3–6.8°C, with all of the sites being significantly different from at least one other site (H=25.94, df=3, n=404, p<0.001).

Comparisons between the upper reach and lower reach indicated considerable differences in the water temperature of the river, egg pocket depth, shallow hyporheic zone, and deep hyporheic zone ($p<0.001$ for all tests). In all cases, the mean water temperature in the upper reach was greater, and had a larger range, than that in the lower reach (Figure 2). The difference in mean temperature between the upper and lower reaches for the river, egg pocket depth, shallow hyporheic zone, and deep hyporheic zone was 1.0°C, 0.9°C, 0.8°C, and 0.6°C, respectively.

2003 – 2004 temperature

Temperature patterns within all of the study sites were similar to those during the 2002–2003 water year. At 6 of the 10 study sites, there was a significant difference ($p<0.05$) in mean water temperature among the river, egg pocket depth, shallow hyporheic zone and deep hyporheic zone. The post-hoc multiple comparison tests indicated that none of the sites had significant differences between the river temperature and egg pocket temperature. Five study sites had a significant temperature difference between the river and shallow hyporheic zone, while six sites had a significant temperature difference between the river and deep hyporheic zone (Table 3). As during the 2002–2003 water year, the four sites with no significant differences in mean water temperature were all located in the upper reach. Three of these four sites also showed no significant differences in mean water temperature during the 2002–2003 water year, including 196.0 ($H=2.02$, $df=3$, $n=420$, $p=0.57$), 240.6 ($H=6.06$, $df=3$, $n=413$, $p=0.11$), and 244.5 ($H=2.26$, $df=3$, $n=384$, $p=0.52$).

Indications of rapid advection of river water into the artificial egg pockets continued during the 2003–2004 water year, as 6 of the 10 study sites had an average egg pocket temperature within 0.3°C of the river temperature (Table 3). At sites in the lower reach, the mean temperature gradient between the river and the deep hyporheic zone was 0.3–1.8°C (Table 3). Over the duration of the fall Chinook salmon egg incubation period, this temperature gradient ranged 0.0–2.8°C among sites in the lower reach. The mean temperature gradient between the river and the deep hyporheic zone was smaller in the upper reach (0.1–1.5°C, Table 3), ranging 0.0–2.5°C. The mean temperature gradient between the river and the shallow hyporheic zone was 0.5–1.0°C in the lower reach, and 0.0–1.3°C in the upper reach (Table 3). Over the duration of the fall Chinook salmon egg incubation period the temperature gradient between the river and the shallow hyporheic zone ranged 0.2–2.4°C in the lower reach, and 0.0–1.3°C in the upper reach.

Comparisons among sites within the upper reach indicated significant differences in the water temperature of the shallow hyporheic zone and deep hyporheic zone. Mean shallow hyporheic zone temperatures in the upper reach ranged 5.4–6.5°C, with 3 of the 8 upper reach sites being significantly different from at least one other site (H=22.02, df=7, n=780, p=0.003). Mean deep hyporheic zone temperatures in the upper reach ranged 5.6–7.2°C, with all of the sites being significantly different from at least one other site (H=51.58, df=7, n=819, p<0.001). As in the upper reach, comparisons between the two sites in the lower reach indicated significant differences in the water temperature of the shallow and deep hyporheic zone (p=0.01 and p<0.001, respectively).

As during the 2002–2003 water year, comparisons between the upper reach and lower reach indicated differences in the water temperature of the river, egg pocket depth, and shallow hyporheic zone (p<0.05 for all tests). However, these differences were smaller than those observed during the 2002–2003 water year. The difference in mean temperature between the upper and lower reaches for the river, egg pocket depth, shallow hyporheic zone, and deep hyporheic zone was 0.7°C, 0.8°C, 0.5°C, and 0.3°C, respectively. Mean water temperature in the deep hyporheic zone was not significantly different between the two reaches (p=0.66). In all cases, the mean water temperature in the upper reach was greater, and had a larger range, than that in the lower reach (Figure 3).

2004 – 2005 temperature

At all four of the study sites, there was a significant difference ($p<0.05$) in mean water temperature among the river, egg pocket depth, shallow hyporheic zone and deep hyporheic zone. The post-hoc multiple comparison tests indicated that none of the sites had significant differences between the river temperature and egg pocket temperature, while all of the sites had significant differences between the river and the shallow and deep hyporheic zone (Table 4). The temperature patterns at each of the four study sites were similar to when they were sampled in previous water years. For example, at sites 152.3, 198.2, and 222.7 there was a small temperature gradient between the river and artificial egg pockets and a much larger gradient between the river and the deep hyporheic zone, as was the case during 2002–2003 and 2003–2004 (Tables 2–4).

As during the 2002–2003 and 2003–2004 water years, there were indications of rapid advection of river water into the artificial egg pockets, as 3 of the 4 study sites had an average egg pocket temperature within 0.2°C of the river temperature (Table 4). At the two lower reach sites, the mean temperature gradient between the river and the deep hyporheic zone was 0.9–1.3°C (Table 4). Over the duration of the fall Chinook salmon egg incubation period, this temperature gradient ranged 0.0–3.8°C at sites 152.3 and 175.2. The mean temperature gradient between the river and the deep hyporheic zone was 1.2°C in the upper reach (Table 4), ranging 0.7–2.4°C at sites 198.2 and 222.7. The mean temperature gradient between the river and the shallow hyporheic zone was 0.6–0.9°C in the lower reach, and 0.5–1.5°C in the upper reach (Table 4). Over the duration of the fall Chinook salmon egg incubation period the temperature gradient between the river and the shallow hyporheic zone ranged 0.0–3.0°C in the lower reach, and 0.2–1.7°C in the upper reach.

Comparisons between sites in the upper reach indicated significant differences only in the water temperature of the shallow hyporheic zone ($p<0.001$). Water temperature in the river, artificial egg pockets, shallow hyporheic zone, and deep hyporheic zone were all significantly different between sites in the lower reach (p<0.001 for all tests).

Comparisons between the upper reach and lower reach indicated considerably larger differences in the water temperature of the river, egg pocket depth, shallow hyporheic zone and deep hyporheic zone (p<0.001 for all tests), than during the 2002–2003 and 2003–2004 water years. In all cases, the mean water temperature in the upper reach was greater, and had a larger range, than that in the lower reach (Figure 4). The difference in mean temperature between the upper and lower reaches for the river, egg pocket depth, shallow hyporheic zone, and deep hyporheic zone was 1.4°C, 1.1°C, 1.7°C, and 1.5°C, respectively.

Accumulated temperature units

At nearly all of the study sites, and during all water years studied, the artificial egg pockets accumulated temperature units at approximately the same rate as the surface water, owing to the small temperature gradient between the river and artificial egg pocket depth. During 2002–2003, the artificial egg pockets at all of the study sites reached 1066 ATU within five days of the surface water reaching 1066 ATU. There were similar observations during the 2003–2004 and 2004–005 water years, when the artificial egg pockets at all of the study sites reached 1066 ATU within 5 and 8 days, respectively, of the surface water reaching 1066 ATU (Table 5).

Within each site, the number of days required to reach 1066 ATU was highly variable among the different depths within the riverbed. The within-site difference between the surface water and the shallow hyporheic zone in the number of days required to reach 1066 ATU ranged from 1 day at sites 196.0 and 244.5 to 22 days at site 222.7 during 2002–2003 (Table 5). Similar large variability was observed during the 2003–2004 and 2004–2005 water years, when the within-site difference between the surface water and the shallow hyporheic zone in the number of days required to reach 1066 ATU ranged from 0 days at site 244.5 to 20 days at site

222.7. During 2002–2003, the within-site difference between the surface water and the deep hyporheic zone in the number of days required to reach 1066 ATU ranged from 2 days at sites 196.0 to 28 days at site 238.6 (Table 5). This difference increased to 33 days (site 198.2) during the 2003–2004 water year, and was 23 days during the 2004–2005 water year (site 222.7).

Among all the study sites, and during all the water years studied, the number of days required to reach 1066 ATU was also highly variable. At sites in the lower reach, the mean (range) number of days required to reach 1066 ATU was 163 (1) in the river, 161 (4) in the artificial egg pockets, 157 (5) in the shallow hyporheic zone, and 146 (7) in the deep hyporheic zone during the 2002–2003 water year (Figure 5). During the same water year a much larger range occurred among the sites in the upper reach, where the mean (range) number of days required to reach 1066 ATU was 139 (7) in the river, 137 (7) in the artificial egg pockets, 130 (24) in the shallow hyporheic zone, and 123 (26) in the deep hyporheic zone (Figure 5). Similar large variability within and between reaches was observed during the 2003–2004 water year. For example, the mean (range) number of days required to reach 1066 ATU in the artificial egg pockets was 170 (1) and 155 (5) in the lower and upper reach, respectively (Figure 5). During the 2004–2005 water year the differences between the upper and lower reach increased, wherein the number of days required to reach 1066 ATU was much smaller at all measurement locations in the upper reach than at those in the lower reach (Figure 5).

Discussion

The results of this study indicate that riverbed temperatures are warmer than water column temperatures during the Snake River fall Chinook salmon incubation period. During each of the three water years studied, the water temperatures measured in the riverbed and water column varied significantly among all the study sites, among the study sites within each reach, and between sites located in the upper and lower reaches. The positive vertical temperature gradient with depth into the riverbed resulted in a concomitant increased rate of accumulated temperature units (ATU) with depth into the riverbed. At some sites using water column and riverbed temperatures to estimate median emergence timing resulted in very small differences, while at other sites the result was very large differences in emergence timing. During each of the three water years studied, the largest differences in emergence timing estimates resulted from comparisons of riverbed temperatures between the upper and lower reaches. Collectively, the findings reported in this paper indicate that the use of riverbed temperatures from more than one site within each reach would produce the most accurate estimates of fall Chinook salmon emergence timing in the Snake River.

The magnitude of the temperature difference between the riverbed and water column increased with depth into the riverbed, a finding not uncommon among studies of riverbed temperatures (Crisp, 1990; Malcolm *et al.,* 2002; Malcolm *et al.,* 2004). At all sites, and during all three water years studied, the temperature gradient between the riverbed surface and the artificial egg pocket depth was very small, indicating that river water rapidly mixed into the artificial egg pockets. This was likely a combined function of the shallow burial depth of the temperature sensor within the egg pocket, and very high hydraulic conductivity in the egg pocket resulting from egg pocket construction (Crisp and Carling, 1989; Kondolf, 2000). While there are no empirical data for the depth of natural Snake River fall Chinook salmon egg pockets, it is likely that the artificial egg pockets used in this study, especially at those sites using baskets during the 2003–2004 and 2004–2005 water years (Table 1), were on the lower end of the depth range (19–37 cm) reported for Columbia River fall Chinook salmon egg pockets (Chapman *et al.*, 1986). Therefore, temperature data from the artificial egg pockets may not be indicative of water temperatures within most natural Snake River fall Chinook salmon egg pockets.

The deeper locations within the riverbed sampled for this study may be as similar (more similar) to the depth of natural fall Chinook salmon egg pockets as (than) the artificial egg pockets used for the study. The temperature sensors in the shallow hyporheic zone piezometers were located at depths (30 cm) below the riverbed surface that were well within the range (19–37 cm) of observed fall Chinook salmon egg pocket depths in the Columbia River (Chapman *et al.*, 1986). Indeed, these authors suggested that the measured mean depth (29 cm) to the bottom of the egg pockets was an underestimate due to their measurement method (Chapman *et al.*, 1986). Chinook salmon egg pocket depths in other rivers have been measured as deep as 80 cm (DeVries, 1997), with most eggs located in the deepest portion of the redd (Chapman, 1988). The research reviewed by Chapman (1988) also indicates that egg pockets dug early during redd construction are deeper below the riverbed surface than those dug later. While egg pockets are buried by mounds of excavated riverbed material (tailspills), it is thought that most Chinook salmon egg pockets lie upstream of the tailspill crest (Chapman, 1988), and therefore are not likely to be scoured any deeper than the adjacent riverbed (Rennie and Millar, 2000). Considering the large range of the depth of Chinook salmon egg pockets observed in other rivers (DeVries, 1997), and the description of natural egg pocket construction observed by Chapman *et al.* (1986), the depth to incubating Snake River fall Chinnok salmon embryos could be comparable to the depth below the riverbed surface at which the temperature sensors in the shallow and deep hyporheic zone were located.

While the depth of the shallow and deep hyporheic zone temperature sensors may be indicative of natural fall Chinook salmon egg pocket depths, it is uncertain whether the substrate composition and structure of the riverbed environment that was sampled is comparable to that of a natural egg pocket. Because the shallow and deep hyporheic zone temperature was measured in the undisturbed riverbed, a reduced hydraulic conductivity at these locations may have contributed to the large temperature gradient observed at some sites. Previous research has indicated that redd excavation by spawning female salmon reduces the fine sediment content and increases the hydraulic conductivity of egg pockets (Kondolf, 2000). Other research has indicated a lack of persistence in egg pocket architecture, wherein the substrate grain size distributions in the egg pocket returned to prespawning conditions during the egg incubation period (Peterson and Quinn, 1996). However, there is still much uncertainty regarding how long the initial egg pocket substrate composition and structure persists after initial redd construction.

The water temperatures measured in the riverbed and water column varied significantly among the fourteen study sites, suggesting that measured water temperatures from any one site would not produce accurate estimates of fall Chinook salmon emergence timing for the entire Hells Canyon Reach of the Snake River. During all three water years studied, the largest temperature differences were observed in comparisons between sites located upstream (upper reach) and downstream (lower reach) of the Salmon River confluence. Water temperatures measured in the river, artificial egg pockets, shallow hyporheic zone and deep hyporheic zone were all significantly warmer in the upper reach than in the lower reach. These differences were expected, given the differences in physiography between the two reaches and the large increase in discharge contributed to the lower reach by the unregulated Salmon River and Grande Ronde River. Indeed, the water column temperature results were consistent with previous work in the Snake River (Connor *et al.,* 2003), wherein the mean temperature in the upper reach was larger than in the lower reach. However, the magnitude of this difference was larger for the water years reported in this paper (0.7°C, 1.0°C, 1.4°C) than for the water years reported by Connor *et al.* (2003) (0.4°C, 0.7°C, -0.8°C). The variability between these two datasets may be attributed to the one lower reach measurement location used by Connor *et al.* (2003) being located 18 km upstream of the mouth of the Grande Ronde River, and 51 km upstream of the downstream-most site used in the present study. It is likely that the Grande

Ronde River contributes significantly to the river temperature variability in the lower reach of the Snake River study area. The Grande Ronde watershed encompasses 6400 km^2 with elevations ranging from 3050 m in the mountainous headwaters to 250 m at the mouth of the Grande Ronde River.

Large variability in the magnitude of average riverbed temperature gradients in salmon spawning areas has been observed across a range of spatial scales. Ringler and Hall (1975) documented temperature gradients as large as 7.5°C within one spawning area of a coastal stream, while no temperature gradient existed within spawning areas of another stream in the same watershed. Even along a short reach in one small stream, temperature gradients in Atlantic salmon spawning areas have been observed to range from 0.1°C to more than 5.0°C (Malcolm *et al.,* 2002; Malcolm *et al.,* 2004; Youngson *et al.,* 2004). Similar findings have been documented in much larger rivers, including temperature gradients ranging from 0.0°C to 6.7°C in salmon spawning areas of the Columbia River (Geist *et al.,* 2002).

The water temperatures measured in the riverbed and water column varied significantly among the sites located within each reach as well, suggesting that water temperature data from more than one site in each reach would be necessary to produce accurate estimates of fall Chinook salmon emergence timing for the respective reach. Within both reaches the differences in water column and artificial egg pocket temperatures among the sites were small, whereas differences in hyporheic zone temperatures among sites within a reach were much larger. This finding indicates that the variability in riverbed temperatures contributes more to the differences among study sites than does the difference in water column temperatures.

The variability in riverbed temperatures among the sites within each reach is not surprising, given the complex hydrologic exchange (water and heat) processes occurring at multiple spatial and temporal scales (Clark *et al.,* 1999). The processes controlling this hydrologic exchange at the study sites are likely to be bedform-induced advective pumping, turbulence at the riverbed surface, and large-scale piezometric gradients along the longitudinal profile of the riverbed (Hanrahan, In review). The mobile riverbed at all of the study sites allows the development of local undulations of the riverbed surface, including those caused by spawning Chinook salmon (i.e., redd pits and tailspills) as well as by local bed scour and deposition. These bedforms promote advective pumping exchange between the river and riverbed, whereby the acceleration of flow over the bedform and flow separation at the crest create localized pressure variations that induce flow into and out of the bed (Savant *et al.*, 1987; Elliott and Brooks, 1997). Because all of the study sites have coarse bed surfaces (d_g of 24–80 mm) and high surface water velocities (0.4–1.4 m s^{-1}) (TP Hanrahan, unpublished data), it is likely that advective pumping and turbulent diffusion are major processes controlling hydrologic exchange between the river and the upper 1 m of the riverbed (Hanrahan, In review a). This is particularly evident at the depth of artificial egg pockets, where the temperatures were nearly isothermal with the river water. Heat transfer between surface water and the riverbed is realized through these exchange flows (i.e., advection) and in the absence of exchange flows through molecular diffusion processes (i.e., conduction) (Comer and Grenney, 1977; Sinokrot and Stefan, 1993; Hondzo and Stefan, 1994; Evans *et al.,* 1995; Clark *et al.,* 1999). Heat transfer through both advection and conduction is controlled by sedimentological properties of the riverbed material, including hydraulic conductivity, thermal conductivity, heat capacity, and thermal diffusivity (Lapham, 1989). Regardless of the mechanisms responsible for the hydrologic exchange between the river and riverbed at each site, the results of this study indicate that there is significant variability in riverbed temperature gradients throughout the Hells Canyon reach of the Snake River. This variability is an important consideration in estimating fall Chinook salmon emergence timing in the Snake River.

The positive vertical temperature gradient with depth into the riverbed resulted in a corresponding increased rate of accumulated temperature units (ATU) with depth into the riverbed. At some sites using water column and riverbed temperatures to estimate median emergence timing (1066 ATU for Snake River fall Chinook salmon (Connor *et al.,* 2003)) resulted in very small differences, while at other sites the result was very large differences in emergence timing. Other researchers working on smaller streams have reported similar variability of emergence timing estimates based on water column and riverbed temperatures. Acornley's (1999) predictions of brown trout (*Salmo trutta* L.) fry emergence based on riverbed temperatures were 17 days earlier than predictions based on water column temperatures. In comparisons between two sites, predictions of trout fry emergence based on water column temperatures showed little differences, while emergence predictions based on riverbed temperatures differed by 9 days (Acornley, 1999). Shepard *et al.* (1986) reported that their initial estimates of Pacific salmon (*Oncorhynchus* spp.) fry emergence timing based on water column temperatures differed by 9 days from the actual observed fry migration data. Their corrected emergence timing estimates based on intragravel temperatures resulted in predicted emergence occurring on the same date as observed fry migration (Shepard *et al.,* 1986). Similarly, Crisp (1990) reported that brown trout eggs incubated 20 cm below the riverbed surface at two sites in a small stream would hatch 10–11 days earlier than eggs incubated at the riverbed surface, although the effect on emergence timing was expected to be considerably less. Other predictions of brown trout and Atlantic salmon fry emergence timing based on riverbed temperatures have shown small differences (0–5 days) from predictions based on water column temperatures (Clark *et al.,* 1999; Malcolm *et al.,* 2002).

In this paper, the largest differences in emergence timing estimates come from comparisons among the measurement locations (river, artificial egg pocket, shallow hyporheic, deep hyporheic) between the upper and lower reach. When including data from just the river and shallow hyporheic zone locations, the differences between the upper and lower reaches in the days required to reach 1066 ATU ranged from 13 to 75 days for the three water years studied. Using just river temperatures during the three water years studied, emergence timing estimates for the upper and lower reach differed by 16 to 55 days. In another study specific to the Hells Canyon Reach of the Snake River, Connor *et al.* (2003) estimated that the emergence timing between the upper and lower reach differed by 7 to 10 days, based on three different years of water column temperature data. Their estimated reach differences in emergence timing are less than half of the average reach differences reported in this paper (14 to 48 days), based on water column temperatures. The different estimates from the two studies may be attributed to differences among water years studied, differences in the time periods used to calculate ATU, and the use of only one monitoring point in each reach by Connor *et al.* (2003). The use of one sampling point in the lower reach, upstream of the Grande Ronde River, by Connor *et al.* (2003) may have significant implications for emergence timing estimates, as 64% of the fall Chinook salmon redds in the lower reach are located downstream of the Grande Ronde River (Garcia *et al.*, 2004). In the present study, emergence timing estimates within the lower reach, upstream and downstream of the Grande Ronde River, differed by 9 days in 2004–2005 based on river temperatures.

Even within each reach, differences in emergence timing estimates among the measurement locations was large. When including data from just the river and shallow hyporheic zone locations, the differences in the days required to reach 1066 ATU ranged from 8 to 26 days for the three water years studied. These findings reinforce the suggestion that riverbed temperatures from more than one site within each reach would produce the most accurate estimates of fall Chinook salmon emergence timing in the Snake River. This suggestion is consistent with findings from previous research indicating that the large variability of riverbed temperature gradients hinders the ability to generalize the effects of egg burial depth on emergence timing from one site to another (Shepard *et al.,* 1986; Crisp, 1990; Acornley, 1999; Clark *et al.,* 1999; Malcolm *et al.,* 2002).

The emergence timing of salmon fry from the riverbed is directly related to the temperature at which the eggs are incubated. The fundamental growth mechanism driving emergence is yolk absorption. Of all the abiotic variables affecting egg-embryo development, temperature is the most important to yolk absorption (Beer and Anderson, 2001). While variability in behavior and life-history patterns do affect emergence timing, it is likely that the primary controlling factor of emergence is attainment of a development state between maximum alevin wet weight (including up to 40% of the weight as yolk) and complete yolk absorption (Murray and Beacham, 1987; Beacham and Murray, 1989; Beer and Anderson, 1997; Beer 1999). Salmon embryo survival and voluntary emergence from the riverbed is affected by other variables in addition to temperature (Beer and Anderson, 1997; Beer, 1999; Malcolm *et al.,* 2005), however it is temperature and the associated ATU that is used by management agencies as an indicator of emergence timing.

Snake River basin management agencies are tasked with managing the discharge operations of Hells Canyon Dam for multiple uses, including tradeoffs between providing sufficient downstream flow to protect incubating embryos of imperiled fall Chinook salmon and limiting downstream flow in order to refill reservoirs. Because these water management decisions are based on the emergence timing of fall Chinook salmon, there is a need to quantify the temperature gradient between the river and riverbed in fall Chinook salmon spawning areas, as temperature is the primary basis for emergence timing estimates. The findings reported in this paper indicate that the use of riverbed temperatures from more than one site within each reach would produce the most accurate estimates of fall Chinook salmon emergence timing in the Snake River. Because of the observed variability in riverbed temperatures among the study sites, it may be prudent to adopt a risk-based approach to monitoring riverbed temperatures when making decisions on flow management changes. This approach could emphasize a level of riverbed temperature monitoring that is proportional to the spawning habitat use of a site, such that sites with the most spawning activity are most intensely monitored. The monitoring of riverbed temperature gradients at a range of spatial scales throughout the Snake River, and other regulated river systems, will provide better information for making water policy decisions, and will aid in the design and interpretation of future empirical research into the ecological significance of physical riverine processes.

Acknowledgments

This research was funded by the U.S. Department of Energy Bonneville Power Administration (BPA) under the Northwest Power and Conservation Council's Fish and Wildlife Program. Co-funding was provided by Idaho Power Company (IPC). I extend my gratitude Brad Alcorn, Jim Chandler and Phil Groves at IPC, and Scott Abernethy, Evan Arntzen, and David Geist the Pacific Northwest National Laboratory (PNNL) for their cooperation and collaboration on the research project. Some of the data presented in this paper are included in PNNL Report 14850, a contract report to BPA. PNNL is operated by Battelle Memorial Institute for the U.S. Department of Energy under contract DE-AC06-76RLO-1830.

References

Acornley RM. 1999. Water temperatures within spawning beds in two chalk streams and implications for salmonid egg development. *Hydrological Processes* **13**: 439–446.

Armstrong JD, Grant JWA, Forsgren HL, Fausch KD, DeGraaf RM, Fleming IA, Prowse TD, and Schlosser IJ. 1998. The application of science to the management of Atlantic salmon (*Salmo salar*): integration across scales. *Canadian Journal of Fisheries and Aquatic Sciences* **55**: 303–311.

Baxter JS and McPhail JD. 1999. The influence of redd site selection, groundwater upwelling, and over-winter incubation temperature on survival of bull trout (*Salvelinus confluentus*) from egg to alevin. *Canadian Journal of Zoology* **77**: 1233–1239.

Beacham TD and Murray CB. 1989. Variation in developmental biology of sockeye salmon (*Oncorhynchus nerka*) and chinook salmon (*O. tshawytscha*) in British Columbia. *Canadian Journal of Zoology* **67**: 2081–2089.

Beer NW. 1999. Comparison of mechanistic and empirical methods for modeling embryo and alevin development in chinook salmon. *North American Journal of Aquaculture* **61**: 126–134.

Beer NW and Anderson JJ. 2001. Effect of spawning day and temperature on salmon emergence: interpretations of a growth model for Methow River chinook. *Canadian Journal of Fisheries and Aquatic Sciences* **58**: 943–949.

Beer NW and Anderson JJ. 1997. Modelling the growth of salmonid embryos. *Journal of Theoretical Biology* **189**: 297–306.

Berland G, Nickelsen T, Heggenes J, Okland F, Thorstad EB, and Halleraker J. 2004.

Movements of wild Atlantic salmon parr in relation to peaking flows below a hydropower station. *River Research and Applications* **20**: 957–966.

Brown LE, Hannah DM, and Milner AM. 2005. Spatial and temporal water column and streambed temperature dynamics within an alpine catchment: implications for benthic communities. *Hydrological Processes* **19**: 1585–1610.

Chapman DW. 1988. Critical review of variables used to define effects of fines in redds of large salmonids. *Transactions of the American Fisheries Society* **117**: 1–21.

Chapman DW, Weitkamp DE, Welsh TL, Dell MB, and Schadt TH. 1986. Effects of river flow on the distribution of chinook salmon redds. *Transactions of the American Fisheries Society* **115**: 537–547.

Clark E, Webb BW, and Ladle M. 1999. Microthermal gradients and ecological implications in Dorset rivers. *Hydrologic Processes* **13**: 423–438.

Comer LE and Grenney WJ. 1977. Heat transfer processes in the bed of a small stream. *Water Research* **11**: 743–744.

Connor WP, Piston CE, and Garcia AP. 2003. Temperature during incubation as one factor affecting the distribution of Snake River fall chinook salmon spawning areas. *Transactions of the American Fisheries Society* **132**: 1236–1243.

Constantz J. 1998. Interaction between stream temperature, streamflow, and groundwater exchanges in alpine streams. *Water Resources Research* **34**: 1609–1615.

Crisp DT. 1990. Water temperature in a stream gravel bed and implications for salmonid incubation. *Freshwater Biology* **23**: 601–612.

Crisp DT and Carling PA. 1989. Observations on siting, dimensions and structure of salmonid redds. *Journal of Fish Biology* **34**: 119–134.

DeVries P. 1997. Riverine salmonid egg burial depths: Review of published data and implications for scour studies. *Canadian Journal of Fisheries and Aquatic Sciences* **54**: 1685–1698.

Dole-Olivier MJ and Marmonier P. 1992. Effects of spates on the vertical distribution of the interstitial community. *Hydrobiologia* **230**: 49–61.

Elliott AH and Brooks NH. 1997. Transfer of nonsorbing solutes to a streambed with bed forms: theory. *Water Resources Research* **33**: 123–136.

Evans EC, Greenwood MT, and Petts GE. 1995. Thermal profiles within river beds. *Hydrological Processes* **9**: 19–25.

Evans EC, McGregor GR, and Petts GE. 1998. River energy budgets with special reference to river bed processes. *Hydrological Processes* **12**: 575–595.

Folt CL, Nislow KH, and Power ME. 1998. Implications of temporal and spatial scale for Atlantic salmon (*Salmo salar*) research. *Canadian Journal of Fisheries and Aquatic Sciences* **55**: 9–21.

Garcia A, Bradbury S, Arnsberg B, Rocklage S, and Groves P. 2003. *Fall Chinook salmon spawning ground surveys in the Snake River basin upriver of Lower Granite Dam*. BPA Report DOE/BP-00004700-2. Bonneville Power Administration, Portland, OR.

Garcia A, Bradbury S, Arnsberg B, Rocklage S, and Groves P. 2004. *Fall Chinook salmon spawning ground surveys in the Snake River basin upriver of Lower Granite Dam*. BPA Report DOE/BP-00004700-3. Bonneville Power Administration, Portland, OR.

Geist DR, Hanrahan TP, Arntzen EV, McMichael GA, Murray CJ, and Chien Y-J. 2002. Physicochemical characteristics of the hyporheic zone affect redd site selection by chum salmon and fall chinook salmon in the Columbia River. *North American Journal of Fisheries Management* **22**: 1077–1085.

Gibbins CN and Acornley RM. 2000. Salmonid habitat modelling studies and their contribution to the development of an ecologically acceptable release policy for Kielder Reservoir, north-east England. *Regulated Rivers: Research and Management* **16**: 203–224.

Gibbins CN, Moir HJ, Webb JH, and Soulsby C. 2002. Assessing discharge use by spawning Atlantic salmon: A comparison of discharge electivity indices and PHABSIM simulations. *River Research and Applications* **18**: 383–395.

Groves PA and Chandler JA. 1999. Spawning habitat used by fall chinook salmon in the Snake River. *North American Journal of Fisheries Management* **19**: 912–922.

Hanrahan TP, Geist DR, Arntzen EV, and Abernethy CS. 2004. *Effects of hyporheic exchange flows on egg pocket water temperature in Snake River fall Chinook salmon spawning areas*. PNNL–14850: Pacific Northwest National Laboratory, Richland, WA.

Hanrahan TP. In review. Effects of river discharge on hyporheic exchange flows in a large gravel-bed river. To be submitted to *Hydrological Processes*.

Harvey JW, Wagner BJ, and Bencala KE. 1996. Evaluating the reliability of the stream tracer approach to characterize stream-subsurface water exchange. *Water Resources Research* **32**: 2441–2451.

Helsel DR and Hirsch RM. 2002. Statistical methods in water resources, Book 4, Chapter A3. In: U. S. Geological Survey (ed), Techniques of water-resources investigations of the United

States Geological Survey, U. S. Government Printing Office, Reston, VA.

Hendricks SP and White DS. 1991. Physicochemical patterns within a hyporheic zone of a northern Michigan river, with comments on surface water patterns. *Canadian Journal of Fisheries and Aquatic Sciences* **48**: 1645–1654.

Hendry K, Cragg-Hine D, O'Grady M, Sambrook H, and Stephen A. 2003. Management of habitat for rehabilitation and enhancement of salmonid stocks. *Fisheries Research* **62**: 171–192.

Hondzo M and Stefan HG. 1994. Riverbed heat conduction prediction. *Water Resources Research* **30**: 1503–1513.

Independent Scientific Group. 1996. *Return to the river: Restoration of salmonid fishes in the Columbia River ecosystem*. Northwest Power Planning Council, Portland, OR.

Johnson SL. 2004. Factors influencing stream temperatures in small streams: substrate effects and a shading experiment. *Canadian Journal of Fisheries and Aquatic Sciences* **61**: 913–923.

Kondolf GM. 2000. Assessing salmonid spawning gravel quality. *Transactions of the American Fisheries Society* **129**: 262–281.

Lapham WW. 1989. *Use of temperature profiles beneath streams to determine rates of vertical ground-water flow and vertical hydraulic conductivity*. Water-Supply Paper 2337. U. S. Geological Survey, Denver, CO.

Malcolm IA, Soulsby C, and Youngson AF. 2002. Thermal regime in the hyporheic zone of two contrasting salmonid spawning streams: ecological and hydrological implications.

Fisheries Management and Ecology **9**: 1–10.

Malcolm IA, Soulsby C, Youngson AF, and Hannah DM. 2005. Catchment-scale controls on the groundwater-surface water interactions in the hyporheic zone: Implications for salmon embryo survival. *River Research and Applications* **21**: 977–989.

Malcolm IA, Soulsby C, Youngson AF, Hannah DM, McLaren IS, and Thorne A. 2004. Hydrological influences on hyporheic water quality: implications for salmon egg survival. *Hydrologic Processes* **18**: 1543–1560.

Marmonier P and Creuze des Chatelliers MC. 1991. Effects of spates on interstitial assemblages of the Rhone River: importance of spatial heterogeneity. *Hydrobiologia* **210**: 243–251.

Miller S, Glanzman D, Doran S, Parkinson S, Buffington J, and Milligan J. 2002. *Geomorphology of the Hells Canyon Reach of the Snake River*. Technical Report Appendix E.1.2 to FERC Relicensing Application. Idaho Power Company, Boise, ID.

Murray CB and Beacham TD. 1987. The development of chinook (*Oncorhynchus tshawytscha*) and chum salmon (*Oncorhynchus keta*) embryos and alevins under varying temperature regimes. *Canadian Journal of Zoology* **65**: 2672–2681.

National Marine Fisheries Service (NMFS). 1992. Threatened status for Snake River spring/summer chinook salmon, threatened status for Snake River fall chinook salmon. *Federal Register* **57**: 14653–14663.

Peterson NP and Quinn TP. 1996. Spatial and temporal variation in dissolved oxygen in natural egg pockets of chum salmon, in Kennedy Creek, Washington. *Journal of Fish Biology* **48**: 131–143.

Rennie CD and Millar RG. 2000. Spatial variability of stream bed scour and fill: a comparison of scour depth in chum salmon (*Oncorhynchus keta*) redds and adjacent bed. *Canadian Journal of Fisheries and Aquatic Sciences* **57**: 928–938.

Ringler NH and Hall JD. 1975. Effects of logging on water temperature and dissolved oxygen in spawning beds. *Transactions of the American Fisheries Society* **104**: 111–121.

Savant SA, Reible DD, and Thibodeaux LJ. 1987. Convective transport within stable river sediments. *Water Resources Research* **23**: 1763–1768.

Shepherd BG, Hartman GF, and Wilson WJ. 1986. Relationships between stream and intragravel temperatures in coastal drainages, and some implications for fisheries workers. *Canadian Journal of Fisheries and Aquatic Sciences* **43**: 1818–1822.

Silliman SE and Booth DF. 1993. Analysis of time-series measurements of sediment temperature for identification of gaining vs. losing portions of Juday Creek, Indiana. *Journal of Hydrology* **146**: 131–148.

Silliman SE, Ramirez J, and McCabe RL. 1995. Quantifying downflow through creek sediments using temperature time series: one-dimensional solution incorporating measured surface temperature. *Journal of Hydrology* **167**: 99–119.

Sinokrot BA and Stefan HG. 1993. Stream temperature dynamics: measurements and modeling. *Water Resources Research* **29**: 2299–2312.

Sinokrot BA and Stefan HG. 1994. Stream water-temperature sensitivity to weather and bed parameters. *Journal of Hydraulic Engineering* **120**: 722–736.

Stanley EH and Boulton AJ. 1993. Hydrology and the distribution of hyporheos: perspectives from a mesic river and a desert stream. *Journal of the North American Benthological Society* **12**: 79–83.

Triska FT, Kennedy VC, Avanzino RJ, Zellweger GW, and Bencala KE. 1989. Retention and transport of nutrients in a third-order stream in northwestern California: hyporheic processes. *Ecology* **70**: 1893–1905.

Webb BW and Zhang Y. 1997. Spatial and seasonal variability in the components of the river heat budget. *Hydrological Processes* **11**: 79–101.

Webb BW and Zhang Y. 1999. Water temperatures and heat budgets in Dorset chalk water courses. *Hydrological Processes* **13**: 309–321.

White DS, Elzinga CH, and Hendricks SP. 1987. Temperature patterns within the hyporheic zone of a northern Michigan river. *Journal of the North American Benthological Society* **6**: 85–91.

Youngson AF, Malcolm IA, Thorley JL, Bacon PJ, and Soulsby C. 2004. Long-residence groundwater effects on incubating salmonid eggs: low hyporheic oxygen impairs embryo development. *Canadian Journal of Fisheries and Aquatic Sciences* **61**: 2278–2287.

Tables

Table 1. Snake River fall Chinook salmon spawning areas sampled during 2002–2003, 2003–2004, and 2004–005. The use of artificial egg pockets at each study site is summarized for the three water years studied. Container types used for deploying temperature sensors are listed, along with their depth below the riverbed surface during deployment and retrieval.

Year	Reach	Site	# egg pockets	Container type	Average deployed depth below riverbed (cm)	Average retrieval depth below riverbed (cm)
2002 - 2003	Lower	148.5	3	tube	22	
		149.2	3	tube	23	
		152.3	3	tube	24	
		156.8	3	tube	23	
	Upper	196.0	3	tube	21	
		198.2	3	tube	23	
		198.8	3	tube	23	
		211.9	3	tube	22	
		218.7	3	tube	25	
		219.3	3	tube	24	
		222.7	3	tube	22	
		238.6	3	tube	21	
		240.6	3	tube	26	
		244.5	3	tube	27	
2003 - 2004	Lower	152.3	3	basket	20	11
		175.2	3	basket	20	11
	Upper	196.0	2	tube	24	
		198.2	3	basket	23	12
		198.8	3	tube	25	
		211.9	3	tube	25	
		219.3	1	tube	23	
		238.6	3	basket	19	12
		240.6	3	tube	25	
		244.5	2	tube	24	
2004 - 2005	Lower	152.3	1	basket	20	8
		175.2	3	basket	20	12
	Upper	198.2	1	basket	20	20
		222.7	1	basket	21	12

Table 2. Summary results from Kruskal-Wallis multiple comparisons (α=0.05) of mean water temperature during the fall Chinook salmon egg incubation period (18 November 2002 – 2 March 2003). Cells with the same letters indicate homogeneous groups within a site.

		Mean water temperature (C)			
Reach	Site	River	Egg pocket	Shallow hyporheic	Deep hyporheic
Lower	148.5	5.39^{A}	5.51^{AB}	5.70^{B}	6.34^{C}
	149.2	5.37^{A}	5.62^{A}	5.69^{A}	6.43^{B}
	152.3	5.22^{A}	5.48^{A}	6.28^{B}	6.79^{C}
	156.8	5.29^{A}	5.72^{B}	6.13^{B}	6.58^{C}
Upper	196.0	6.45^{A}	6.56^{A}	6.47^{A}	6.56^{A}
	198.2	6.69^{A}	6.28^{A}	6.92^{A}	7.40^{B}
	198.8	6.53^{A}	6.63^{AB}	7.02^{BC}	7.41^{C}
	211.9	6.13^{A}	6.54^{A}	6.37^{AB}	6.72^{B}
	218.7	6.38^{A}	6.58^{A}	7.12^{B}	8.04^{C}
	219.3	6.21^{A}	6.08^{A}	6.40^{AB}	6.86^{B}
	222.7	6.36^{A}	6.74^{AB}	7.37^{BC}	7.76^{C}
	238.6	6.27^{A}	6.22^{A}	7.13^{B}	7.55^{B}
	240.6	6.26^{A}	6.13^{A}	6.47^{A}	6.53^{A}
	244.5	6.10^{A}	6.36^{A}	6.27^{A}	6.31^{A}

Table 3. Summary results from Kruskal-Wallis multiple comparisons (α=0.05) of mean water temperature during the fall Chinook salmon egg incubation period (18 November 2003 – 2 March 2004). Cells with the same letters indicate homogeneous groups within a site.

		Mean water temperature (C)			
Reach	Site	River	Egg pocket	Shallow hyporheic	Deep hyporheic
Lower	152.3	4.89^{A}	4.91^{A}	5.92^{B}	6.66^{C}
	175.2	4.90^{A}	4.92^{AB}	5.36^{B}	5.21^{AB}
Upper	196.0	6.01^{A}	5.93^{A}	5.97^{A}	5.58^{A}
	198.2	6.00^{A}	5.54^{A}	6.10^{A}	7.18^{B}
	198.8	5.13^{A}	5.87^{AB}	6.39^{BC}	6.61^{C}
	211.9	5.36^{A}	5.81^{AB}	6.41^{B}	5.90^{AB}
	219.3	5.66^{A}	5.47^{A}	5.87^{A}	5.78^{A}
	238.6	5.40^{A}	5.88^{A}	6.51^{B}	6.62^{B}
	240.6	5.66^{A}	5.61^{A}	6.29^{A}	5.89^{A}
	244.5	5.70^{A}	5.89^{A}	5.38^{A}	5.58^{A}

Table 4. Summary results from Kruskal-Wallis multiple comparisons (α=0.05) of mean water temperature during the fall Chinook salmon egg incubation period (18 November 2004 – 2 March 2005). Cells with the same letters indicate homogeneous groups within a site.

		Mean water temperature (C)			
Reach	Site	River	Egg pocket	Shallow hyporheic	Deep hyporheic
Lower	152.3	4.50^{A}	5.05^{AB}	5.39^{BC}	5.82^{C}
	175.2	5.30^{A}	5.54^{AB}	5.88^{BC}	6.15^{C}
Upper	198.2	6.20^{A}	6.30^{A}	6.73^{B}	7.37^{B}
	222.7	6.44^{A}	6.55^{A}	7.97^{B}	7.63^{B}

Table 5. Summary results of the number of days required to reach 1066 accumulated temperature units (ATU) in the river, artificial egg pockets, shallow hyporheic zone, and deep hyporheic zone at each site during the three water years studied.

			Days to 1066 ATU			
Year	Reach	Site	River	Egg pocket	Shallow hyporheic	Deep hyporheic
2002 - 2003	Lower	148.5	162	162	155	147
		149.2	163	162	158	145
		152.3	163	161	160	150
		156.8	163	158	155	143
	Upper	196.0	139	139	138	137
		198.2	135	135	132	117
		198.8	140	137	129	121
		211.9	142	137	130	124
		218.7	138	133	119	113
		219.3	141	139	132	130
		222.7	138	133	116	111
		238.6	139	137	125	111
		240.6	141	138	135	128
		244.5	141	140	140	136
2003 - 2004	Lower	152.3	171	170	158	158
		175.2	171	169	163	164
	Upper	196.0	158	154	156	156
		198.2	155	156	146	122
		198.8	156	152	146	143
		211.9	158	153	147	143
		219.3	158	156	153	151
		238.6	156	153	149	135
		240.6	157	155	151	146
		244.5	157	157	157	152
2004 - 2005	Lower	152.3	169	161	156	147
		175.2	160	158	144	145
	Upper	198.2	119	113	107	97
		222.7	114	111	94	91

List of figures

Figure 1. The study area extended from Hells Canyon Dam downstream to near the confluence with Asotin Creek. Study sites (□) are identified by their river mile location.

Figure 2. Reach comparisons of water temperature in (a) the river, (b) egg pocket depth, (c) the shallow hyporheic zone, and (d) the deep hyporheic zone, during the 2002–2003 fall Chinook salmon egg incubation period (18 November – 2 March). Each boxplot represents a summary of hourly water temperature. The point in the center of the boxplot indicates the mean, the box is equal to one standard deviation, and the whiskers represent the range.

Figure 3. Reach comparisons of water temperature in (a) the river, (b) egg pocket depth, (c) the shallow hyporheic zone, and (d) the deep hyporheic zone, during the 2003–2004 fall Chinook salmon egg incubation period (18 November – 2 March). Each boxplot represents a summary of hourly water temperature. The point in the center of the boxplot indicates the mean, the box is equal to one standard deviation, and the whiskers represent the range.

Figure 4. Reach comparisons of water temperature in (a) the river, (b) egg pocket depth, (c) the shallow hyporheic zone, and (d) the deep hyporheic zone, during the 2004–2005 fall Chinook salmon egg incubation period (18 November – 2 March). Each boxplot represents a summary of hourly water temperature. The point in the center of the boxplot indicates the mean, the box is equal to one standard deviation, and the whiskers represent the range.

Figure 5. Comparison of the number of days required to reach 1066 accumulated temperature units (ATU) in the river, artificial egg pockets, shallow hyporheic zone, and deep hyporheic zone of the lower (○) and upper (□) reach during each of the three water years studied. The point at the center of each plot represents the mean for the reach, while the whiskers indicate the range. The daily average temperature of the river and at each depth within the riverbed is the basis for the ATU.

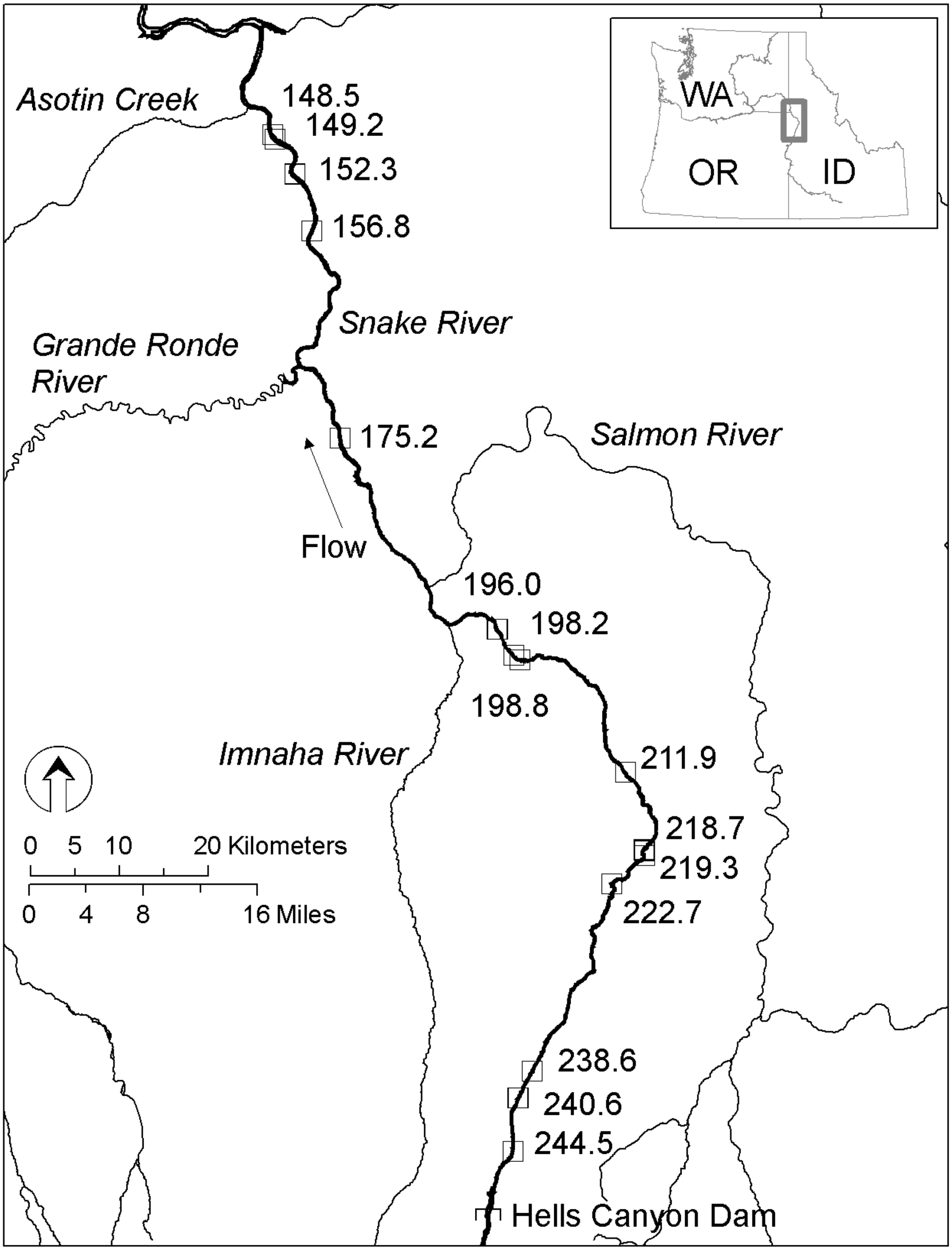
Asotin Creek
148.5
149.2
152.3
156.8
Snake River
Grande Ronde River
175.2
Salmon River
Flow
196.0
198.2
198.8
Imnaha River
211.9
218.7
219.3
222.7
238.6
240.6
244.5
Hells Canyon Dam
0 5 10 20 Kilometers
0 4 8 16 Miles
WA
OR
ID

Figure 1

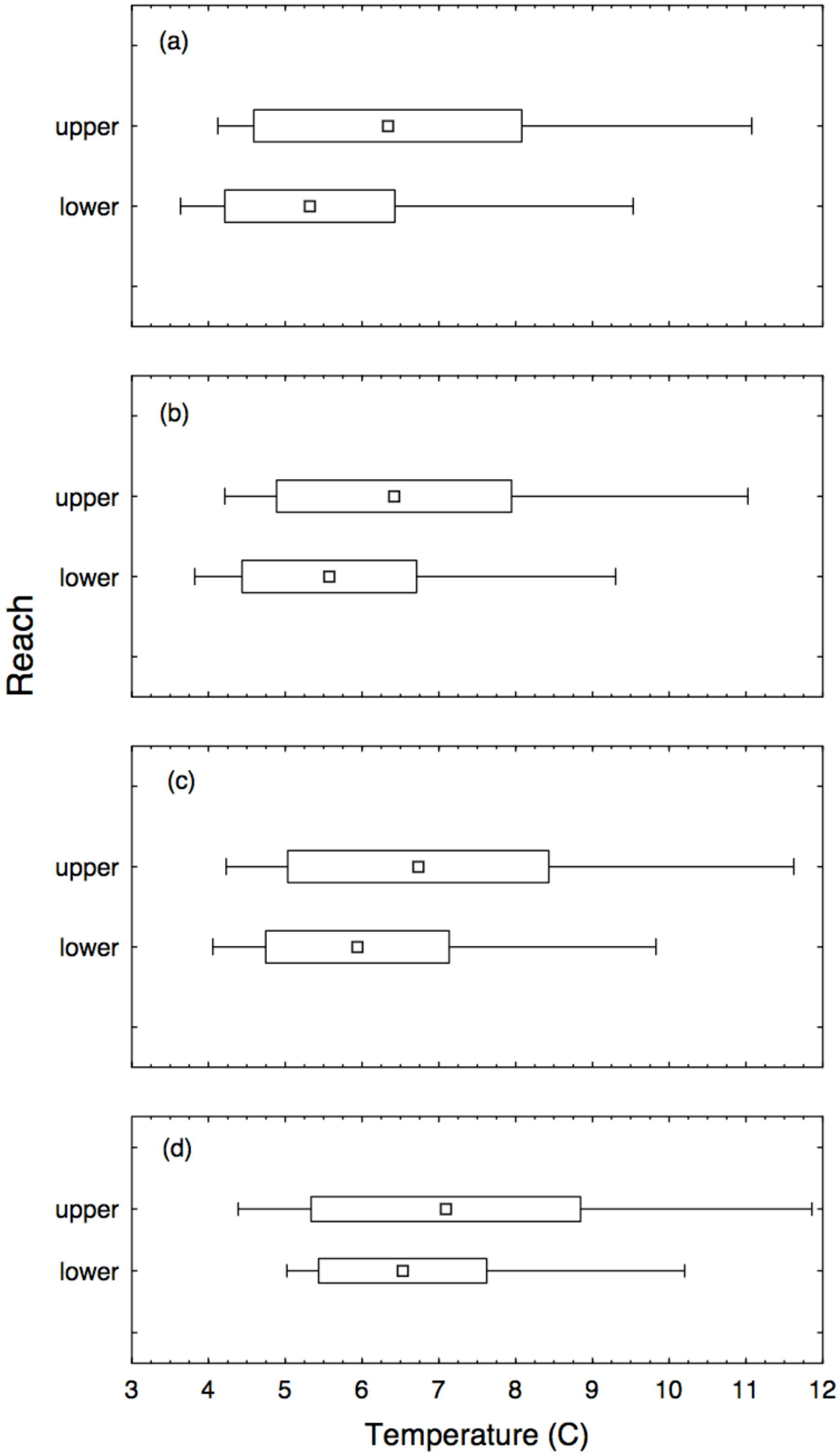
(a)
upper
lower
(b)
upper
lower
Reach
(c)
upper
lower
(d)
upper
lower
3
4
5
6
7
8
9
10
11
12
Temperature (C)

Figure 2

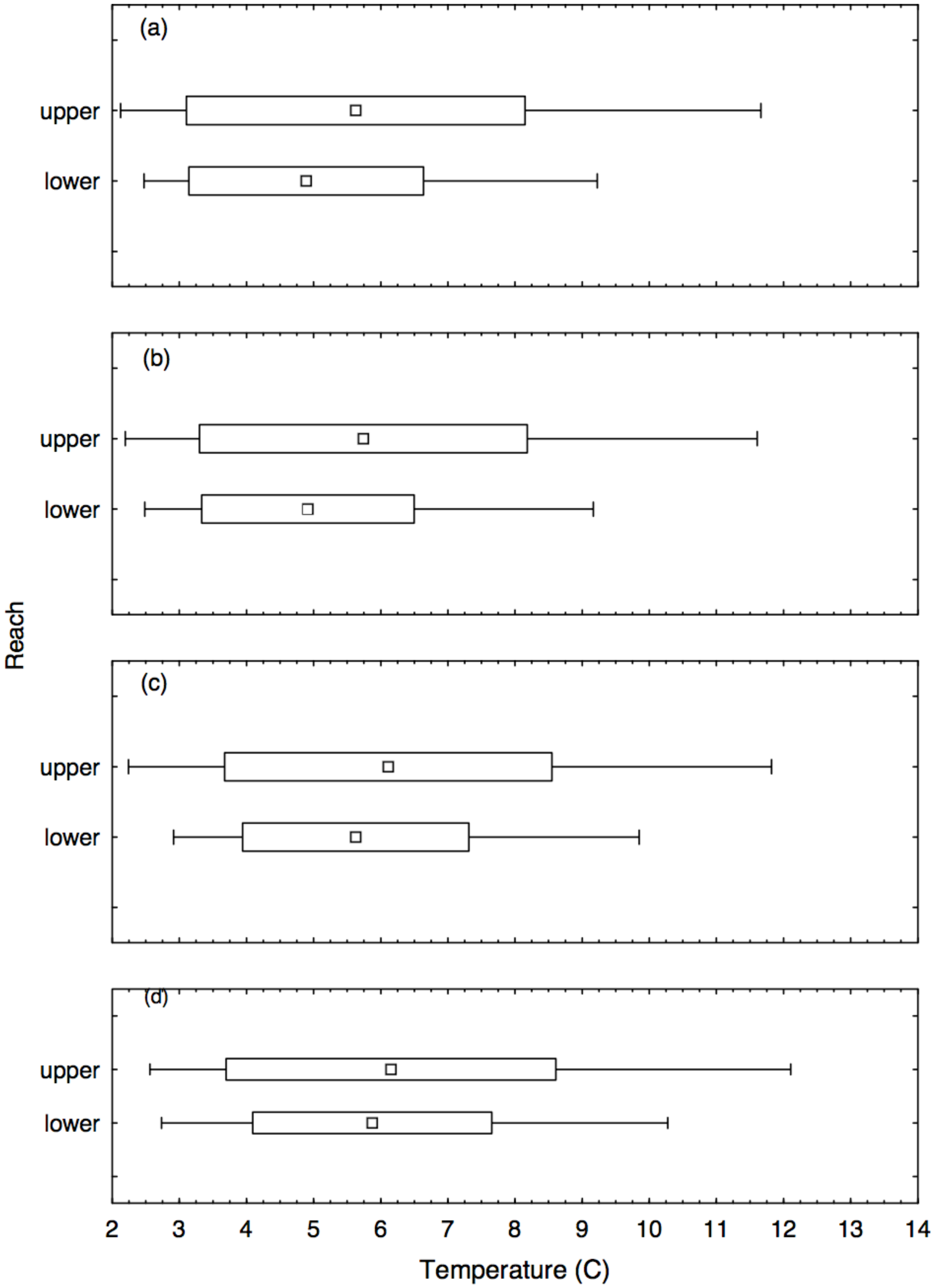
(a)
upper
lower
(b)
upper
lower
(c)
upper
lower
(d)
upper
lower
Reach
2
3
4
5
6
7
8
9
10
11
12
13
14
Temperature (C)

Figure 3

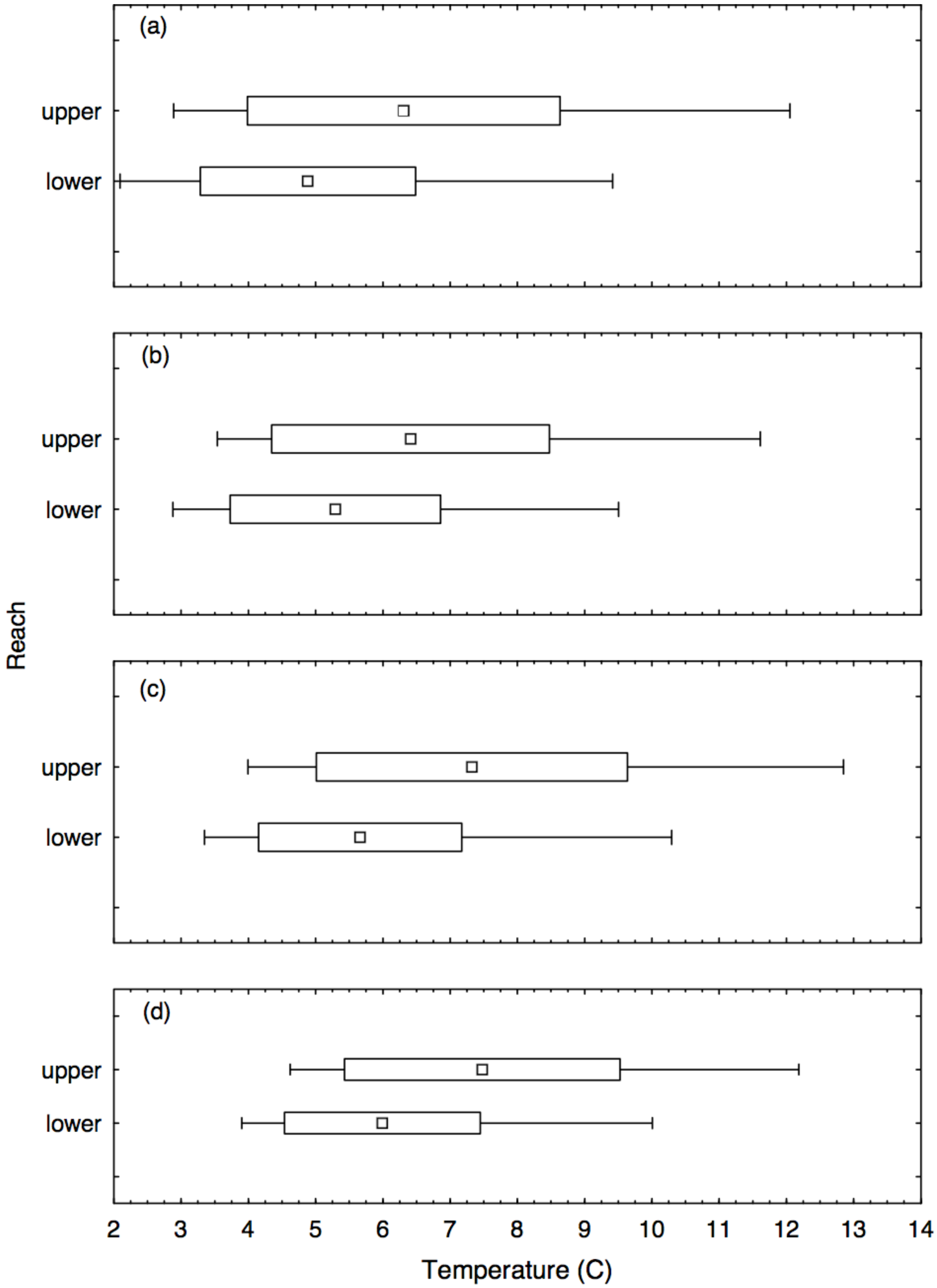
(a)
upper
lower
(b)
upper
lower
(c)
upper
lower
(d)
upper
lower
Reach
2
3
4
5
6
7
8
9
10
11
12
13
14
Temperature (C)

Figure 4

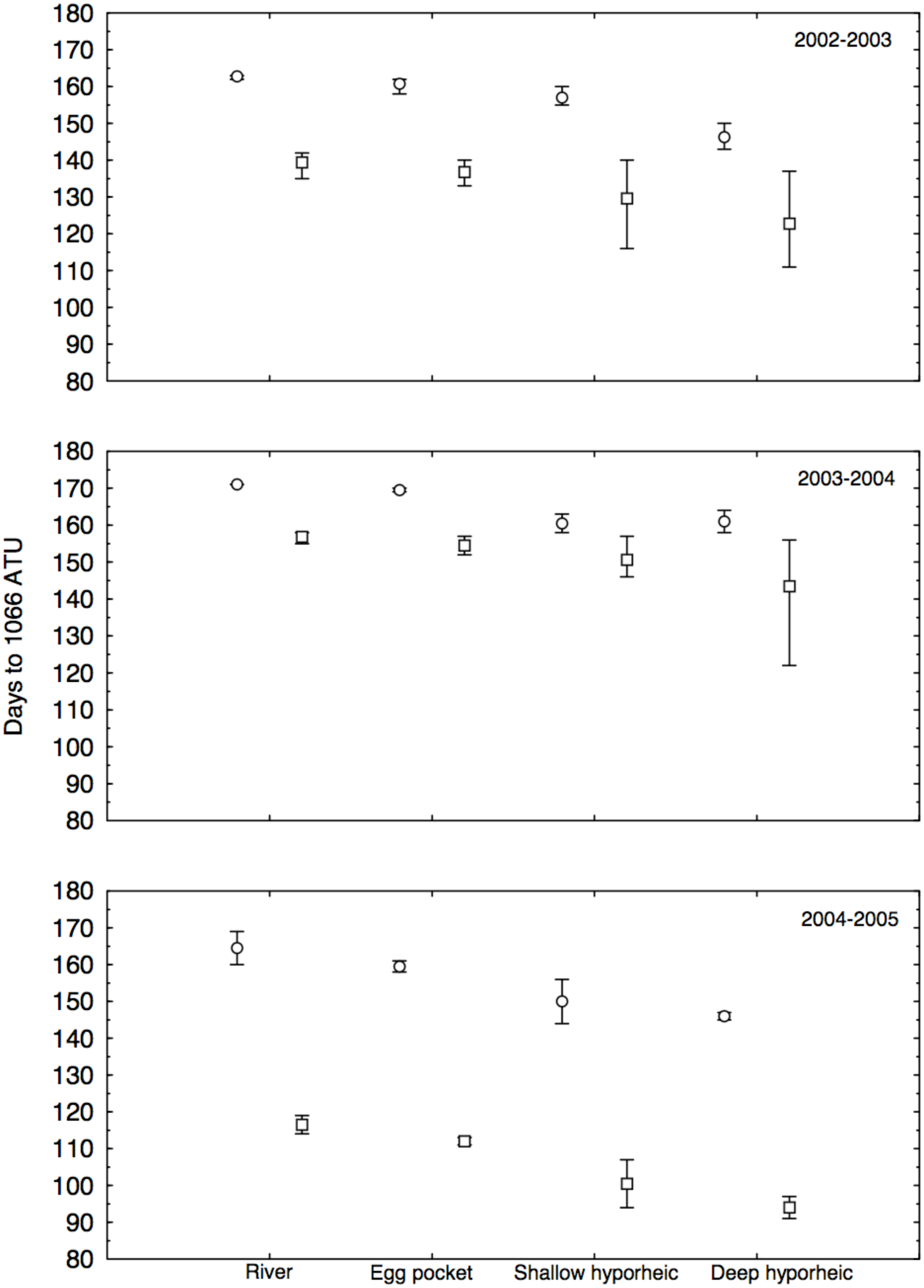
Days to 1066 ATU
2002-2003
2003-2004
2004-2005
180
170
160
150
140
130
120
110
100
90
80
River
Egg pocket
Shallow hyporheic
Deep hyporheic

Figure 5

SUMMARY

SUMMARY

The findings reported in manuscript one provide a quantitative association between salmon spawning habitat and geomorphic features, an association that previous research has documented in qualitative terms. The results indicate that most Snake River fall Chinook salmon spawning occurs in riffles, and at a vertical location within 80% of the riffle crest elevation. The findings provide an important context for estimating the spawning habitat potential of Snake River fall Chinook salmon and other salmon populations. The objective identification and quantification of stage-independent pool-riffle bed forms will result in more accurate estimates of salmon spawning habitat potential, as microhabitat characteristics (e.g., depth, velocity, substrate size) in salmon spawning areas encompass such a large range that their predictive potential is often limited. For example, incorporating the quantitative association between salmon spawning habitat and riffles into habitat modeling will improve the predictive potential of such models by providing a quantitative means of identifying the suitable microhabitat located in riffles, and not elsewhere along the longitudinal profile. Such an approach is not possible through visual planform mapping of pools and riffles, as the identified geomorphic units are stage-dependent, subject to individual interpretation, and provide no quantitative metric that can be incorporated into habitat models. Incorporating the quantitative linkages between bed forms and other microhabitat variables, such as hydrologic exchange, when predicting habitat potential will also result in more accurate estimates of suitable habitat. Improvements to the predictive potential of habitat models will help management and regulatory agencies in the Snake River basin and elsewhere to develop realistic recovery goals for salmon abundance.

While pool-riffle bed forms may be controlling factors of fish habitat, quantifying their location in the longitudinal profile also provides a useful framework for evaluating general ecological implications of riverine processes in large gravel-bed rivers. The identification of bed forms and application of the Riffle Proximity Index described in manuscript one provide a quantitative framework for testing hypotheses regarding the associations between riverine processes and ecological function (e.g., benthic macroinvertebrate habitat, nutrient cycling, biofilm development). For example, the location along the longitudinal profile may be used as an independent variable to evaluate the magnitude of hydrologic exchange between the river and riverbed, the local turbulence characteristics of the flow field, and the local bedload sediment transport capacity as it affects bed material grain size distributions, all of which affect the functioning of benthic habitats. Thus, the framework described in manuscript one for quantifying the longitudinal riverbed profile will aid in the design and interpretation of future empirical research into the ecological significance of physical riverine processes.

Regional management agencies in the Snake River basin are considering modifications to the discharge operations of Hells Canyon Dam as part of recovery efforts for imperiled fall Chinook salmon populations. Before modifications to discharge operations are implemented, additional information regarding the effects of river discharge on hydrologic exchange between the river and riverbed in fall Chinook salmon spawning areas is necessary. The results reported in manuscript two suggest that manipulated variations of river discharge from Hells Canyon Dam have a negligible effect on vertical hydrologic exchange. Because variation in river discharge have a negligible effect on riverbed temperature gradients, manipulations of river discharge from Hells Canyon Dam would likely have a negligible effect on accelerating fall Chinook salmon egg incubation and growth.

The findings reported in manuscript two indicate that hydrologic exchange within the upper 1 m of the riverbed in Snake River fall Chinook salmon spawning areas is controlled primarily by surface water hydraulics at the scale of individual redds, and secondarily by the channel morphology at the scale of several pool-riffle sequences. It is likely that the surface water hydraulic processes of advective pumping and turbulent diffusion are major processes controlling the hydrologic exchange on the smaller scale, and within the upper 1 m of the riverbed. Because of the high longitudinal riverbed slope within the study area, and the geomorphically-confined nature of the river corridor, the upstream–downstream piezometric gradients likely contribute significantly to the surface–subsurface exchange at the larger scale of several pool-riffle sequences. The high longitudinal riverbed gradient of the Hells Canyon reach of the Snake River, and the pool-riffle morphology, dictates that hydrologic exchange in fall Chinook salmon spawning areas is controlled longitudinally and is much less susceptible to flux reversals resulting from discharge changes. Given the context of these hydrologic controls, the findings reported in manuscript two are more comparable with other gravel-bed rivers in similar physical settings regardless of river size, than with other large gravel-bed rivers in different physical settings.

Snake River basin management agencies are tasked with managing the discharge operations of Hells Canyon Dam for multiple uses, including tradeoffs between providing sufficient downstream flow to protect incubating embryos of imperiled fall Chinook salmon and limiting downstream flow in order to refill reservoirs. Because these water management decisions are based on the emergence timing of fall Chinook salmon, there is a need to quantify the temperature gradient between the river and riverbed in fall Chinook salmon spawning areas, as temperature is the primary basis for emergence timing estimates. The results reported in manuscript three indicate that riverbed temperatures are warmer than water column temperatures during the Snake River fall Chinook salmon incubation period. During each of the three water years studied, the water temperatures measured in the riverbed and water column varied significantly among all the study sites, among the study sites within each reach, and between sites located in the upper and lower reaches. The findings indicate that the use of riverbed temperatures from more than one site within each reach would produce the most accurate estimates of fall Chinook salmon emergence timing in the Snake River. Because of the observed variability in riverbed temperatures among the study sites, it may be prudent to adopt a risk-based approach to monitoring riverbed temperatures when making decisions on flow management changes. This approach could emphasize a level of riverbed temperature monitoring that is proportional to the spawning habitat use of a site, such that sites with the most spawning activity are most intensely monitored.

The large variability in riverbed temperatures within and among the study sites suggests the need to better understand this variability in order to better manage the limited water resources in the highly-regulated Snake River basin. By incorporating the knowledge of hydrologic exchange processes into water management planning, regional agencies will be better prepared to manage the limited water resources among competing priorities that include salmon recovery, flood control, irrigation supply, hydropower production, and recreation.

Collectively, the results of this research improve upon the understanding of physical habitat characteristics (channel morphology, hydrologic exchange, temperature gradients) affecting Snake River fall Chinook salmon spawning and incubation environments. This knowledge will foster science-based water management planning and recovery activities for this imperiled salmon population, and those elsewhere in the world.